Victor Beccari Dieguez Campo

Bachelor of Biological Sciences

Junho, 2021

The sauropodomorph dinosaurs from the Late Triassic (Norian) of Jameson Land, East Greenland

Dissertação para obtenção do Grau de Mestre em Paleontologia

Advisor: Doutor Octávio João Madeira Mateus, Professor Associado com Agregação, Faculdade de Ciências e Tecnologia da Universidade Nova de Lisboa

Júri:

Presidente: Prof. Doutor Paulo Alexandre Rodrigues Roque Legoinha (FCT-UNL)

Arguente: Doutor Oliver Wings (ZNS)

Vogal: Prof. Doutor Octávio João Madeira Mateus (FCT-UNL)

FACULDADE DE CIÊNCIAS E TECNOLOGIA
UNIVERSIDADE NOVA DE LISBOA

The sauropodomorph dinosaurs from the Late Triassic (Norian) of Jameson Land, East Greenland

Acknowledgements

My everlasting dream of becoming a palaeontologist hits another milestone with the present thesis, and it would not be possible without the help I got along the way. I am humbled to have participated in a project in which I believe and gave me so much joy. Therefore, I want to firstly thank my advisor, Prof. Octávio Mateus, who allowed me to work on the amazing specimens described in this thesis. He helped me grow as a researcher and trusted me to follow my leads and path. I would like to thank the team responsible for finding and collecting the specimens in this study, William W. Amaral, William R. Downs, Stephen M. Gatesy, Neil H. Shubin and Niels Bonde and Farish Jenkins. And to be able to segment the high-resolution CT-Scans of the material that made this thesis both more enjoyable and substantial I have Marco Marzola, Filippo Rotatori and Alexandra Fernandes to thank. For the discussions about sauropodomorphs I would like to thank Lars Clemmensen, Oliver Rauhut and Rodrigo Müller, all who gave me good advises and ideas for this thesis.

Others helped me get here, to a different country in a different continent. Among them are my former bachelor advisor, Prof. Luiz Eduardo Anelli, and the co-author of my first paper, Prof. Felipe Pinheiro. Both pushed me to be better and taught me lessons I will take for the rest of my life. As this journey had ups and (very deep) downs, to meet people at the right time was substantial, and one person that reignited my passion for palaeontology was Prof. Aline Ghilardi, to whom I will always be thankful. Also, from Brazil, the friends that believed in me and helped me throughout my life are many to thank, but here I will try my best. So, here is a big thank you to my school friends Gustavo W. Rauscher, Leandro Hayashi, Vitor Takahasi, Aleksei Manz, Alexandre Vasconcelos, and all my friends from 12C, to my college friends Anna Carolina Dias de Almeida, Leonardo Barolo, Imo, Aloha, Luiza Sandoval, Ade, Taran, Rafael Hauy, Bernardo, Mari, Heitor, Ana Luiza Fontenelle and many others, and my dear colleagues of Alef, Beatriz Aceto, Jacqueline Oliveira, Lucas, Rapha, Torugo, Tambor and Mauricio. And finally, to the amazing Marta Alvin, thank you dearly for all your support. Those are all friends I want to keep close for the rest of my life.

Here in Portugal, I had the opportunity to meet brilliant researchers and friends, who all helped me during dire times and were always ready to guide me when I needed to. To my thesis-tutor André Saleiro, my palaeontological friends, Xana, Pippo, Eduardo Puértolas-Pascual, Alexandre Guillaume, Victor López, Dário, João Russo, Francisco, Simone, Simão, Miguel Marx, Marco and Maciej, my boss Miguel Moreno-Azanza, my classmates and friends Rita, Catarina, Mahima, Filipe and Gonçalo and my non-paleo European friends Alexandre Audigane, Lope, Ana Luz and Remmert, a big thank to all of you. Life would lose much of its charm if I could not go out and have drinks, hunt mushrooms and

travel with you. I would also like to thank the GEAL Museu da Lourinhã (ML), Nature History Museum of Denmark (NHMD) and Møns Klint for hosting me and providing the specimens for my thesis.

And my thanks would not be complete without my family, especially my mother, who endured me during the worst phase of my life and keeps making sure I am alive and well, and my brother Pedro and my cousin Bia, both of whom sheltered me on my first few weeks in Europe and are always present.

Abstract

The Late Triassic (Norian) outcrops of Malmros Klint Formation, Jameson Land, central East Greenland, are home to non-sauropod sauropodomorphs that are yet to be thoroughly described. The material recovered to this locality comprises of almost complete and sometimes articulated specimens, preserving both cranial and postcranial elements, and tracks. These fossils were briefly reported in the literature and were assigned to the taxon *Plateosaurus trossingensis*. However, with new findings for the clade of early non-sauropod sauropodomorphs around the globe, the material should be revised. The goal of the present thesis is to fully describe the specimens housed in Lourinhã Museum (ML), Lourinhã, Portugal, using µCT-Scan and Photogrammetry, when available, to understand the taxonomy, systematics and palaeobiogeography of these animals. The specimens in this study consist in two almost complete and articulated skulls. The Greenland sauropodomorph skulls were compared with other plateosaurid sauropodomorphs and closely related taxa for a full anatomical description. The specimens represent a single taxon of different ontogenetic stages, an early-stage juvenile (NHMD 164758) and a late-stage juvenile (NHMD 164741). This taxon differs from all other sauropodomorphs by a set of unique traits (1) the presence of a small foramen at the medial surface of the premaxilla at the base of the lateral process of the premaxilla; 2) an anteroposteriorly elongated dorsoposterior process of the squamosal; 3) a quadrate relatively tall in comparison to the rostrum height; 4) a well-developed, square-shaped in lateral view posterodorsal process of the articular) that are not explained by taphonomy, ontogeny and intraspecific variation. The Greenland sauropodomorph was recovered in the most recent phylogenetic analysis as the first non-*Plateosaurus* plateosaurid of Laurasia.

Keywords: Plateosauridae, ontogeny, Malmros Klint Formation, taxonomy, image segmentation.

Resumo

Os afloramentos do Triássico Superior (Noriano) da Formação Malmros Klint, Jameson Land, Leste da Groelândia, fornecem sauropodomorfos não-saurópodes que carecem de descrições completas. O material recolhido desta localidade contém espécimes muitas vezes articulados e quase completos, que preservam material craniano e pós-craniano, e trilhos de pegadas. Esses fósseis foram brevemente descritos na literatura e atribuídos ao táxon *Plateosaurus trossingensis*. Porém, com novas descobertas de sauropodomorfos não-saurópodes ao redor do mundo, esse material deve ser revisto. O objetivo desta tese é de descrever os espécimes depositados no Museu da Lourinhã (ML), Lourinhã, Portugal, utilizando µCT e fotogrametria, quando possível, para entender a taxonomia, sistemática e paleobiogeografia desses animais. Os espécimes deste estudo consistem em dois crâneos quase completos e articulados. Os crânios de sauropodomorfos da Groelândia estudados nesse trabalho representam uma única espécie em dois estágios ontogenéticos distintos, um juvenil em estágio inicial de desenvolvimento (NHMD 164758), e um juvenil tardio (NHMD 164741). Esse táxon difere de todos os outros sauropodomorfos por um conjunto de características únicas (1) presença de um pequeno forámen na face medial da premaxila; 2) um processo posterodorsal alongado do esquamosal; 3) um quadrado relativamente alto em comparação com o rostro; 4) presença de um processo robusto posterodorsal do articular, quadrado em vista lateral) que não podem ser explicadas por tafonomia, ontogenia ou variação intraespecífica. O sauropodomorfos da Groelândia foi recuperado nas análises filogenéticas recentes como o primeiro plateosaurídeo não-*Plateosaurus* da Laurásia.

Palavras-chave: Plateosauridae, ontogenia, Formação Malmros Klint, taxonomia, segmentação de imagem.

Graphic Abstract

Institutional abbreviations

AMNH FARB, American Museum of Natural History, Fossil Amphibian, Reptile and Bird collection, New York, USA; BP, Bernard Price Institute for Palaeontological Research, University of the Witwatersrand, Johannesburg, South Africa; BRSMG, Bristol City Museum and Art Galleries, Bristol, UK; CAPPA/UFSM, Centro de Apoio à Pesquisa Paleontológica da Quarta Colônia da Universidade Federal de Santa Maria, Rio Grande do Sul, Brazil; GPIT, Institut und Museum für Geologie und Paläontologie der Universität Tübingen, Germany; IVPP, Institute of Vertebrate Paleontology and Paleoanthropology, Beijing, People's Republic of China; MB.R., Museum für Naturkunde, collection of fossil Reptilia, Berlin, Germany; MCP, Museu de Ciências e Tecnologia Pontifícia Universidade Católica do Rio Grande do Sul, Porto Alegre, Brazil; MSF, Sauriermuseum Frick, Frick, Switzerland; NHMD, GeoCenter Møns Klint, Møns Klint, Denmark; PVL, Paleontolgía de Vertebrados, Instituto Muíguel Lillo, Tucumán, Argentina; SAM-PK, Iziko South African Museum, Cape Town, South Africa; SMA, Sauriermuseum Aathal, Aathal-Seegräben, Switzerland; SMNS, Staatliches Museum für Naturkund, Stuttgart, Germany; UFRGS-PV, Paleovertebrate Collection of the Laboratório de Paleovertebrados da Universidade Federal do Rio Grande do Sul, Porto Alegre, Brazil; UFSM, Universidade Federal de Santa Maria, Brazil; ULBRA-PVT, Universidade Luterana do Brasil, Coleção de Paleovertebrados, Canoas, Brazil.

Table of Contents

Contents

Table of Figures

Table of Tables

1 Introduction

1.1 Late Triassic sauropodomorphs

The clade Sauropodomorpha comprises the largest animals ever to walk the Earth, with remarkable long necks and small heads. Sauropodomorpha includes iconic animals such as *Diplodocus carnegii* Hatcher, 1901 and *Brachiosaurus altithorax* Riggs, 1903, as well as some of the earliest dinosaurs. The first sauropodomorphs date back to the late Carnian stage (Late Triassic) of Santa Maria Supersequence, southern Brazil and Ischigualasto Formation, Northwestern Argentina (Sereno *et al.*, 1993; Martinez & Alcober, 2009; Ezcurra, 2010; Cabreira *et al.*, 2016; Langer *et al.*, 2018; Müller *et al.*, 2018a; Müller & Garcia, 2020). From the Southwestern Gondwana, the sauropodomorphs soon diversified and conquered the whole globe during the late Norian, becoming the most common large herbivore of the Late Triassic (Brusatte *et al.*, 2010; Button *et al.*, 2017; Langer *et al.*, 2010).

With the numerous new findings of basal sauropodomorphs in South America in the last decade, the understanding of this clade early evolution increased significantly. These new taxa (i.e., *Pampadromaeus barberenai* Cabreira *et al.*, 2011, *Buriolestes schultzi* Cabreira *et al.*, 2016, *Macrocollum itaquii* Müller *et al.*, 2018b and *Bagualosaurus agudoensis* Pretto *et al.*, 2019) suggest that sauropodomorphs were already highly diverse during the late Carnian to late Norian Müller & Garcia, 2020. The earliest forms of basal sauropodomorphs were small faunivorous and gracile animals from the late Carnian (i.e., *Saturnalia tupiniquim* Langer *et al.*, 1999 and *Buriolestes*). These taxa possessed ziphodont teeth and possibly agile bodies, whereas coeval sauropodomorphs such as *Panphagia protos* Martinez & Alcober, 2009 and *Pampadromaeus* were likely omnivorous (Müller & Garcia, 2020) and *Unaysaurus tolentinoi* Leal *et al.*, 2004 already shows adaptations towards herbivory, such as larger denticles and relatively larger body size in comparison to other coeval sauropodomorphs (Pretto *et al.*, 2019; Müller & Garcia, 2020) (Fig. 1.1).

This high diversity at the base of Sauropodomorpha can be tentatively explained through some hypotheses proposed by Müller & Garcia, (2020). The lack of accurate geochronological data for the late Carnian of South America could argue to a low diversity anachronic scenario, where the first forms gradually evolved. Another scenario that would argue for an actual lower diversity during the initial stages of evolution is the lack of understanding of the alpha taxonomy of these dinosaurs. Studies of intraspecific variation and ontogeny are still rare when it comes to early sauropodomorphs but have received more attention in the last few years (Nesbitt *et al.*, 2009; Müller *et al.*, 2017; Nau *et al.*, 2020; Lallensack *et al.*, 2021). However, it is still unclear if the taxonomy of early sauropodomorphs is well

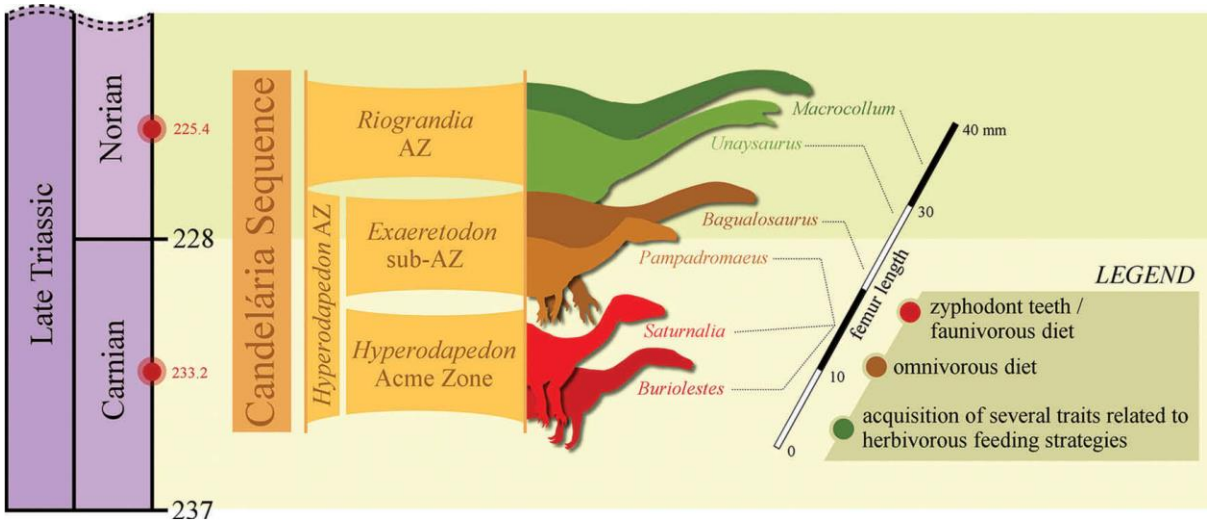

Figure 1.1 – Sauropodomorphs from the Late Triassic of Candelária Sequence, Brazil. The radiometric data were recovered in Langer *et al.* (2018). Dinosaur silhouette colours indicate possible diet (Müller & Garcia, 2020).

resolved for the taxa in Brazil and Argentina, and this could change with new material and more studies. A third hypothesis argues for a true high diversity of basal sauropodomorphs due to possible niche partitioning. This is corroborated by the diverse teeth morphology and body size of these animals, and a better time calibration could be a plausible outcome (Müller & Garcia, 2020).

Whatever scenario can explain the early evolution of the clade, sauropodomorphs became the main components of the herbivorous fauna by the mid to late Norian (Brusatte *et al.*, 2010). This event of faunal turnover was coined “Dynasty V” or “Prosauropod Empire” by Bakker, (1977) and Benton, (1983), respectively. Therefore, the earliest sauropodomorphs in Europe already bore herbivorous adaptations, such as large denticles of teeth forming oblique angles with its margin and large body with a relatively small head (Müller *et al.*, 2018b). However, the European sauropodomorph *Thecodontosaurus antiquus* Morris, 1843 from the Late Triassic (possibly Rhaetian, see Whiteside *et al.*, 2016) of south-western England possesses well-developed flocculi and anterior semicircular canal that points towards an agile and stable gaze that could be related to facultative carnivory (Ballell *et al.*, 2020a). *Thecodontosaurus* is nested at the base of Sauropodomorpha, although not being the first sauropodomorph to arrive in Europe. The mid-Norian stage of the Late Triassic of Germany bore numerous fossils of the first European sauropodomorphs, such as *Efraasia minor* Huene, 1932 from Nordwürttemberg, *Ruehleia bedheimensis* Galton, 2001 from Schleusingen and *Plateosaurus* Meyer, 1837, the most abundant sauropodomorph from Germany (see section 1.2 in this thesis) (Fig. 1.2). *Efraasia* and *Ruehleia* are usually recovered in phylogenetic analyses as more derived sauropodomorphs than *Thecodontosaurus*, but outside Plateosauria (see section 1.3 of this thesis). Both *Efraasia* and *Ruehleia* were large, possibly bipedal herbivores and mark the rise of sauropodomorphs at around 216 Ma in Europe. The events that made possible the migration from Gondwana to Laurasia

are still unclear. However, some authors argue for environmental changes such as an increase in humidity that allowed the crossing of the dry central Pangea at around 218 to 215 Ma (Kent & Clemmensen, 2021).

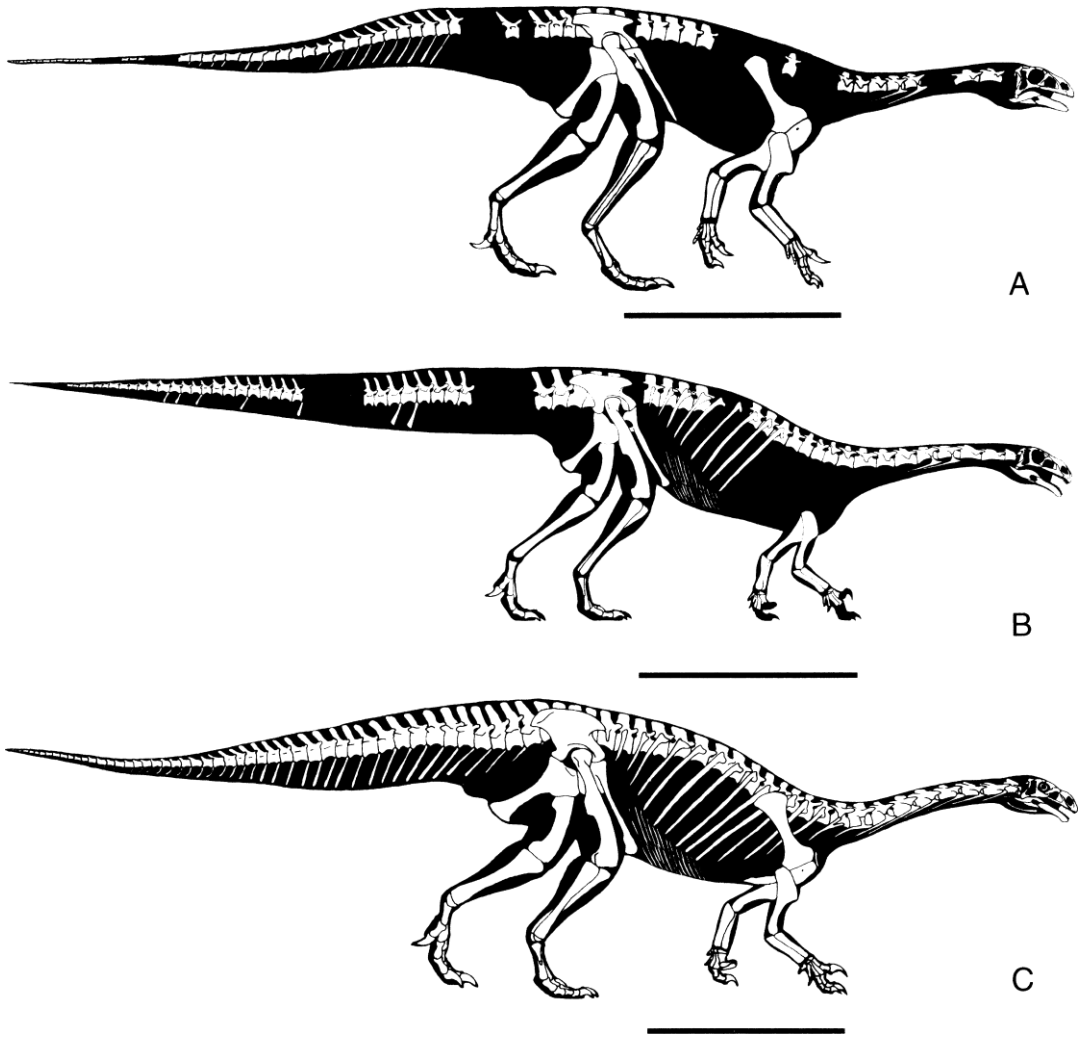

Figure 1.2 - Reconstructed skeletons of the Löwenstein Formation, Late Triassic of Germany, sauropodomorphs. A, *Efraasia minor* based upon specimens SMNS 11838, 12354 and 17928; B, *P. gracilis* based on SMNS 5175, GPIT 18392 and 18318a; C, *P. trossingensis* based on SMNS 13200. From Yates, 2003.

1.2 The sauropodomorph *Plateosaurus*

1.2.1 The taxonomy of *Plateosaurus*

Five years before Richard Owen coined the term Dinosaur in 1842, *Plateosaurus engelhardti* was reported, being the first dinosaur to be scientifically named outside England (Yates, 2003). But although being reported by Meyer in 1837, it took almost 20 years for the *Plateosaurus engelhardti* holotype to be described and illustrated (Meyer, 1855). The described specimen consisted of complete vertebrae

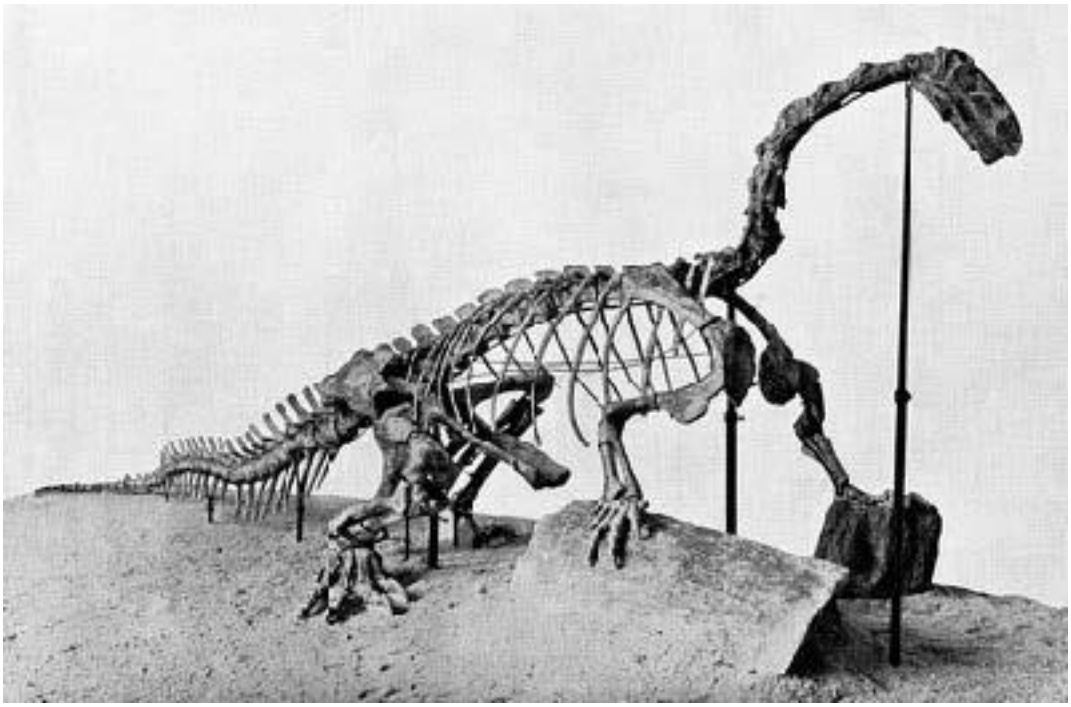

Figure 1.3 - Skeletal mount of *P. trossingensis* holotype, SMNS 13200 (from Moser, 2003).

and limb bones. Three bones initially attributed to the holotype of *Plateosaurus* were then found to be from a different individual due to their large sizes (Huene, 1908). Galton, (1984) further excluded two skeletal remains from the holotype, one pertaining to a proganochelyid turtle and one to a theropod dinosaur. The autapomorphic characters of *P. engelhardti* were revised and include the second sacral rib originating posteriorly to the centrum, and the straight distal part of the femur in anteroposterior view (Galton, 2000; Moser, 2003).

Numerous specimens were since assigned to the genus *Plateosaurus*. Such is the case of *Plateosaurus ingens* Galton, 1986, formerly *Gresslyosaurus ingens* Rütimeyer, 1856, *Plateosaurus erlenbergiensis* Huene, 1905, *Plateosaurus gracilis* Yates, 2003, formerly *Sellosaurus gracilis* Huene, 1908, and *Plateosaurus trossingensis* Fraas, 1913. The validity of these specimens has been debated over the last few decades, with one main alternative of *Plateosaurus* classification being the most accepted. Most authors recognize three valid species, *P. gracilis* as a sister taxon of *P. engelhardti* and *P. ingens* (Yates, 2007b, 2010; Galton & Kermack, 2010; Apaldetti *et al.*, 2011). The material assigned to *P. ingens* is under preparation for a redescription, as it possibly pertains to a new genus (Rauhut *et al.*, 2020). The main issue with *Plateosaurus* taxonomy arises due to the fragmentary nature of the holotype. Galton (2012) proposed that the specimen SMNS 13200 (Fig. 1.3), assigned to *P. trossingensis*, should be the neotype of *Plateosaurus*, which was accepted by the decision of the International Commission on Zoological Nomenclature (ICZN, 2019).

The specimen SMNS 13200 was recovered from the lower bonebed at the Obere Mühle location at Trossingen, Germany. It was first reported by Fraas, (1913) and then fully described and figured by Huene (Huene, 1926). The holotype consists of an almost complete skeleton with skull. Further cranial materials of *P. trossingensis* were recovered from Trossingen, Halberstadt and Frick, and were described and pictured on different occasions (Galton, 1985, 1986, 2000; Yates, 2003; Prieto-Márquez & Norell, 2011; Lallensack *et al.*, 2021). Yates, (2003) gave the emended diagnosis for *P. trossingensis* that includes four cranial autapomorphies: a broad lateral sheet of bone of the lacrimal covering the posterodorsal corner of the antorbital fenestra; a short jugal with a dorsoventrally deep suborbital bar; a centrally located, ventral, peg-like process of the palatine; and a deep interbasipterygoid septum, with paired median processes, which fills the whole space between the basipterygoid processes. The newly described skulls from Frick were identified by these autapomorphies, except for the palatine, which could not be observed (Lallensack *et al.*, 2021). *P. trossingensis* differs from the stratigraphically older *P. gracilis* as the latter possesses a pair of sharp-rimmed fossae behind the basal tubera in the basioccipital and no lateral sheet of bone on the lacrimal. The *Plateosaurus* species share the cranial autapomorphies of five (or more) premaxillary teeth, a broad antorbital fossa (however, this feature is highly variable among specimens, as showed in Lallensack and collaborators, 2021) and a nasal longer than half the skull roof length (Yates, 2003; Galton & Upchurch, 2004; Prieto-Márquez & Norell, 2011; Lallensack *et al.*, 2021) (Fig. 1.4).

1.2.2 Plateosaurus paleobiology

Although its taxonomy is still under debate, *Plateosaurus* is one of the best-known and studied Triassic dinosaur genera (Galton & Upchurch, 2004; Mallison, 2010a; Lallensack *et al.*, 2021). This sauropodomorph was recovered originally from the Late Triassic (Norian) of Trossingen (Germany), by dr. Johann Friedrich Phillip Engelhart in 1834, and then was found in other parts of Central and North Europe, i.e., Germany, France, Switzerland, and Norway; (Sander, 1992; Moser, 2003; Galton & Upchurch, 2004; Hurum *et al.*, 2006; Mallison, 2010b; Prieto-Márquez & Norell, 2011; Nau *et al.*, 2020), and Greenland (Jenkins *et al.*, 1994; Marzola *et al.*, 2018; Kent & Clemmensen, 2021).

Plateosaurus bonebeds were found in Trossingen and Halberstadt, both from Germany, and Frick, in Switzerland. The abundance and completeness of *Plateosaurus* material in an upright posture and buried feet have been interpreted as size-selective miring muds (Sander, 1992). These assemblages, however, are biased towards adult specimens, with few juveniles and subadults described so far (Hofmann & Sander, 2014; Nau *et al.*, 2020; Lallensack *et al.*, 2021). This resulted in the first material

of a juvenile *Plateosaurus* to be formally described over a century after the first reports of the genus (Hofmann & Sander, 2014; Nau *et al.*, 2020; Lallensack *et al.*, 2021). The *Plateosaurus* bonebeds from Germany have been excavated since the first half of the 20th century, whereas excavations at the Frick bonebed in Switzerland began in 1976 (Schoch & Seegis, 2014; Lallensack *et al.*, 2021).

The skeleton of *Plateosaurus* was digitized on different occasions, being used in works to determine the paleobiology of this taxon. The skull MB.R.1937 of an adult *P. trossingensis* was scanned using computed tomography (CT-scan), segmented and retrodeformed to study its myology and biomechanics (Button *et al.*, 2016) (Fig. 1.5), whereas the specimen MB.R.5586-1 was CT-scanned and segmented for the reconstruction of its brain anatomy (Bronzati *et al.*, 2017; Ballell *et al.*, 2020a). The post-cranium of the specimen GPIT 1 of *P. trossingensis* was CT-scanned and segmented to create a virtual mount of the specimen and study its locomotion capabilities and body mass (Mallison, 2010a, 2010b).

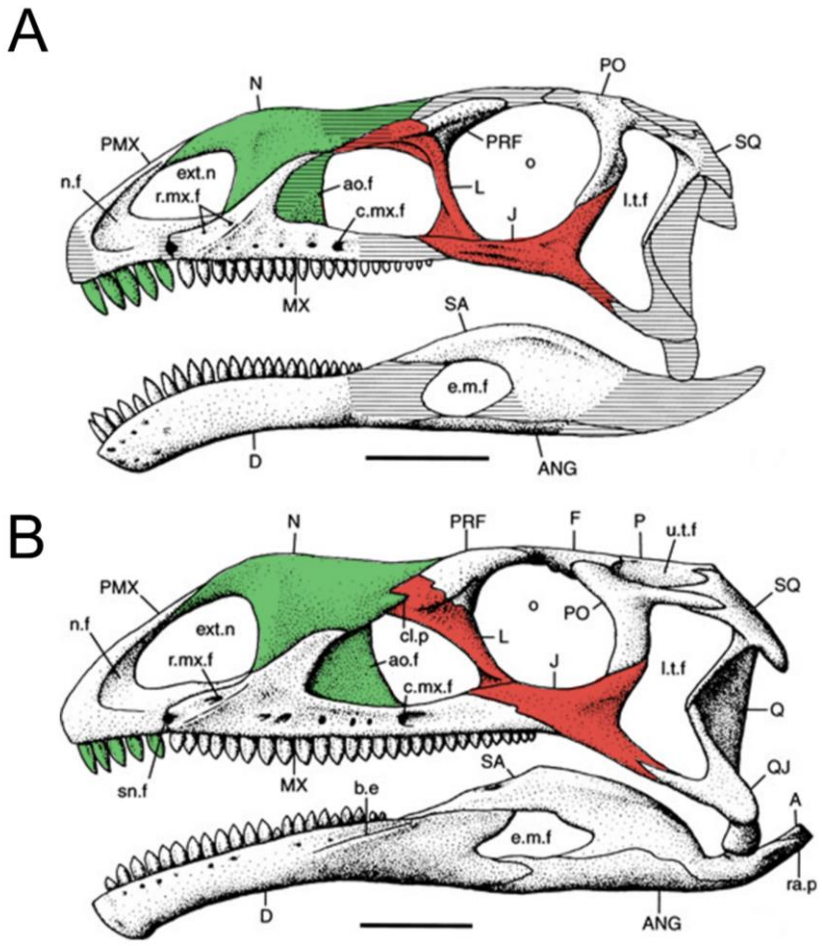

Figure 1.4 - Skulls of *Plateosaurus*. Skull of *P. gracilis* based on GPIT 18318a and the skull of *P. trossingensis* based on specimen SMNS 13200. In green: shared autapomorphies for *Plateosaurus*. In red: differences between both *Plateosaurus* species. Scale bars = 50 mm. Modified from Yates, 2003.

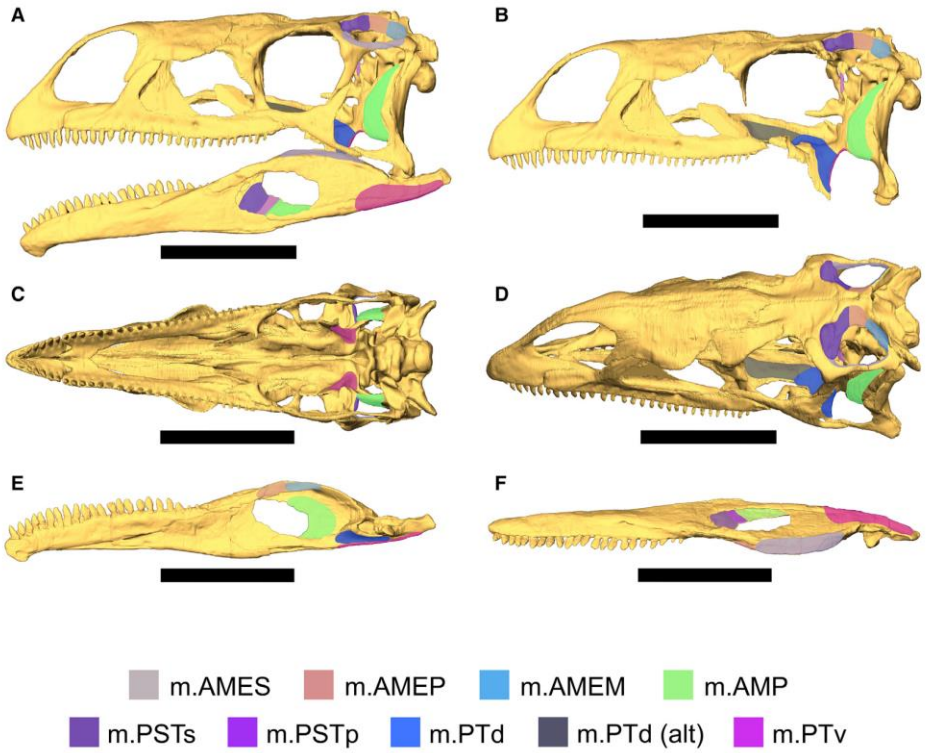

Figure 1.5 - *P. trossingensis* skull and jaw adductor reconstruction based on specimen MB.R.1937. Modified from Button *et al.*, 2016.

The leaf-shaped maxillary and dentary teeth of *Plateosaurus* were adapted either to an herbivore or omnivore diet, due to its coarse serrations on both mesial and distal margins of the crown and mesiodistally expanded crowns (Barrett & Upchurch, 2007; Nesbitt, 2011; Müller *et al.*, 2018b). The long snout and tooth row of *Plateosaurus* suggests a speedy jaw closure (Button *et al.*, 2016, 2017). This feature is not important for herbivory, however, facilitates a facultative omnivore diet for the taxon. This would place the obligatory herbivory at the base of Sauropoda, as suggested by some authors (Barrett *et al.*, 2010; Lautenschlager *et al.*, 2016; Button *et al.*, 2016, 2017). The endocast of *Plateosaurus* was firstly illustrated in Galton, 1985 and later segmented. A reduction of the floccular fossae lobe (FFL) was observed in *Plateosaurus* and is usually associated with herbivory (Bronzati *et al.*, 2017).

Mallison, (2010a, 2010b) tested the various hypothesis on the gait, posture and body mass estimation of *Plateosaurus* using the digitized skeleton GPIT 1 from Trossingen. Up until that point, the locomotion of *Plateosaurus* was debated by many authors, ranging from a digitigrade, obligatory bipedal locomotion (Huene, 1908, 1926), to plantigrady, obligatory quadrupedal gait (Jaekel, 1910; Fraas, 1913; Sullivan *et al.*, 2003), to facultative bipedality (Galton, 1976, 2000; Moser, 2003). *Plateosaurus* skeleton offers extensive support for a bipedal gait, whereas a quadrupedal gait would

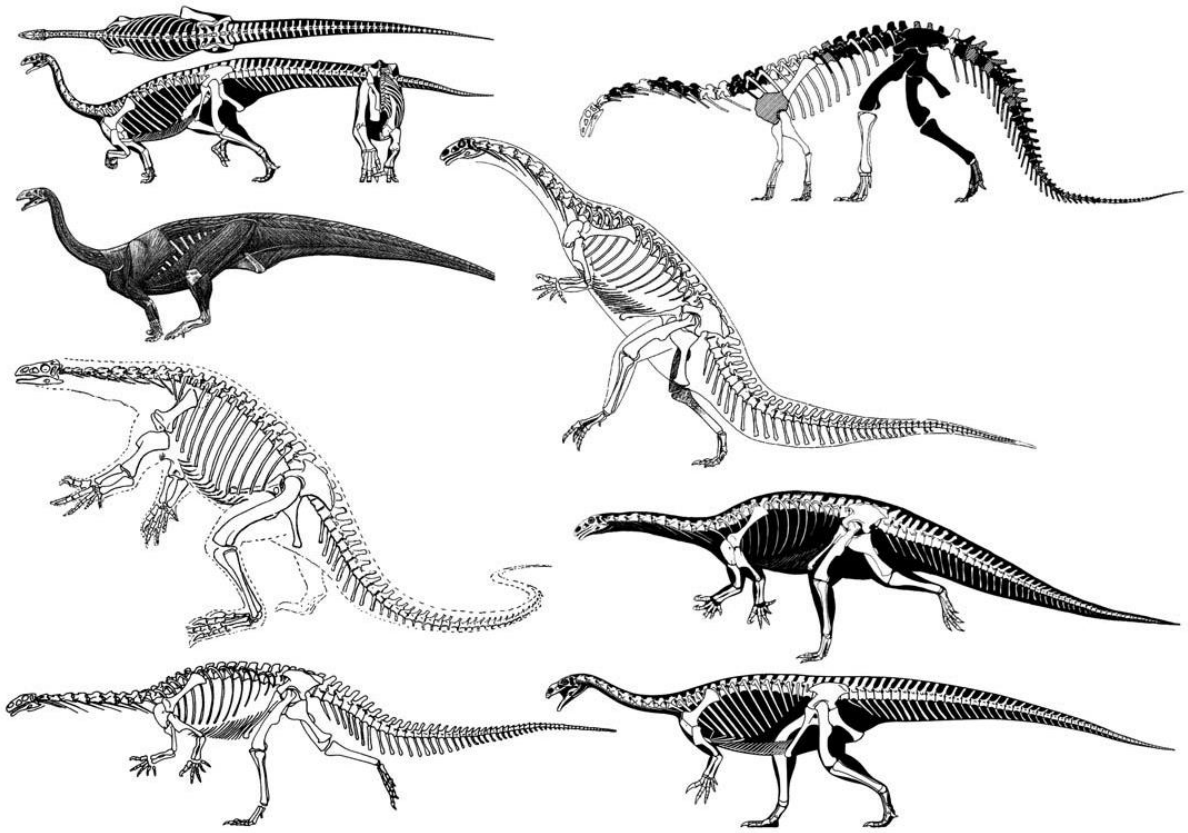

Figure 1.6 - Skeletal reconstruction of *Plateosaurus* through time. Modified from Mallison, 2010b.

result in locomotive disadvantages (Mallison, 2010a). The range of motion of forelimbs and the proper articulation of the skeleton agree for an obligatory bipedality locomotion for *Plateosaurus* (Mallison, 2010a, 2010b). Mallison, (2010b) compared the skeletal poses proposed by earlier authors to his findings, and brought a yet up-to-date reconstruction of a *Plateosaurus* skeleton (Fig. 1.6). The body-mass estimations applied in Mallison, (2010a) range from 430 kg for the smallest adult *Plateosaurus* (around 4.8 m in total length) and over 4,000 kg for the largest (around 10 m in total length). This agrees with the proposed body mass by Sander and Klein, (2005). It is worth mentioning that this large range of sizes for adult *Plateosaurus* was recovered through histology of specimens found in the *Plateosaurus* bonebeds (Sander & Klein, 2005; Klein & Sander, 2007). This attests to high developmental plasticity in *P. trossingensis*, which was then confirmed by its skull material (Lallensack *et al.*, 2021).

The ontogeny of *Plateosaurus* is yet understudied, as most specimens recovered so far represent fully grown adults (Sander, 1992; Sander & Klein, 2005). The minimum age for a fully grown adult was recovered at 12 years, whereas the youngest specimen sampled was 9 years old (Sander & Klein, 2005). The first juvenile specimen of *P. trossingensis* from Frick was described by Hofmann and Sander, (2014). The osteological immaturity of *Plateosaurus* was attested by the lack of fusion of the vertebral neural arches to the centra (Brochu, 1996; Hofmann & Sander, 2014; Nau *et al.*, 2020). As mentioned

Figure 1.7 - Skeletal reconstruction of the early-stage juvenile of *P. trossingensis* MSF 15.8B. From Nau *et al.*, 2020.

above, the size of *Plateosaurus* has a poor correlation with age (Sander & Klein, 2005; Klein & Sander, 2007). Both the cranial and postcranial skeleton of *Plateosaurus* is conservative throughout ontogeny, with minor changes observed so far (Lallensack *et al.*, 2021) (Fig. 1.7). The cranial ontogenetic differences are the unossified tip of the premaxilla in juveniles, the reduced gap of the first premaxillary tooth and the tip of the premaxilla, and the dentary tooth count (being less than 20 dentary teeth in juveniles) (Lallensack *et al.*, 2021). Other characters that may be associated with the ontogeny of *Plateosaurus* are the elongation of the skull throughout ontogeny, the posterior deflection of the dorsal process of the premaxilla and a proportionally larger orbit in immature specimens (Lallensack *et al.*, 2021).

1.3 Plateosauridae

The interrelationships of basal sauropodomorphs and the phylogenetic relationship of *Plateosaurus* are receiving increasing attention with the novel taxa described for the Late Triassic of Brazil, South Africa and Europe in the past few decades but it is still plagued by issues that are yet to be resolved (Yates, 2007a; McPhee *et al.*, 2020; Müller, 2020; Rauhut *et al.*, 2020). McPhee *et al*., (2020) listed the major issues with basal sauropodomorph taxonomy, such as (1) disagreeing and poorly understood character conceptions; (2) fragmentary material and missing data for key specimens; (3) lack of complete descriptions and access to several Chinese taxa; and (4) the inclusion of chimeric specimens as operational taxonomic units (OTUs). Among the first attempts to assess *Plateosaurus* interrelationships was the phylogenetic analysis done by (Yates, 2007a). In his work, *Plateosaurus* was recovered at the base of Plateosauria, defined as the least inclusive clade containing *Plateosaurus* and Sauropoda (*sensu* Yates, 2007a) (Fig. 1.8.). The clade that includes species closer to *Plateosaurus trossingensis* than to Sauropoda was referred as Plateosauridae in the same work (Yates, 2007a) and is recovered in most cladistic analyses with *Unaysaurus* as the sister taxon to *Plateosaurus* (Yates, 2007a; Apaldetti *et al.*,

2011; McPhee *et al.*, 2015, 2020; Rauhut *et al.*, 2020). However, this comes as no surprise as the dataset used to assess non-sauropod sauropodomorphs usually derives from the work of Yates, (2007a).

McPhee *et al*., (2020) tested the position of *Unaysaurus* as the sister taxon to *Plateosaurus* and, although relatively constant in his analysis, the clade Plateosauridae is only supported by two unambiguous

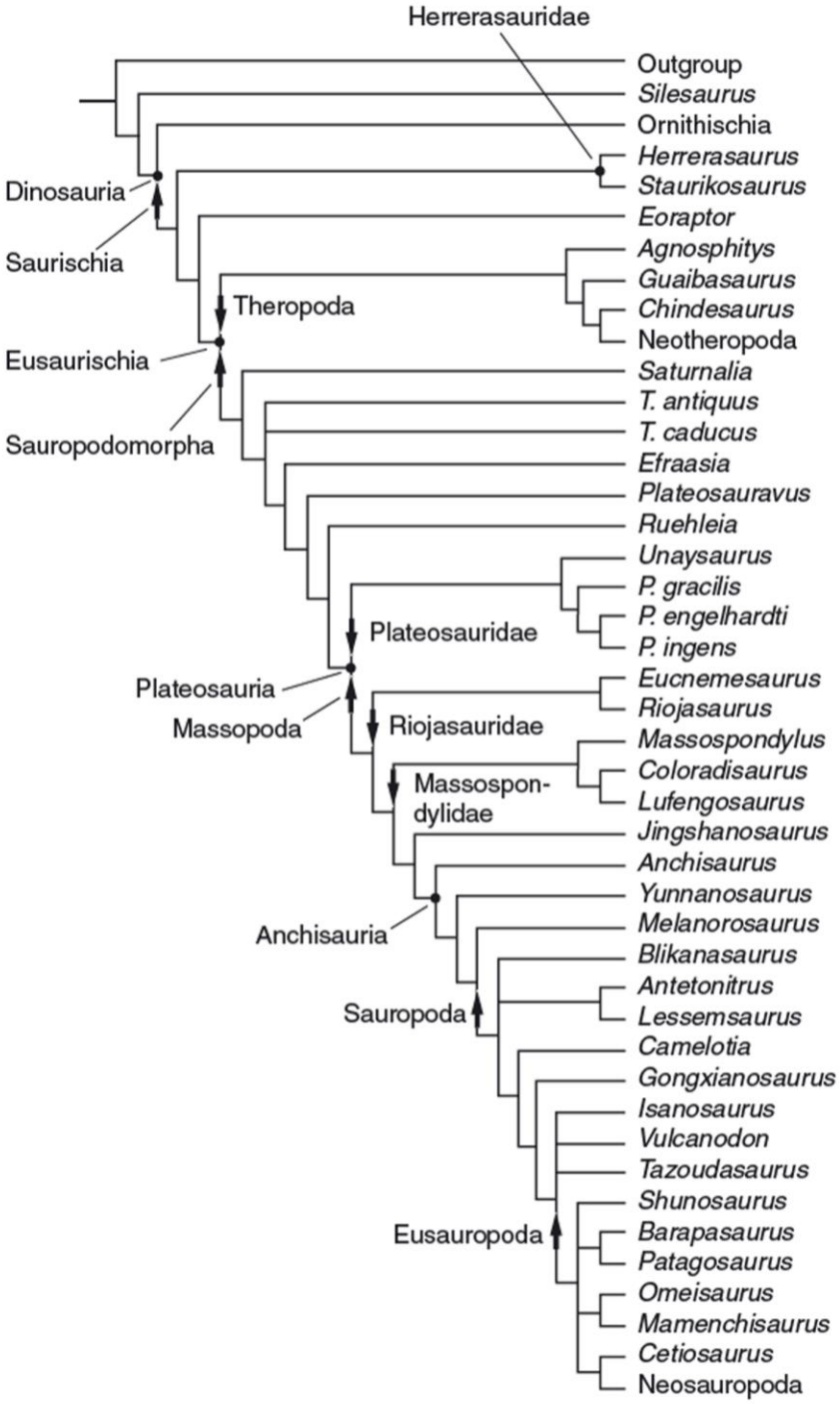

Figure 1.8 - Strict-consensus tree of Sauropodomorpha. Modified from Yates, 2007.

synapomorphies of the humerus: a non-convex humeral head [character 220, state (1)] and length of humerus being three times that of the transverse width of the distal condyles [226 (0)]. This latter, however, is shared with several other non-sauropod taxa. The introduction of *Macrocollum* in recent phylogenetic analyses placed *Unaysaurus* as a sister taxon to *Macrocollum*, both forming with the Indian sauropodomorph *Jaklapallisaurus asymmetrica* Novas *et al.*, 2010 the clade Unaysauridae (Müller *et al.*, 2018b; Müller, 2020) (Fig. 1.9). Unaysauridae was first recovered as a sister clade to Plateosauridae (in his analyses composed only of the *Plateosaurus* species) and then shifted to a more derived position inside of Massopoda (*sensu* Yates, 2007a) (Müller *et al.*, 2018b; Müller, 2020). Although the close relationship of the coeval sauropodomorphs from Brazil is expected, the validity of Unaysauridae suffers from the missing data and fragmentary nature of specimens. For instance, one synapomorphy of unaysaurids is related to the astragalus and cannot be observed in *Unaysaurus*,

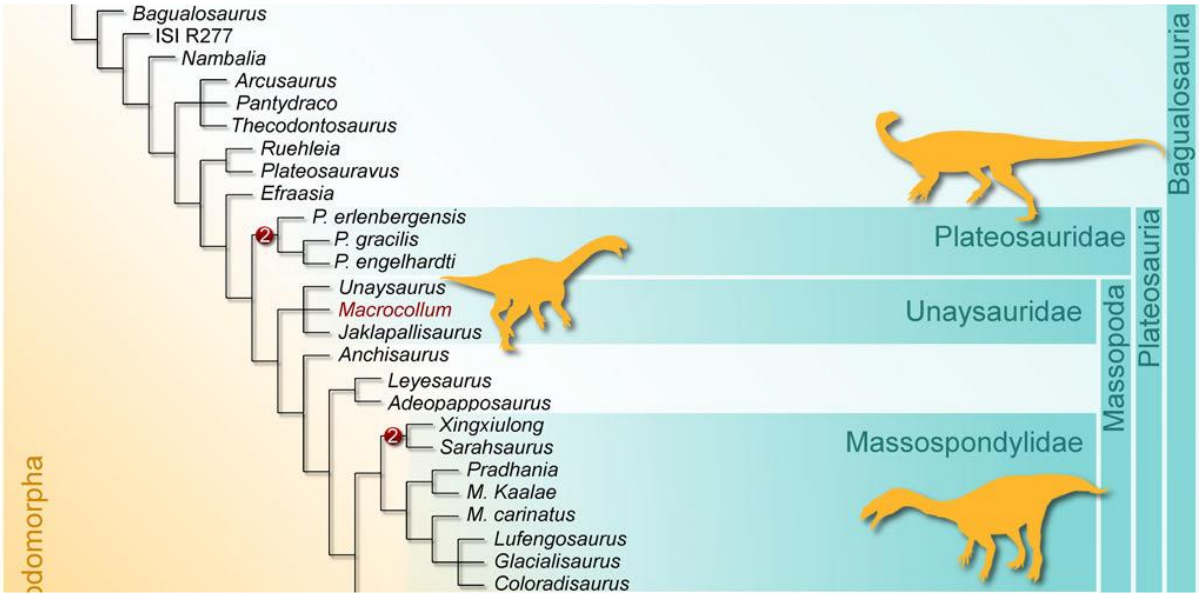

Figure 1.9 - Reduced strict-consensus tree of Sauropodomorpha, showing the different hypothesis for the interrelationships of Plateosauridae and Unaysauridae. Modified from Müller, 2020.

whereas a second synapomorphy, the presence of a promaxillary fenestra, cannot be observed in *Jaklapallisaurus*. This goes to show that the relationships of this part of the sauropodomorph phylogeny are unresolved.

1.4 Greenland sauropodomorphs

Jenkins *et al.*, (1994) reported for the first time the presence of a basal sauropodomorph in Late Triassic rocks (Norian) of Fleming Fjord Group (formerly Fleming Fjord Formation, see Clemmensen *et al.*, 2020), of Jameson Land, central East Greenland. In their work, Jenkins and colleagues, (1994) briefly described a skull (NHMD 164741, formerly MCZ Field no. 61/91G) from the Malmros Klint Formation

(formerly Malmros Klint Member, see Clemmensen *et al.*, 2020). This specimen was collected in Summer 1991 by a team lead by Farish Jenkins. The specimen was assigned to *Plateosaurus engelhardti* (=*P. trossingensis*) due to its dental structure and number of teeth, a single dorsal process of the premaxilla, and a Y-shaped quadratojugal. However, the lack of a thorough description renders the precise allocation of this specimen to *P. trossingensis* as tentative, at most, and recent studies advise that this classification should be taken with caution (Marzola *et al.*, 2018). Also, the Norian sauropodomorphs described in the past few decades added new information that should be considered for the taxonomy of these specimens.

To help understand these issues, new specimens were collected from the same locality. At least three new specimens were recovered and are yet to be formally described. Among them are an almost complete skull of a juvenile sauropodomorph (NHMD 164758, formerly 1/G95 or 1/95/G, collected in 1995) and two unpublished individuals with cranial and postcranial material (NHMD 164734, formerly 4.88.G and GM.V 2013-683, collected in 2013; and NHMD 164775, a yet unprepared specimen collected in 2012). Specimens NHMD 164741 and NHMD 164758 were recovered from the same locality, the north side of Macknight Bjerg, Jameson Land, NHMD 164734 comes from Lepidopteriselv, Jameson Land, and NHMD 164775 from the "Iron Cake" Site, Wood Njerg - Macknight Bjerg, Jameson Land, all ranging from the late Norian to early Rhaetian in age (Clemmensen *et al.*, 2020; Marzola *et al.*, 2018) or restricted to late Norian (Kent & Clemmensen, 2021).

The skulls NHMD 164741 and NHMD 164758 are under preparation at Museu da Lourinhã, Portugal, and were digitized using µCT-Scanning in Burgos, Spain. Both specimens consist of almost complete and partially articulated skulls (the latter with postcranial material in storage at GeoCenter Møns Klint, Denmark) of different ontogenetic stages, with NHMD 164741 being associated with a sub-adult whereas NHMD 164758 as an early juvenile. NHMD 164734 (Fig. 1.10) is currently exhibited at GeoCenter Møns Klint and consists of an almost complete skeleton with skull material (i.e., maxilla, lacrimal, postorbital, part of the occipital region, dentary, and other mandibular bones) and an almost complete vertebral series, girdles, and limbs. NHMD 164775 consists of a partially prepared rib cage and cranial and postcranial material under preparation at Dino-Park Münchehagen, Germany.

Figure 1.11 - Greenland sauropodomorph NHMD 164734. Picture by Octávio Mateus.

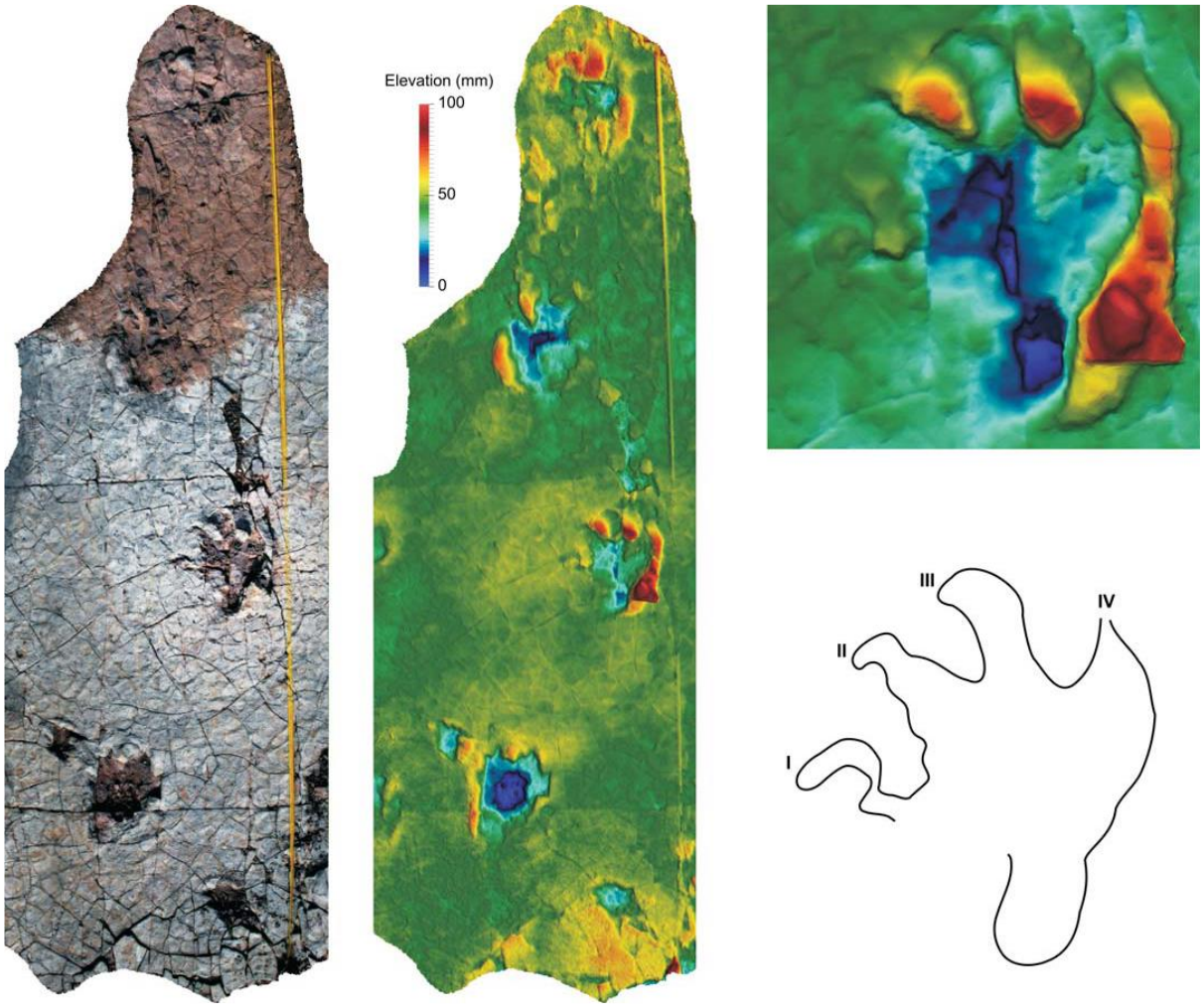

Figure 1.10 - Sauropodomorph trackway S3 from "Track Mountain", Jameson Land, East Greenland. The *Evazoum* isc. trackway S3 was attributed to a non-sauropod sauropodomorph. From Lallensack *et al.*, 2017.

A total of three trackways containing two ichnotaxa assigned to Sauropodomorpha were described for the Late Triassic of Jameson Land (Jenkins *et al.*, 1994; Clemmensen *et al.*, 2016; Lallensack *et al.*,

2017). These trackways come from the "Track Mountain", Tait Bjerg Member, the uppermost part of Fleming Fjord Formation, and are relatively younger (possibly early Rhaetian) than the skeletal remains found on lower levels of the same formation. Two trackways (S1 and S2) were assigned to *Eosauropus* isp. Lockley *et al.*, 2006a. These trackways are the largest known for this morphotype and may be assigned to sauropod dinosaurs, extending the presence of the group to the Late Triassic and being the first evidence of sauropods in Greenland (Lallensack *et al.*, 2017; Marzola *et al.*, 2018). However, Lallensack *et al.*, (2017) does not discard the possibility of a non-sauropod sauropodomorph with a quadrupedal gait being able to leave these footprints behind. Trackway S3 (Fig. 1.11) was assigned to the ichnotaxon *Evazoum* isp. Lockley *et al.*, 2006b and was made by a bipedal animal, possibly a non-sauropod sauropodomorph due to several features (i.e., pes rotated slightly inwards anteriorly, heel-region constriction, more protruded digit III, medially directed claw impressions and lack of digit V impression) (Lallensack *et al.*, 2017). These occurrences of sauropodomorphs are among the first in Europe and are the first for the northernmost part of Laurasia with a paleolatitude of 43ºN at 215 Ma, according to magnetostratigraphy (Kent & Clemmensen, 2021). The German Löwenstein Formation age ranges from circa 217 Ma to 212.5 Ma based on biostratigraphy, marking the first occurrence of *Plateosaurus* possibly 2 million years before the Greenland sauropodomorphs (Bachmann & Kozur, 2004).

1.5 Geology of Malmros Klint Formation

The Jameson Land Basin located in central East Greenland is known for its tetrapod-bearing sediments ranging from the Middle to Late Devonian to the Late Jurassic (Jenkins *et al.*, 1994; Marzola *et al.*,

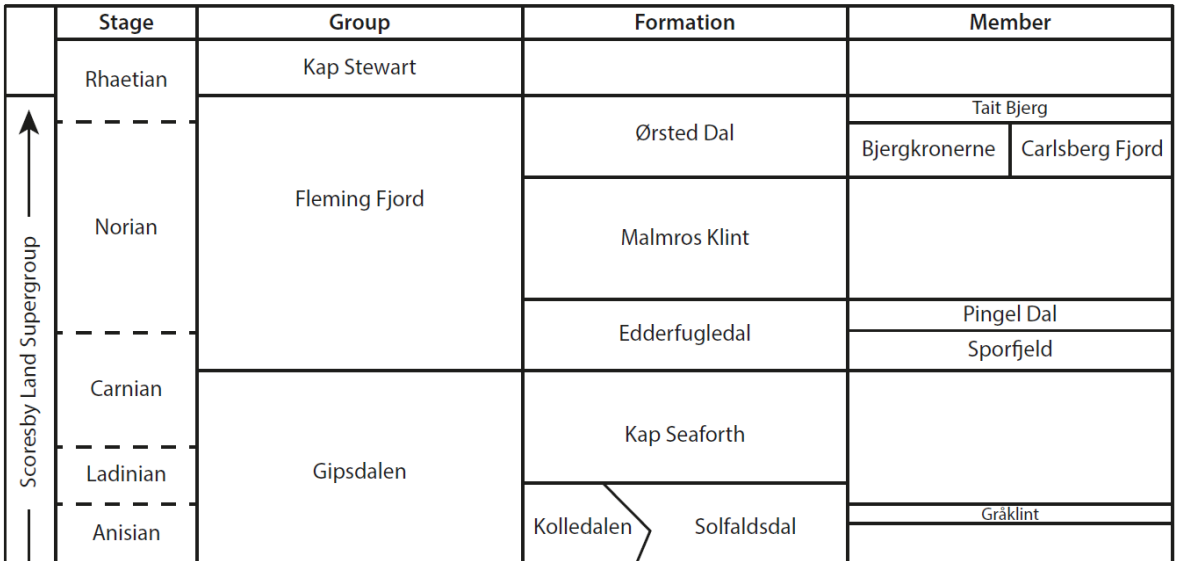

Figure 1.12 - Lithographical subdivision of the Triassic sedimentary rocks of Jameson Land Basin, central East Greenland. Modified from Clemmensen *et al.*, 2020.

2018). The Late Triassic is represented by the Fleming Fjord Group and interpreted as a lacustrine environment with fluvial influences from western source areas (Clemmensen, 1980; Jenkins *et al.*, 1994; Clemmensen *et al.*, 1998, 2016, 2020; Decou *et al.*, 2017). During the Late Triassic (Norian to Rhaetian), the deposits of Fleming Fjord Group were located much south from its current position, at around 43º N (against the current 71º N) (Kent & Tauxe, 2005). This paleolatitude corresponded to the northern part of Pangea in a transitional zone between the supercontinent dry interior and the more humid periphery (Clemmensen *et al.*, 1998). The Fleming Fjord Group was later established as Fleming Fjord Formation Perch-Nielsen *et al.*, 1974 to raise the tetrapod-bearing beds to the formation status (Clemmensen *et al.*, 2020). Three formations are included in the Group: the bottom Edderfugledal Formation, the middle Malmros Klint Formation, and the top Ørsted Dal Formation (Clemmensen *et al.*, 2020) (Fig. 1.12).

Malmros Klint Formation type section is about 200 m thick and located in Malmros Klint (Fig. 1.13). The formation thickness ranges from 220 m around Kap Biot to its shallowest point of 45 m at Pictet Bjerge. This formation is categorized by its brownish to greyish red mudstones and fine-grained sandstone (Fig. 1.13). The Malmros Klint Formation bears a diverse vertebrate fauna of phytosaurs, amphibians, fishes and sauropodomorph dinosaurs (Marzola *et al.*, 2018). This latter was recovered at a fossil-rich site for sauropodomorph material in the middle part of Malmros Klint Formation, at 82 m in the stratigraphic log. The Late Triassic of the Formation was dated to the late Norian stage, around 214 Ma, through cycle stratigraphy and magnetochronology (Clemmensen *et al.*, 1998; Kent & Clemmensen, 2021). Its paleoenvironment during the Triassic represents a playa lake or mudflat deposits that dried seasonally, with an apparent accumulation rate around 55 mm/ka (Clemmensen *et al.*, 1998; Decou *et al.*, 2017).

1.6 Objectives

The present work focuses on the reassessment and thorough description of specimen NHMD 164741, regarded as *P. engelhardti* (=*P. trossingensis*) by Jenkins *et al.*, (1994), and the description of specimen NHMD 164758, a yet undescribed skull from the same locality, using µCT-Scanning for the evaluation of hard to access features. It is also in the scope of this work to include said specimens in the most recent phylogenetic datasets for the group, i.e., Rauhut *et al.*, (2020). The redescription will serve to test if the Greenland sauropodomorphs: a) represent a single taxon; b) represent a different taxon than formerly assigned and is either monospecific or not, and c) describe ontogenetic differences for the Greenland sauropodomorphs.

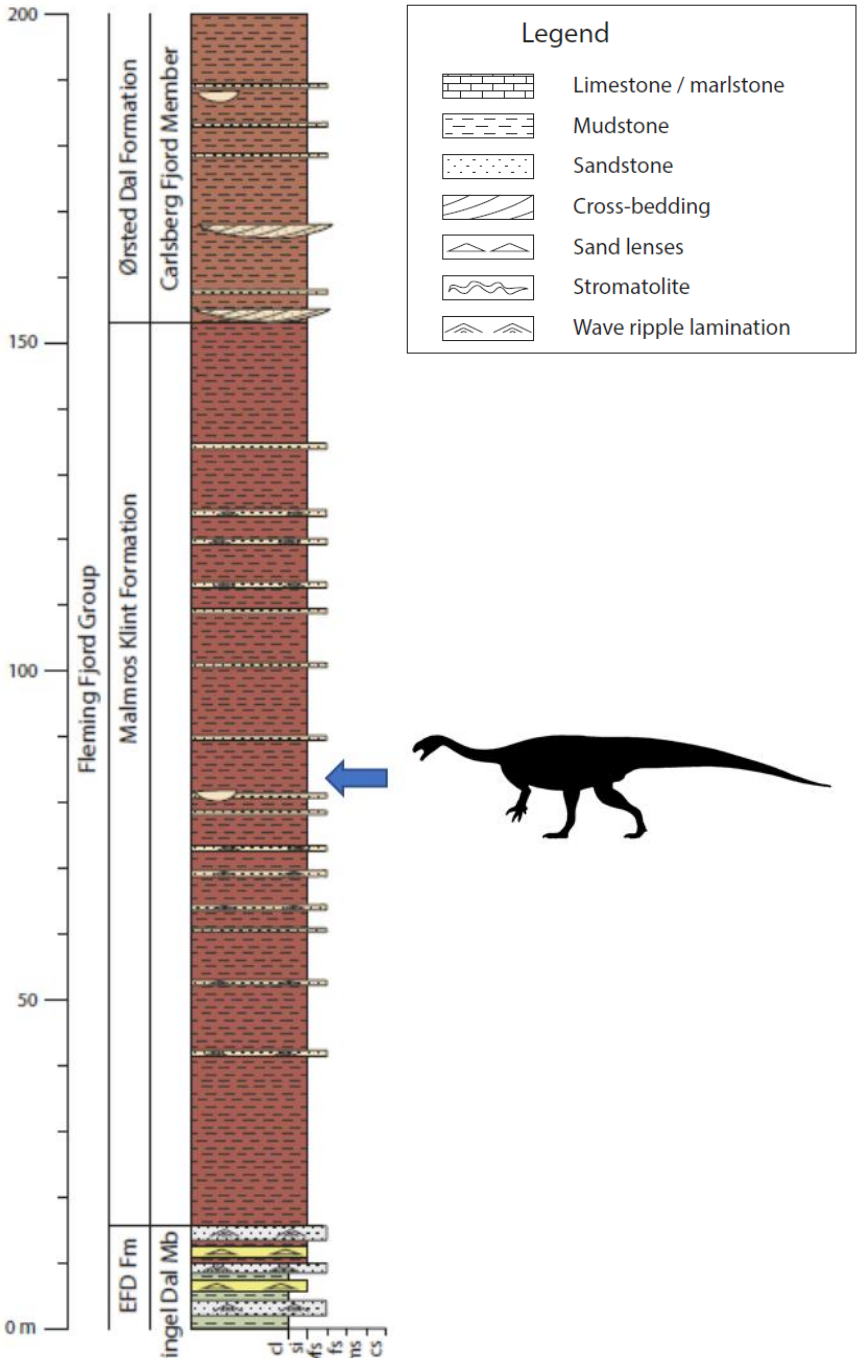

Figure 1.13 - Stratigraphic log of Fleming Fjord Group, Jameson Land Basin, central East Greenland. The sauropodomorph specimens layer is marked by the silhouettes and blue arrow (around 82 m). Modified from Clemmensen *et al*. 2020.

2 Material and Methods

2.1 Specimens in this study

The specimens NHMD 164741 and NHMD 164758 (Fig. 2.1) comprise two skulls, mandible and teeth, recovered from the Late Triassic (Norian) rocks of Malmros Klint Formation, Jameson Land, East Greenland. NHMD 164741 (Fig. 2.1 A) was collected in 07/27/91 by William W. Amaral, William R. Downs, Stephen M. Gatesy, Neil H. Shubin and Niels Bonde, at the Macknight Bjerg site of coordinates 71°23.010′ N, 22°34.114′ W. NHMD 164758 (Fig. 2.1 B) was collected in 1995 at 71°22.993′ N, 22°33.972′ W. Postcranial elements of probably the same individual were collected in the expedition of 2012 but are not described here. These specimens are temporarily deposited at Museu da Lourinhã (ML) for preparation, which was undertaken before the present work. Specimen NHMD 164758 was broken into at least two pieces, separating the anterior and posterior regions of the skull, and glued back together using Paraloid® B-72 dissolved in acetone (equal parts/50%). The specimens were compared to a list of basal sauropodomorph dinosaurs described in the literature (Table 1). In the results section, each specimen is described and compared, providing its systematic identification, and justify the latter in a remarks section by comparative notes.

Table 1 - List of specimens used in this study for purposes of comparative anatomy.

Taxon	**Specimen(s)**	**Source(s)**
Bagualosaurus agudoensis	UFRGS-PV-1009-T	Pretto *et al.*, 2019
Buriolestes schultzi	CAPPA/UFSM 0035; ULBRA-PVT280	Cabreira *et al.*, 2016; Müller *et al.*, 2018a, 2021
Coloradisaurus brevis	PVL 3967	Bonaparte, 1978; Apaldetti *et al.*, 2014
Efraasia minor	SMNS 12667	Galton, 1985; Yates, 2003; Bronzati & Rauhut, 2018
Leyesaurus marayensis	PVSJ 706	Apaldetti *et al.*, 2011
Lufengosaurus huenei	IVPP V15	Barrett *et al.*, 2005
Macrocollum itaquii	CAPPA/UFSM 0001a; CAPPA/UFSM 0001b	Müller *et al.*, 2018b; Müller, 2020
Massospondylus kaalae	SAM-PK-K1325	Barrett, 2009
Ngwevu intlokoi	BP/1/4779	Chapelle *et al.*, 2019
Pampadromaeus berberenai	ULBRA-PVT016	Langer *et al.*, 2019
Plateosaurus trossingensis	AMNH FARB 6810; GPIT-PV-30704; MB.R.1937; MSF 07.M; MSF 08.M; MSF 08.H; MSF 09.2; MSF 11.4; MSF 12.3; MSF 15.4; MSF 15.8; MSF 16.1; MSF 17.4; MSF 23; MSF 33; NAAG_00011238; NAAG_ 00011239; SMA 09.1; SMNS 12949; SMNS 12950; SMNS 13200; SMNS 52968	Galton, 1986, 2001; Yates, 2003; Prieto-Márquez & Norell, 2011; Lallensack *et al.*, 2021
Plateosaurus gracilis	GPIT 18318a	Yates, 2003

Saturnalia tupiniquim	MCP 3845-PV	Langer *et al.*, 1999; Bronzati *et al.*, 2019
Thecodontosaurus antiquus	BRSMG C4529; YPM 2192	Benton *et al.*, 2000; Ballell *et al.*, 2020a, 2020b
Unaysaurus tolentinoi	UFSM 11069	Leal *et al.*, 2004; McPhee *et al.*, 2020

Figure 2.1 - Greenland sauropodomorph specimens NHMD 164741 and NHMD 164758. NHMD 164741 in left lateral view (A) and NHMD 164758 in left lateral view (B).

2.2 Digitization and image treatment

The specimens were digitized using both photogrammetry and µCT-Scanning, allowing the creation of a texturized 3D model as wells as observations of internal structures. The photogrammetry method used was derived from the Walk-Around Method (Mallison & Wings, 2014) using a Nikon 3500d camera. The pictures were taken from the full 360º of each specimen with a 10º interval between each picture. The 3D photogrammetry models were created using Agisoft Metashape v.1.71. The first alignment was set to High accuracy, then the point cloud was cleaned manually and using gradual selection, then a dense point cloud was generated set to High quality. The meshes were generated using the High face count setting and textures were created in 7680/1 Texture size/count setting.

Both specimens were CT-scanned at CENIEH, Burgos, Spain, using MicroCT V|Tome|X s 240 by GE Sensing & Inspections Technologies Phoenix X-Ray. This resulted in a high-resolution stack of 2,848 .tiff images of 0.08999975 mm voxel size and 1922x562x2636 resolution (NHMD 164741) and a stack of 2,821 .tiff images of 0.0679998 mm voxel size and1810x756x2821 resolution (NHMD 164758). The segmentation was carried out using Thermo Fisher Avizo v9.1. Due to the low contrast between bones, the process of segmentation was done mainly using the brush selection tool, slice by slice, and applying interpolation when needed. The "Remove Island" feature of Avizo was applied for islands smaller than 30 pixels to remove the excessive noise of the meshes. The image segmentation process took around 100 hours per specimen and resulted in a total of 65 meshes for NHMD 164741 and 73 meshes for NHMD 164758. The meshes were generated using no smooth operator and exported as wavefront (.obj) files.

All meshes were treated and rendered using Blender 2.92. The segmented meshes were smooth using the Smooth Laplacian modifier with Lambda factor = 1 and 5 repeats and then decimated to 20% of the original face count. The measurements were taken both on the physical specimens and digitally in Blender (Table 2-3). All renders were done using Cycles as a render engine and with an accurate scale bar in the software. All pictures and renders of the specimens were treated in Adobe Lightroom 2021 and Adobe Photoshop CC 2021. The cladograms and vector images were created in Adobe Illustrator 2021.

2.3 Skull reconstruction

The digital reconstruction of the specimens was done by retrodeforming, moving, and mirroring the best-preserved elements using the Mirror modifier in Blender. Bones present in only one specimen were duplicated and rescaled for the other specimen. This allowed for tentative volume visualization and

natural placement of bones of the laterally crushed specimens. The measurements taken in these skeletal reconstructions are approximated.

2.4 Phylogenetic analysis

The specimens NHMD 164741 and NHMD 164758 were scored separately in the data matrix of Rauhut *et al*., 2020, containing 67 OTUs and 382 characters (120 cranial and 262 post-cranial) (appendix 1). *Macrocollum* was scored in this dataset, following the descriptive work of Müller *et al.*, (2018b) and Müller, (2020) to assess the validity of the clade Unaysauridae and its relationship to Plateosauridae. The phylogenetic analysis was conducted using TNT v1.5 Goloboff & Catalano, 2016. The trees were recovered using Traditional Search, with 1,000 Wagner trees replicates, holding 20 trees per replicate, with TBR algorithm and 1 random seed, collapsing the trees after the search. Consistency and retention indexes and Bremer Support were obtained using a premade script. Bootstrap was calculated using absolute frequencies and 100 replicates. All characters were treated with the same weight, and characters 8, 13, 19, 23, 40, 57, 62, 69, 92, 102, 117, 121, 122, 129, 132, 148, 150, 151, 158, 168, 170, 171, 178, 210, 211, 213, 232, 237, 254, 263, 268, 282, 295, 316, 322, 330, 352, 365, 368, 370, 375, and 380 were treated as ordered.

3 Results

3.1 Systematic Paleontology

Dinosauria Owen, 1842

Saurischia Seeley, 1887

Sauropodomorpha Huene, 1932

Plateosauridae Marsh, 1895

3.2 Horizon and age

NHMD 164741 and NHMD 164758 were collected at Malmros Klint Formation, Fleming Fjord Group, of mid Norian stage of the Late Triassic (Clemmensen, 1980; Clemmensen *et al.*, 1998; Kent & Clemmensen, 2021).

3.3 Location

NHMD 164741 and NHMD 164758 were collected at Macknight Bjerg site, Jameson Land, central East Greenland, of coordinates 71°23.010′ N, 22°34.114′ W and 71°22.993′ N, 22°33.972′ W, respectively (Fig. 3.1).

Figure 3.1 - Topographic map of Jameson Land, central East Greenland. The Macknight Bjerg site of the Malmros Klint Formation is marked by the red circle and number 6. Modified from Clemmensen *et al.*, 2020.

3.4 Material

NHMD 164741 (Fig. 3.2-3.3) comprises a nearly complete and partially articulated skull, missing the anteriormost region and most of the right elements. The skull preserves the left premaxilla, both maxillae, both nasals, the left lacrimal, incomplete jugals, incomplete prefrontals, incomplete left postorbital, left squamosal, left quadratojugal, left quadrate, both frontals, the distal part of the left parietal, parts of the braincase (i.e., fragments of the basisphenoid, a fragment of the left laterosphenoid and the left paroccipital process), both pterygoids, the left ectopterygoid, fragments of the palatines,

fragments of the left vomer, both dentaries, the left coronoid process, left splenial, left angular, left surangular, left prearticular, left articular and teeth.

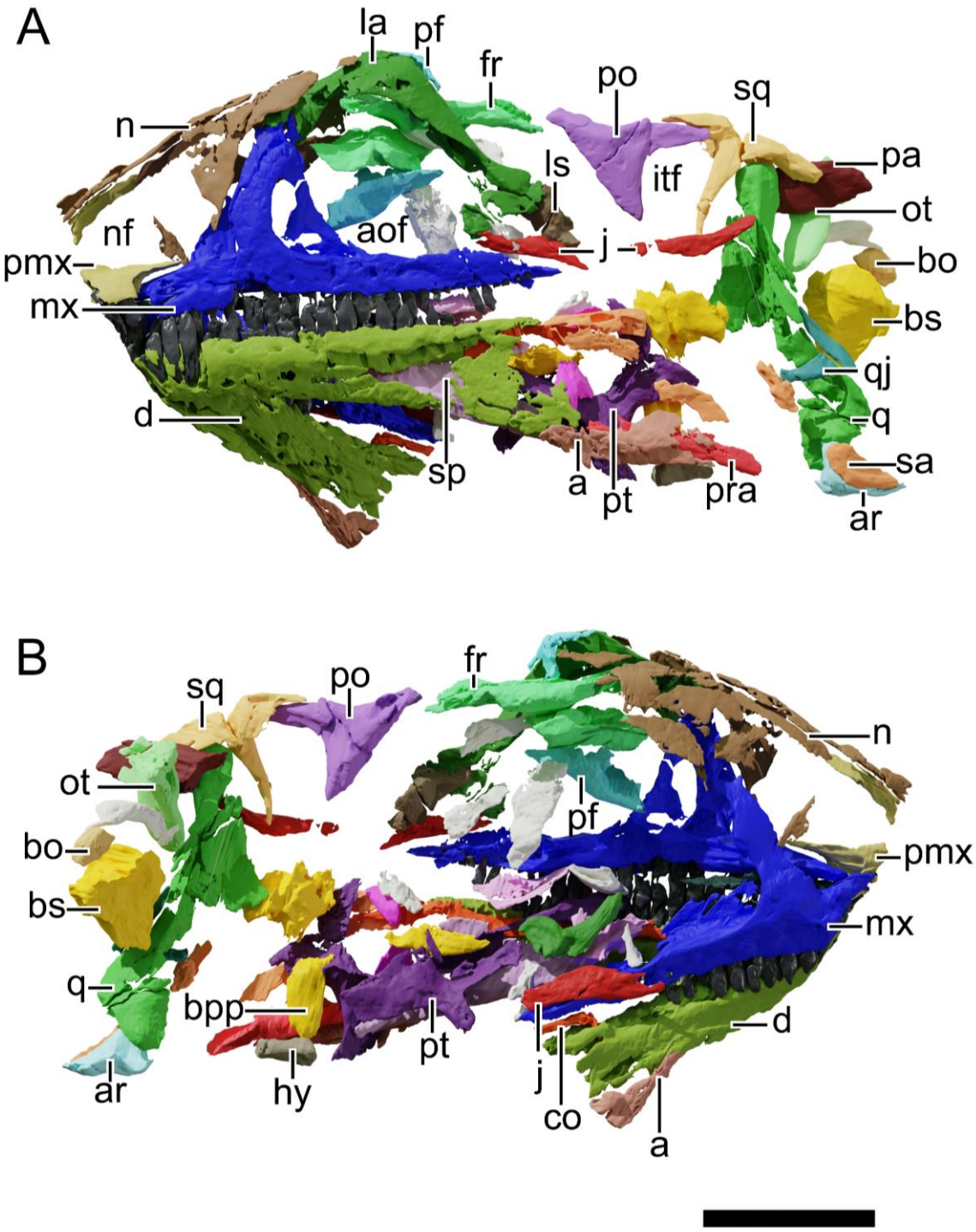

Figure 3.2 - 3D model of the skull of NHMD 164741. A, left lateral view of skull NHMD 164741; B, right lateral view of skull NHMD 164741. Abbreviations: a, angular; aof, antorbital fenestra; ar, articular; bo, basioccipital; bpp, basipterygoid process; bs, basisphenoid; co, coronoid; d, dentary; fr, frontal; hy, hyoid; itf, infratemporal fenestra; j, jugal; la, lacrimal; ls, laterosphenoid; mx, maxilla; n, nasal; nf, narial fenestra; ot, otoccipital; pa, parietal; pf, prefrontal; pmx, premaxilla; po, postorbital; pra, prearticular; pt, pterygoid; q, quadrate; qj, quadratojugal; sa, surangular; sp, splenial; sq, squamosal. Scale bar = 50 mm.

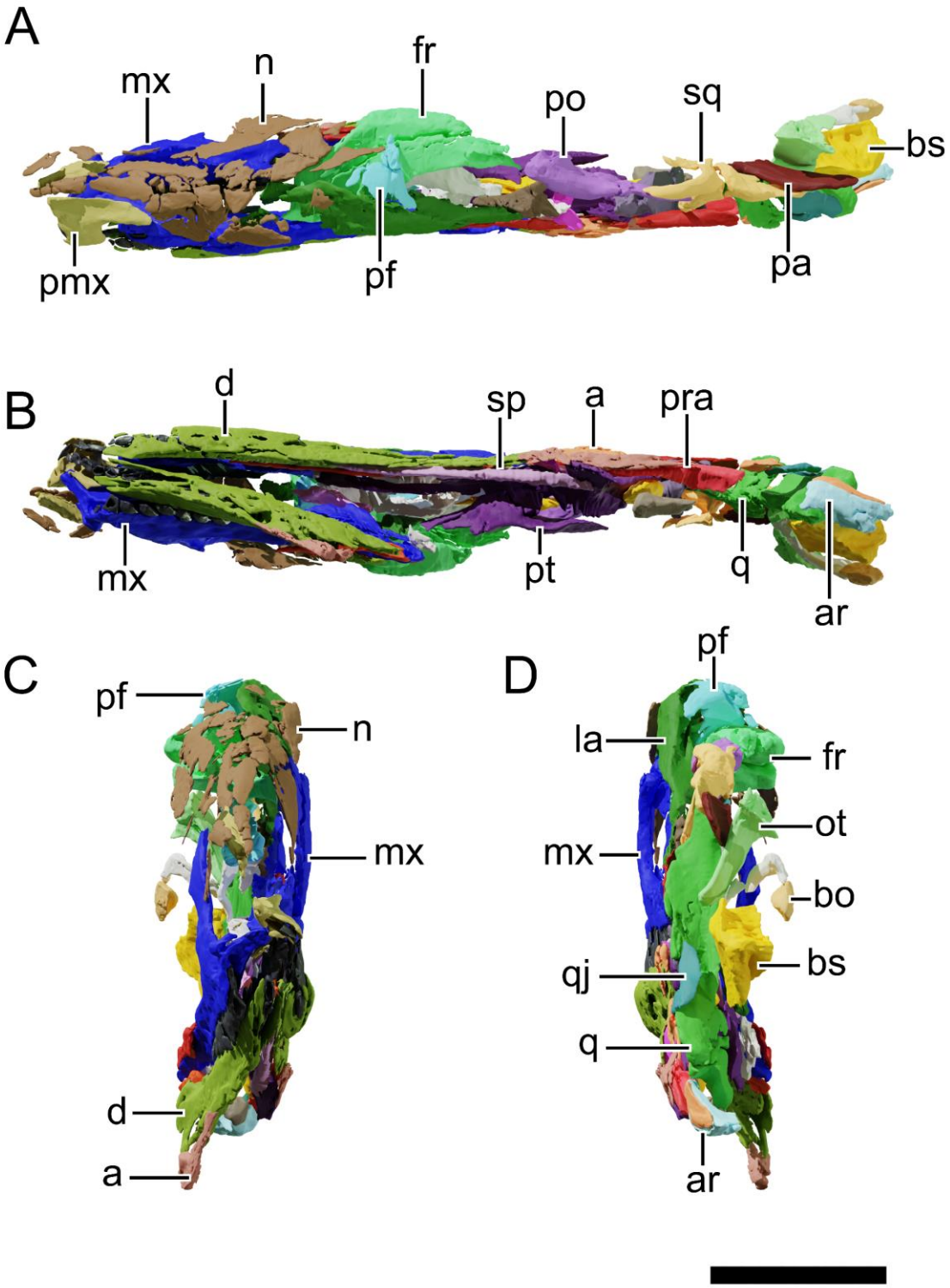

Figure 3.3 - 3D model of the skull of NHMD 164741. A, dorsal view of skull NHMD 164741; B, ventral view of skull NHMD 164741; C, anterior view of skull NHMD 164741; D, posterior view of skull NHMD 164741. Abbreviations: a, angular; ar, articular; bo, basioccipital; bs, basisphenoid; d, dentary; fr, frontal; la, lacrimal; ls, laterosphenoid; mx, maxilla; n, nasal; ot, otoccipital; pa, parietal; pf, prefrontal; pmx, premaxilla; po, postorbital; pra, prearticular; pt, pterygoid; q, quadrate; qj, quadratojugal; sa, surangular; sp, splenial; sq, squamosal. Scale bar = 50 mm.

NHMD 164758 (Fig. 3.4-3.5) comprises a nearly complete and articulated skull with lateral deformation, missing most of the posterodorsal elements posterior to the orbit. The skull preserves both premaxillae, both maxillae, both nasal, both lacrimals, both prefrontals, the left postorbital, both jugals, the condylar area of both quadrates, both frontals, the anterior part of the left parietal, parts of the braincase (i.e., the left orbitosphenoid, the left laterosphenoid, right basipterygoid process and the parasphenoid process of the basisphenoid), the complete palatal region and the complete mandibles.

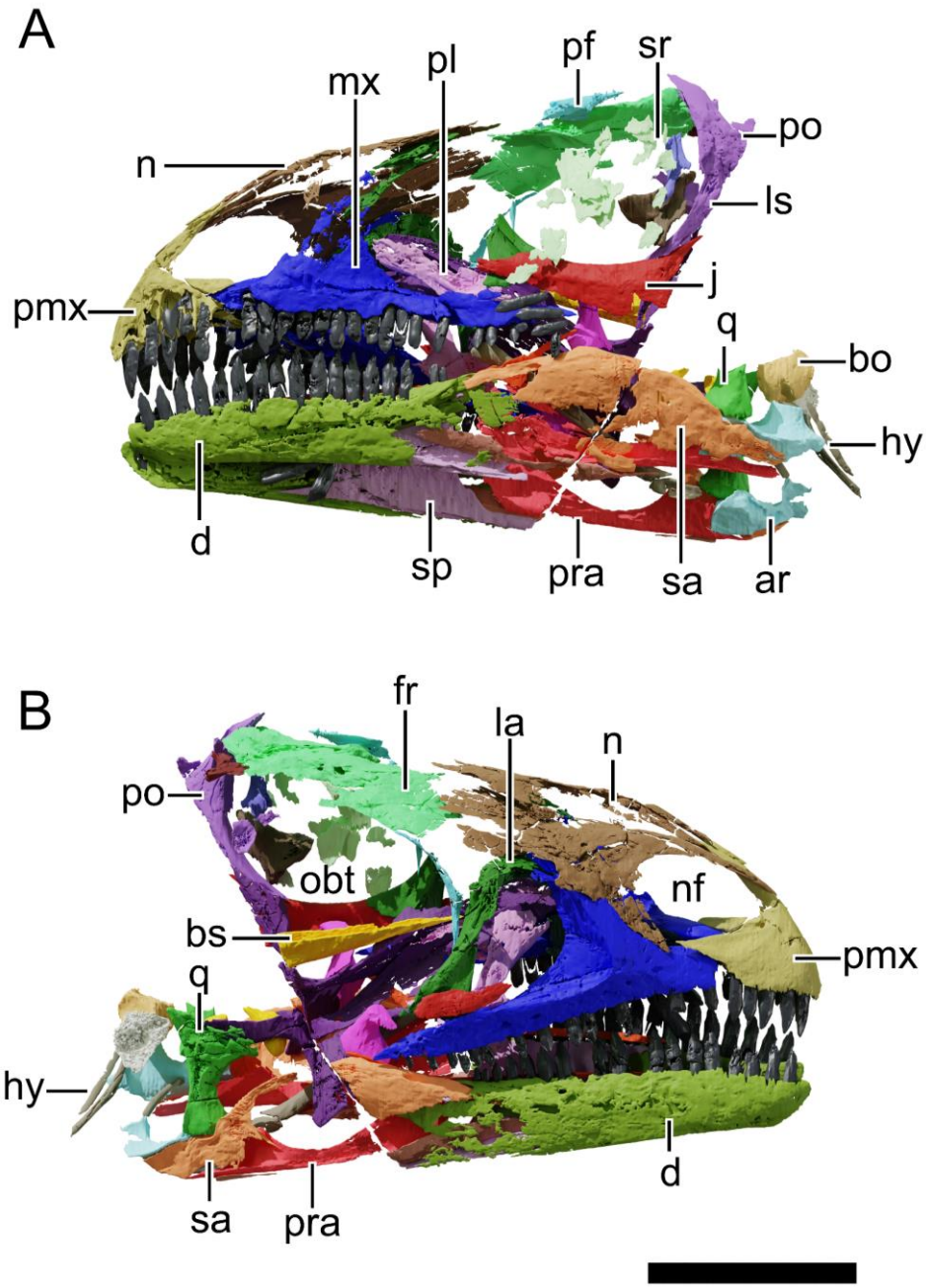

Figure 3.4 - 3D model of the skull NHMD 164758. A, left lateral view of skull NHMD 164758; B, right lateral view of skull NHMD 164758. Abbreviations: ar, articular; bo, basioccipital; bs, basisphenoid; d, dentary; fr, frontal; hy, hyoid; j, jugal; la, lacrimal; ls, laterosphenoid; mx, maxilla; n, nasal; nf, narial fenestra; obt, orbit; pf, prefrontal; pl, palatine; pmx, premaxilla; po, postorbital; pra, prearticular; pt, pterygoid; q, quadrate; sa, surangular; sp, splenial; sr, sclerotic ring. Scale bar = 50 mm.

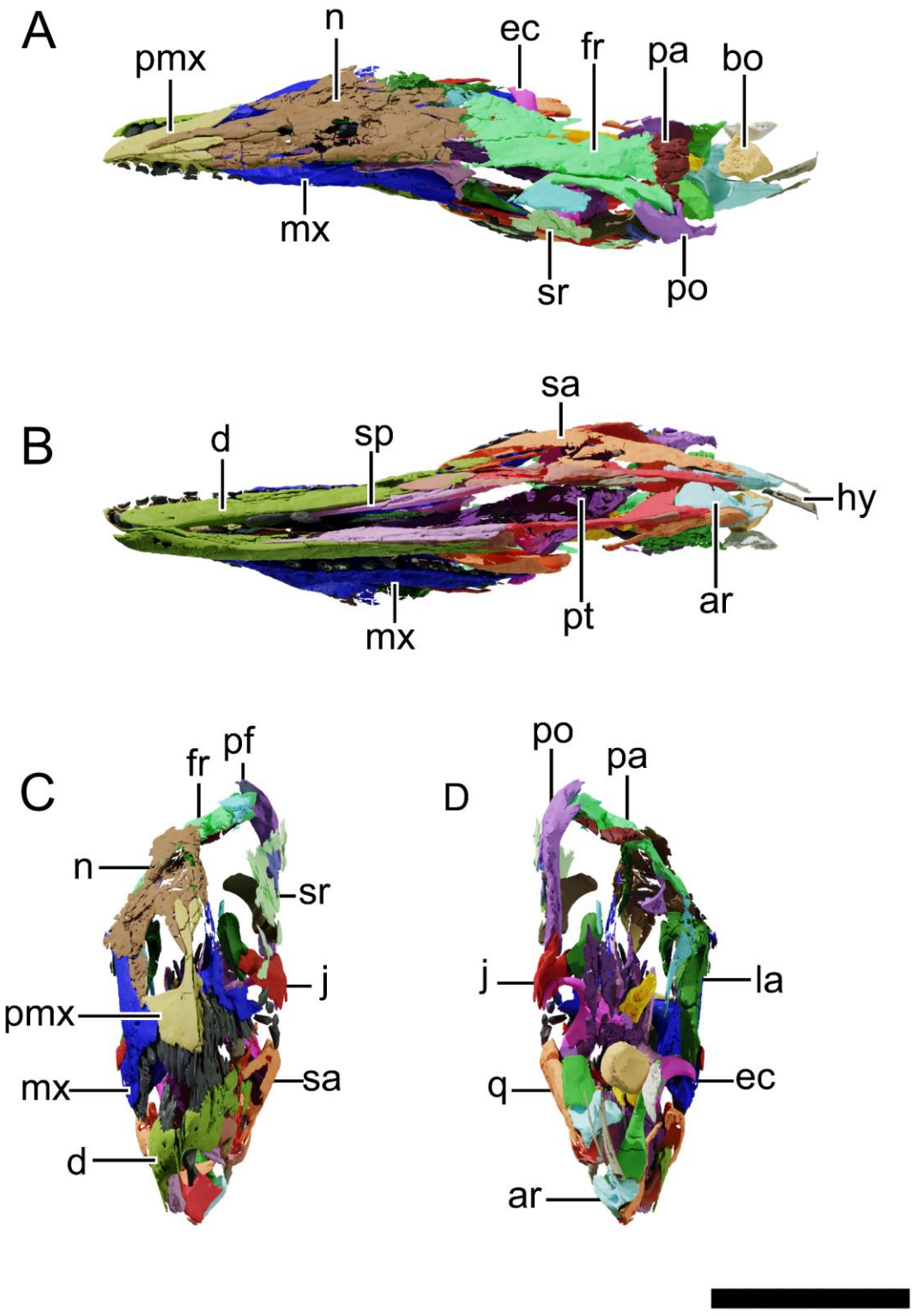

Figure 3.5 - 3D model of the skull NHMD 164758. A, dorsal view of skull NHMD 164758; B, ventral view of skull NHMD 164758; C, anterior view of skull NHMD 164758; D, posterior view of skull NHMD 164758. Abbreviations: ar, articular; bo, basioccipital; d, dentary; ec, ectopterygoid; fr, frontal; hy, hyoid; j, jugal; la, lacrimal; mx, maxilla; n, nasal; pa, parietal; pf, prefrontal; pmx, premaxilla; po, postorbital; pra, prearticular; pt, pterygoid; q, quadrate; sa, surangular; sp, splenial; sr, sclerotic ring. Scale bar = 50 mm.

3.5 Unique traits (contribution for a diagnosis)

Five autapomorphies were identified: 1) the presence of a foramen at the medial surface of the premaxilla; 2) an anteroposteriorly elongated dorsoposterior process of the squamosal (only preserved in NHMD 164741); 3) a quadrate relatively tall in comparison to the rostrum height (only preserved in NHMD 164741); 4) a well-developed, square-shaped in lateral view posterodorsal process of the articular (only preserved in NHMD 164758).

3.6 Description and comparative anatomy

3.6.1 Generalities

NHMD 164741 consists of a partially complete and almost fully articulated skull. The specimen is almost twice as long as tall (length is measured from the anteriormost preserved region to the end of the squamosal and height is measured from the ventral surface of the left dentary to the apex of the left lacrimal), and due to lateral crushing, its overall width is around a fifth of the height (see Table 2 for the skull general measurements). The anteriormost region of the snout (anterior part of left premaxilla and whole right premaxilla) and anterior region of both dentaries are missing. Thus, the total length of the skull cannot be precisely measured, although it would not be much longer than preserved. NHMD 164741 skull is relatively dorsoventrally taller than in other plateosaurids, such as *P. trossingensis*, *Unaysaurus* and *Macrocollum*. Most elements in the skull of NHMD 164741 are preserved in three dimensions, with little deformation, even though the skull is crushed laterally. This lateral compression dislocated most bones at the right side of the skull and disarticulated some elements (i.e., left and right frontals, left postorbital, left quadratojugal). The left elements of the skull are mostly present, showing some fractures, but preserving the overall shape of the skull. The orbital region, however, is poorly preserved due to compaction, with the overall orbital shape only tentatively recovered as semi-circular, according to a slight anterodorsal expansion over the caudal margin of the lacrimal. The right upper and lower jaw joint regions of the skull are missing, whereas the left elements of this region are slightly ventrally dislocated, but mostly still in association (i.e., quadratojugal, quadrate, articular and the posterior part of the surangular). The braincase and occipital region are mostly disarticulated, some of its bones are missing or too fragmented for precise identification.

Table 2 - General skull measurements for the Greenland specimens NHMD 164741 and NHMD 164758. * indicates maximum preserved measurement.

Measurements (in mm)	**NHMD 164741**	**NHMD 164758**

Skull anteroposterior length (from the anterior tip of the premaxilla to posterior margin of occipital condyle)	243.7*	167.9
Skull maximum dorsoventral height at orbit including the mandible	112.7	93.6
Skull dorsoventral height at orbit excluding mandible	75.2	58.3
Rostrum dorsoventral height (measured at the posterior margin of the external naris level)	57.9	40.9
External naris maximum anteroposterior length	35.1	25.1
Orbit length	52.5*	49.9
Orbit height	46.5*	41.0
Premaxilla maximum anteroposterior length	-	36.9
Premaxilla alveolar anteroposterior length	-	24.3
Premaxilla maximum dorsoventral height	40.3	37.8
Narial fossa anteroposterior length	28.7	24.9
Maxilla anteroposterior maximum length	129.9	95.5
Maxilla anteroposterior alveolar length	118.8	85.7
Maxilla dorso ventral height (from the dorsal tip of the dorsal process to ventral margin of maxilla)	57.0	42.0
Antorbital fossa maximum anteroposterior length	46.5	34.8
Nasal anteroposterior length	98.7	80.0
Lacrimal dorsoventral height	64.5	41.9
Lacrimal maximum length of dorsal region	43.1	37.5

Prefrontal dorsoventral maximum height	-	32.3
Frontal maximum anteroposterior length	51.6	42.3
Frontal maximum mediolateral width	49.1	18.7
Postorbital maximum length	48.6	25.5
Postorbital maximum height	40.8	41.6
Squamosal maximum length	49.5	-
Squamosal maximum height	38.9	-
Jugal maximum anteroposterior length	57.8	48.9
Jugal height under the orbit	11.3	10.5
Quadrate dorsoventral height	91.8	-
Quadrate mediolateral width at condylar region	13.9	10.8
Quadrate pterygoid flange anteroposterior length	24.3	17.8
Pterygoid maximum anteroposterior length	92.4	83.8
Pterygoid maximum dorsoventral height	52.4	46.6
Ectopterygoid maximum length of medial flange	29.8	20.5
Ectopterygoid maximum mediolateral width	22.4	21.6
Palatine maximum anteroposterior length	31.3	39.8
Palatine maximum mediolateral width	9.1	13.2
Vomer maximum anteroposterior length	-	42.6

NHMD 164758 is a partially complete and articulated skull. NHMD 164758 skull is relatively smaller than NHMD 164741 (0.69 of NHMD 164741 length), but its elements show less lateral compaction

than NHMD 164741. Therefore, the palatal region is better preserved in NHMD 164758. Similar to NHMD 164741, the skull is relatively dorsoventrally taller than in other plateosaurids (see Table 2). The right elements of the snout are better preserved, as the lateral surface of the left snout elements was eroded. The orbit in NHMD 164758 is subcircular and preserves the left sclerotic ring.

3.6.2 Premaxilla

NHMD 164741 preserves the posterior half of the left premaxilla (Fig. 3.6). NHMD 164758 bears the only complete premaxilla between both specimens (Fig. 3.7). The premaxilla is triangular in lateral profile, encompassing most of the narial fenestra. The main body of the premaxilla is slightly anteroposteriorly longer than dorsoventrally tall and contains five alveoli, the first of which is adjacent to the rostral tip of the premaxilla. The premaxilla bears 5 teeth, a tooth count as in *Plateosaurus* (except for specimens with 6 premaxillary teeth, i.e., HMN XXIV, SMNS 12949 and SMNS 13200), and the position of the first premaxillary tooth is close to the anterior margin of the premaxilla. This characteristic is similar to that of the juvenile MSF 15.8B, which is thought to be related to ontogeny (Lallensack *et al.*, 2021). The main body is perforated by a small foramen at the base of the dorsal process, at the level of the anterior margin of the second premaxillary tooth. Posterior to this foramen, at the dorsal margin of the premaxilla main body, a shallow recess forms the narial fossa. The narial fossa marginates the posterior margin of the dorsal process of the premaxilla, reaching its deepest point at the lateral mid-length of the premaxillary body, around the level of the third premaxillary tooth. The shallow narial fossa is observed on both NHMD 164741 and NHMD 164758, although the exact anterior extend of this structure on the former is unknown. The narial fossa position, depth and shape differ from all other *Plateosaurus* skulls described (i.e., AMNH FARB 6810; HMN XXIV; HMN MB.1927.19.1; MSF 11.4; MSF 16.1; MSF 1; SMNS 52968). The narial fossa on these specimens is marked by a ventral rim and deeply depressed in the premaxilla. The condition observed in NHMD 164758 is closer to the observed in *Unaysaurus tolentinoi* UFSM 11069, *Macrocollum* CAPPA/UFSM 0001a, *Massospondylus* BP/1/4934, and *Ngwevu* BP/1/4779.

The medial surface of the premaxilla is almost straight at the contact with its counterpart, which occurs in the first half of the premaxillary main body. As in *P. trossingensis*, the teeth row is separated by an angle of 20º from the symphysis, resulting in a V-shaped dorsal and ventral profiles. The maxillary articular facet is delimited by a ventral sharp ridge that constitutes the posteroventral process and a smoother dorsal recess that forms the ventral margin of the posterolateral (=maxillary) process of the premaxilla. This later rests on the anterodorsal margin of the maxillary body and tapers to a point posteriorly until it contacts the rostroventral process of the nasal. Both NHMD 164741 and NHMD 164758 possess a round foramen at the dorsomedial surface of the premaxilla main body, at the base of

the dorsal process of the premaxilla (Fig. 3.6-3.7). This foramen is absent in *Plateosaurus*, *Unaysaurus*, and cannot be accessed in *Macrocollum*.

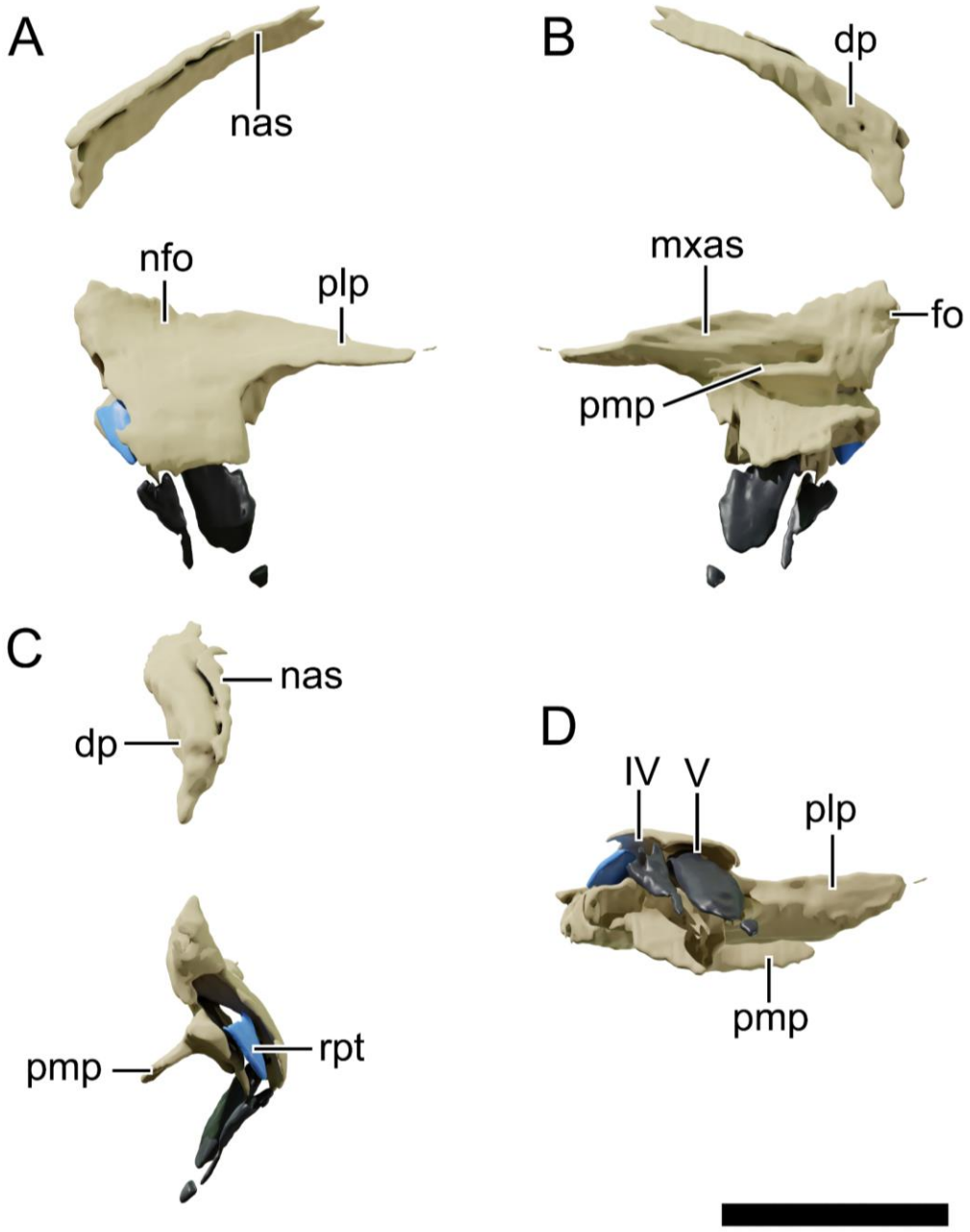

Figure 3.6 - NHMD 164741 left premaxilla. Digital model of the left premaxilla of NHMD 164741 in lateral view (A), medial view (B), anterior view (C) and ventral view (D). Abbreviations: dp, dorsal process; fo, foramen; mxas, articular surface for the maxilla; nas, articular surface for the nasal; nfo, narial fossa; plp, posterolateral process; pmp, posteromedial process; rpt, replacement tooth. IV and V represent the tooth position. Scale bar = 20 mm.

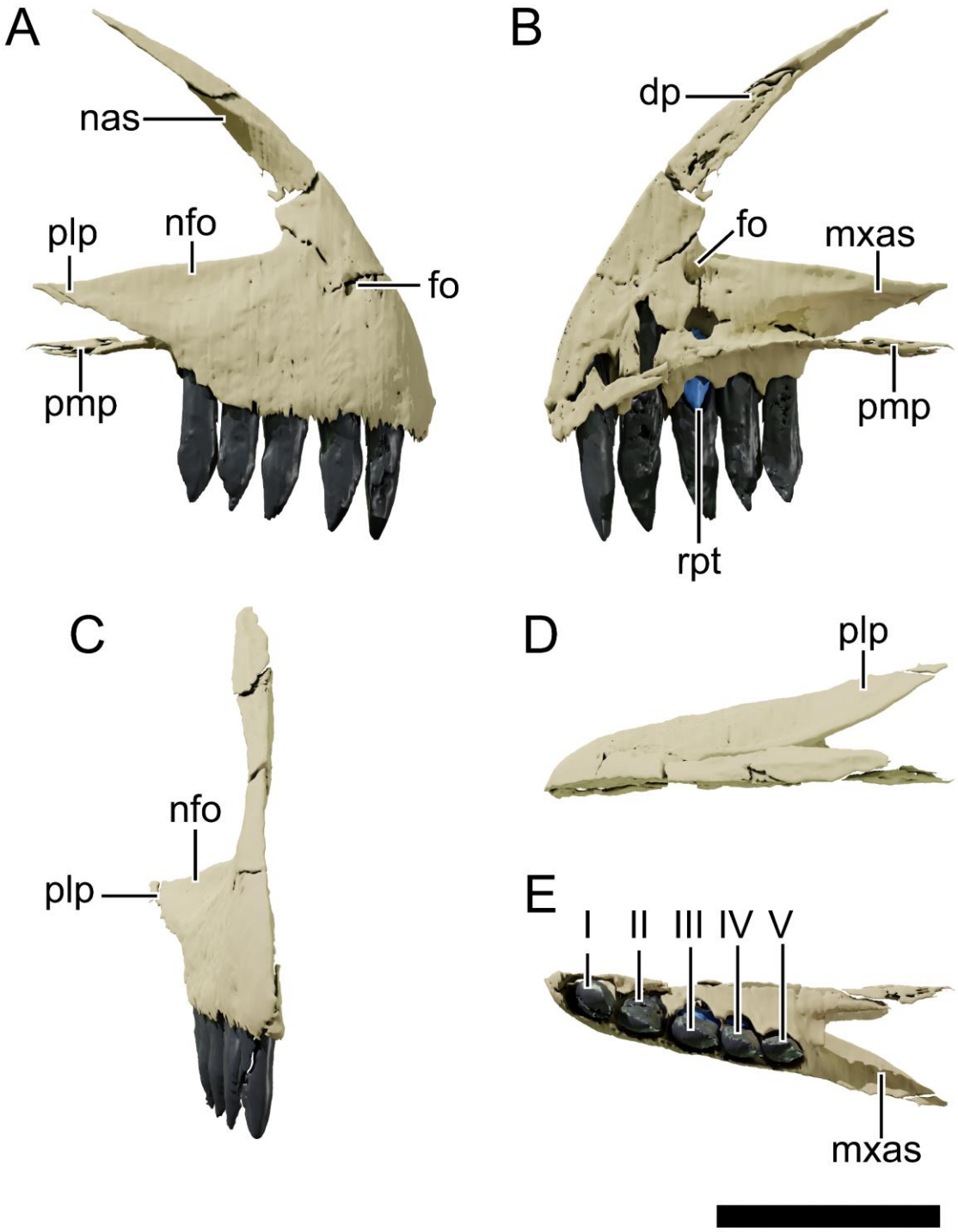

Figure 3.7 - NHMD 164758 right premaxilla. Digital model of the right premaxilla of NHMD 164758 in lateral view (A), medial view (B), anterior view (C), dorsal view (D) and ventral view (E). Abbreviations: dp, dorsal process; fo, foramen; mxas, articular surface for the maxilla; nas, articular surface for the nasal; nfo, narial fossa; plp, posterolateral process; pmp, posteromedial process; rpt, replacement tooth. I to V represent the tooth position. Scale bar = 20 mm.

The dorsal (=nasal) process of the premaxilla slopes posteriorly at an angle of 61º with the main body of the premaxilla. This deflection is lower than in *Macrocollum* (45º), *Unaysaurus* (40º), but similar to some *Plateosaurus* specimens, particularly MB.R.1937. The dorsal process encloses the anterior margin of the narial fenestra and extends posteriorly until the level of the posterior process of the premaxilla. This process contacts its counterpart medially, flattening dorsoventrally at the posterior end. This flattening results in a distal expansion of this process, as in *Plateosaurus*, *Macrocollum*, and *Coloradisaurus brevis* Bonaparte, 1978 PVL 3967.

3.6.3 Maxilla

The best-preserved maxillae are the left ramus in NHMD 164741 (Fig. 3.8) and the right ramus in NHMD 164758 (Fig. 3.9). This bone is triradiate in the lateral profile, with the horizontal main ramus divided by the vertical dorsal process of the maxilla. The main ramus is straight throughout its anteroposterior length, with both dorsal and ventral margins parallel to each other, only tapering at the posteriormost region. The dorsal process deflects slightly posteriorly and marginates the subtriangular antorbital fossa. A maximum of 23 alveoli in NHMD 164758 and 24 alveoli in NHMD 164741 are preserved, both specimens with four alveoli in the anterior segment of the main ramus. In other sauropodomorphs such as *Macrocollum*, *Unaysaurus* UFSM 11069, *Leyesaurus* PVSJ 706, and *Massospondylus* BP/1/4934 there are indeed four alveoli in this segment of the maxilla, but in *Plateosaurus* (such as AMNH FARB 6810, MSF 12.3, SMNS 13200) there are five alveoli anterior to the dorsal process of the maxilla.

The anterior segment of the main ramus of the maxilla is anteroposteriorly shorter than the posterior segment and has no lateral neurovascular foramina. An anterior process of the maxilla extends medial to the premaxilla, tapering to a point anteriorly. This process is gently curved mediolaterally, with a sharp ridge at its dorsal margin, where it contacts laterally the maxillary process of the premaxilla. The anterior process of the maxilla contacts ventrally with the posteroventral process of the premaxilla and medially with the vomer, as in *Plateosaurus*.

The dorsal (=ascending) process of the maxilla tappers dorsally, with a slight dorsoposterior inclination. Anteriorly this process bounds the posterior margin of the external naris and laterally contacts the ventral (=maxillary) process of the nasal. The dorsal margin of the antorbital fossa converges to the dorsal tip of the maxillary dorsal process forming an apex, as in *Lufengosaurus huenei* Young, 1941 IVPP V15, but differing from the posteriorly extended antorbital fossae of *Macrocollum*. In *Plateosaurus*, the antorbital fossa was found to vary among specimens, being plastic and not of significant taxonomic importance (Lallensack *et al.*, 2021). Medially, the dorsal process of the maxilla

forms the anterior margin of the antorbital fossa. In NHMD 164758 the antorbital fossa is fully closed, differing from “unaysaurids” (i.e., *Macrocollum* and *Unaysaurus*, *sensu* Müller *et al.*, 2018b; Müller, 2020), whose antorbital fossae are perforated by a large promaxillary fenestra. In NHMD 164741 this region is fragmented on both left and right ramus of the maxilla. However, in the left antorbital fossa, the presence of the promaxillary fenestra (or a blind ridge, as in the right maxilla of *Macrocollum*

CAPPA/UFSM 0001b, Müller, 2019) is not discarded, as the anteroventral margin of the antorbital fossa possesses an undamaged recess.

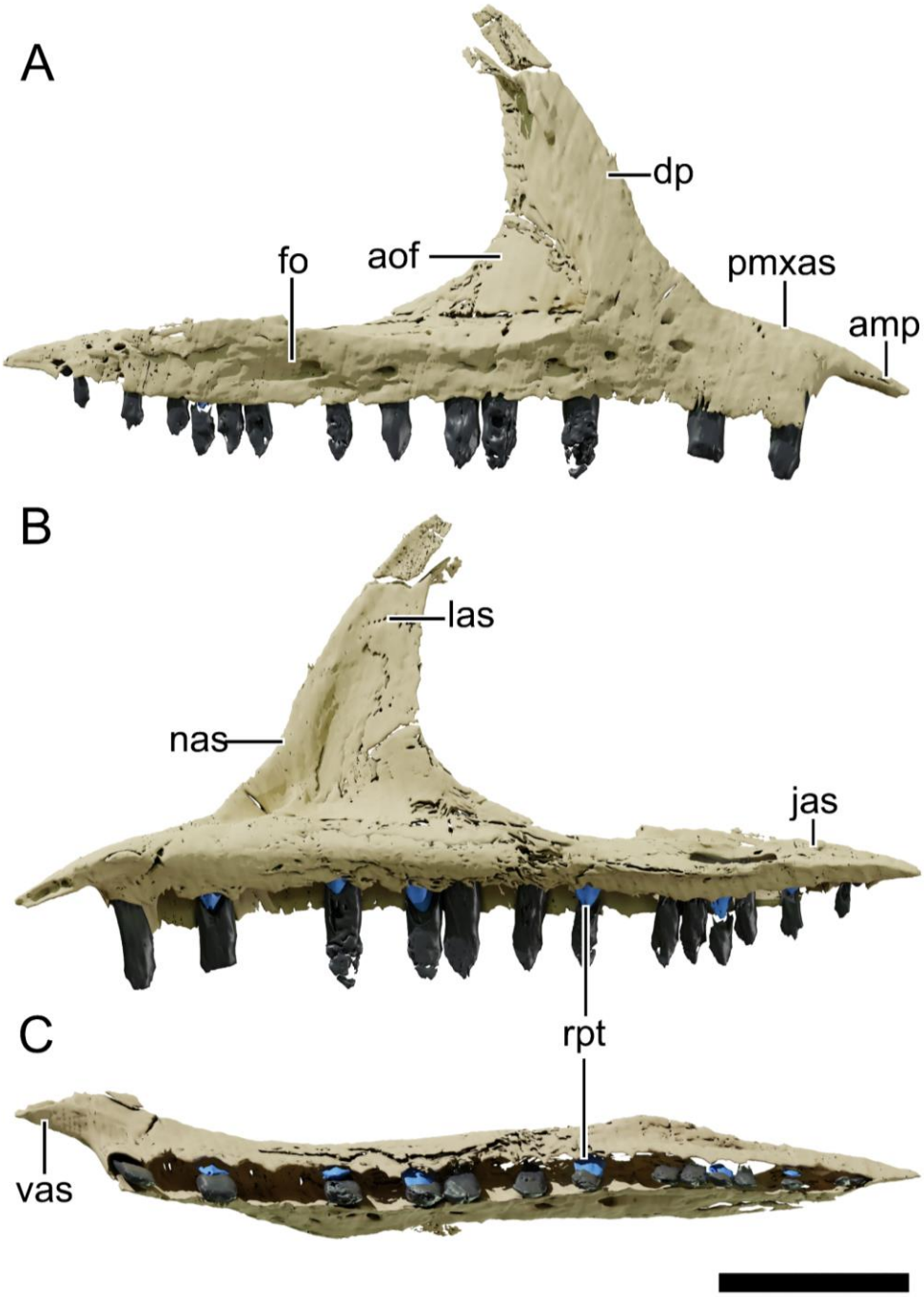

Figure 3.8 - NHMD 164758 right maxilla. Digital model of the right maxilla of NHMD 164758 in lateral view (A), medial view (B) and ventral view. Abbreviations: amp, anteromedial process; aof, antorbital fossa; dp, dorsal process; fo, foramen; jas, articular surface for the jugal; las, articular surface for the lacrimal; nas, articular surface for the nasal; pmxas, articular surface for the premaxilla; rpt, replacement tooth; vas, articular surface for the vomer. Scale bar = 20 mm.

The lateral surface of the posterior process of the maxilla is perforated by foramina, the last of which being the largest and opening posteriorly. The dorsal and ventral margins of the posterior process are parallel throughout most of the length, tapering posteriorly with a slight dorsal deflection. Among this deflection, a medial groove is formed on the dorsal margin, where the jugal articulates with the maxilla.

3.6.4 Nasal

The nasals are dorsoventrally thin tetraradiate bones (Fig. 3.2-3.5), anteroposteriorly longer than lateromedially wide. The nasal is shorter in NHMD 164741 and NHMD 164758 than in *Plateosaurus.* In *Plateosaurus*, the nasal is longer than half the skull roof length, being a distinctive feature for the genus (Galton & Upchurch, 2004; Prieto-Márquez & Norell, 2011; Lallensack *et al.*, 2021). The main body of the nasal is dorsally convex and overlaps laterally the apex of the maxillary dorsal process. At its posterior region, the nasal contacts the prefrontal laterally and the frontal ventrally. Anteriorly, the nasal radiates in two ventrally oriented processes, separated by a dorsal concavity of the nasal. This area encompasses the posterodorsal region of the narial fenestra. The anteromedial (=premaxillary) process of the nasal contacts the dorsal process of the premaxilla laterally. The lateroventral (=maxillary) process marginates the dorsal process of the maxilla as a ventrally oriented triangular blade. Ventrally, this process tapers to a point that finishes just before contacting the posteriormost tip of the posterolateral process of the premaxilla. A point-contact between the distal part of the lateroventral process of the nasal and the posterolateral process of the premaxilla is observed in *Plateosaurus* but not in *Macrocollum* and *Massospondylus*.

3.6.5 Lacrimal

The best-preserved lacrimals are the left element in NHMD 164741 (Fig. 3.10) and the right element in NHMD 164758 (Fig. 3.11), although in the former the distal part of the maxillary process is broken, and in the latter, the lateral surface is weathered. The lacrimal bounds the posterior margin of the antorbital fenestra and the anterior margin of the orbit. As in *Macrocollum* and *Plateosaurus*, the lacrimal is shaped like an inverted L, with a long anterodorsal (=maxillary) process extending anteriorly. This process is obscured dorsally by the nasal. The anterodorsal process of the lacrimal is hollow and subcircular in cross-section, with the dorsal margin tapering into a ridge. This ridge extends from the dorsomedial margin of the main shaft of the lacrimal until it bisects at the anteriormost region of the process. The ventral projection at the bifid junction is longer than the dorsal projection. The anterodorsal process of the lacrimal bends laterally distally to articulate to the medial margin of the dorsal process of the maxilla. The overall shape of the anterodorsal process of the lacrimal differs from that of *P.*

trossingensis AMNH FARB 6810, in which the process is triangular in cross-section at the bifid region, with the dorsal projection of the process being longer than the ventral one.

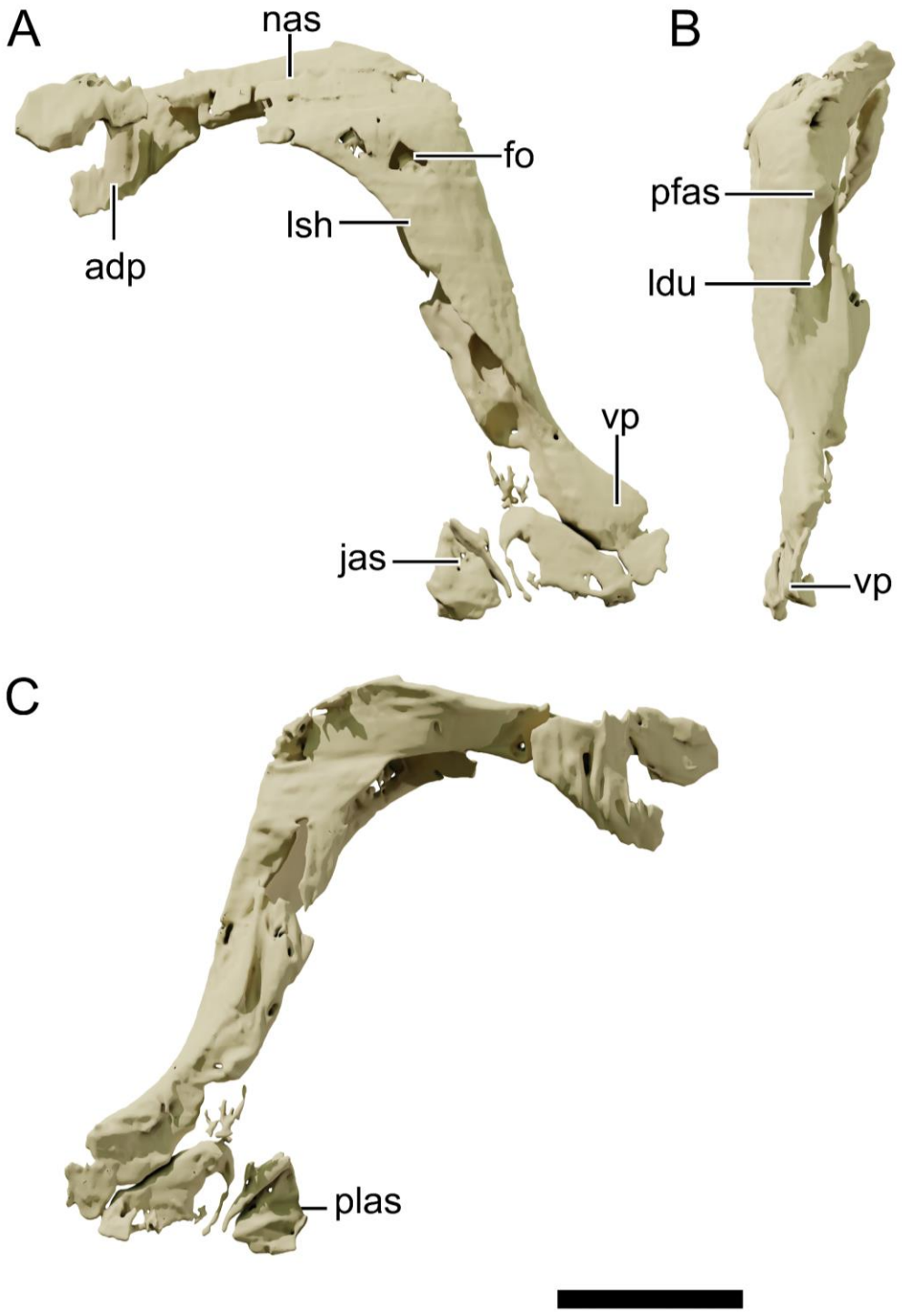

Figure 3.9 - NHMD 164741 left lacrimal. Digital model of the left lacrimal oof NHMD 164741 in lateral view (A); posterior view (B) and medial view (C). Abbreviations: adp, anterodorsal process; fo, foramen; jas, articular surface for the jugal; ldu, lacrimal duct; lsh, lateral sheet of bone; nas, articular surface for the nasal; pfas, articular surface for the prefrontal; plas, articular surface for the palatine; vp, ventral process. Scale bar = 20 mm.

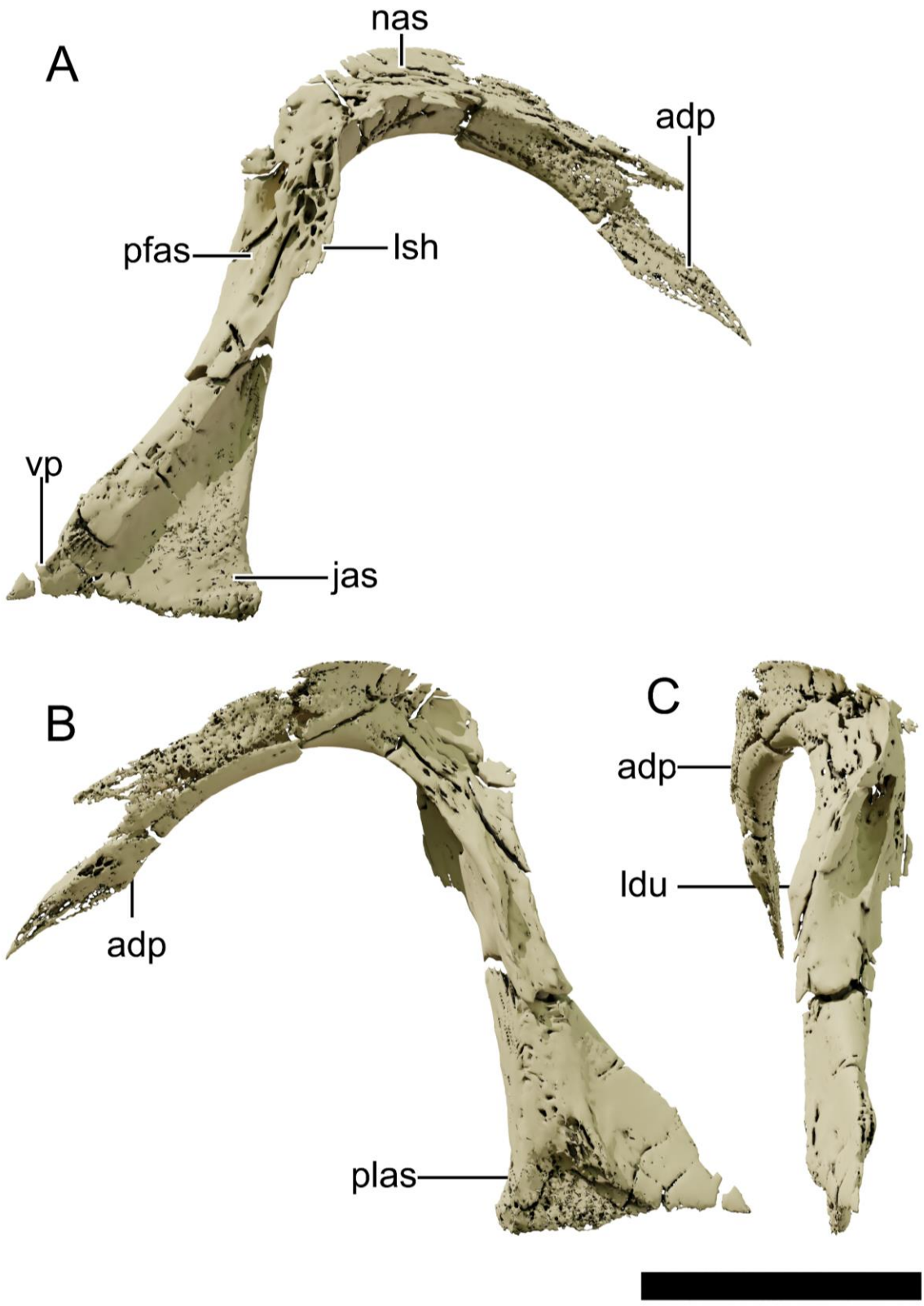

Figure 3.10 - NHMD 164758 left lacrimal. Digital model of the left lacrimal oof NHMD 164758 in lateral view (A); medial view (B) and posterior view (C). Abbreviations: adp, anterodorsal process; fo, foramen; jas, articular surface for the jugal; ldu, lacrimal duct; lsh, lateral sheet of bone; nas, articular surface for the nasal; pfas, articular surface for the prefrontal; plas, articular surface for the palatine; vp, ventral process. Scale bar = 20 mm.

The main shaft of the lacrimal is inclined anteriorly at an angle of 50º to the long axis of the skull, contrasting with the sub-vertical lacrimal of *Macrocollum* and the 30º tilted lacrimal of *Plateosaurus*. The lateral flange of the shaft is well-developed in NHMD 164741, as in *P. trossingensis* and differing from the condition of *Efraasia* and *P. gracilis*. The dorsal half of the anterior margin of this flange is concave in NHMD 164741. In most specimens of *P. trossingensis*, this flange is convex, except for specimens MSF 15.4 and MSF 16.1, where it is concave. However, this concavity may be caused by diagenetic deformation in these specimens. Therefore, the condition in NHMD 164741 is similar to *Ngwevu* and *Lufengosaurus* but differs from *Massospondylus* (Chapelle *et al.*, 2019).

The lateral margin of the lacrimal is perforated by a laterally opened foramen near the dorsal margin of the main shaft in NHMD 164741, as in *Lufengosaurus* IVPP V15 and *Macrocollum*, although on the latter the foramen is reduced in diameter. The posterior margin of the lacrimal is perforated by the ventral-facing lacrimal duct. Ventral to this duct, the lacrimal articulates with the ventral (=lacrimal) process of the prefrontal. The ventral process of the lacrimal projects anteriorly and posteriorly, forming a fin-like shelf, as in *Plateosaurus*. The anterior projection is overlapped laterally by the anterior process of the jugal and medially by the palatine.

3.6.6 Prefrontal

Both NHMD 164741 and NHMD 164758 preserved only fragments of the prefrontals (Fig. 3.2-3.5). The prefrontal is a dorsoventrally slender bone, anteroposteriorly longer than wide. It comprises the anterodorsal margin of the orbit, being slightly concave at its ventral margin, whereas straight at its dorsal margin. In lateral view, the bone is T-shaped, with its posterior process being longer than the anterior, and reaching over half the length of the orbit. This condition is also observed in most post-Carnian sauropodomorphs, but not in *Macrocollum*, in which the posterior process does not reach half the orbital length. Medially, the prefrontal is concave, forming a dorsal and a ventral shelf that project medially. An elongated and slender lacrimal process projects ventrally from the medioventral margin of the postorbital. This process marginates the posterior margin of the lacrimal beneath the lacrimal duct opening and participates in the anterior margin of the orbit, although not reaching the anteroventral corner of the orbit.

The posterior process of the prefrontal is expanded in both NHMD 164741 and NHMD 164758, being anteroposteriorly longer than the anterior process of the prefrontal. However, this elongation does not restrict the participation of the frontal to the orbit, as the derived feature of *Plateosaurus* (Yates, 2003). In dorsal view, this process tapers distally as in *Plateosaurus* and contacts the anterior region of the frontal medially.

3.6.7 Postorbital

Only the left postorbitals are preserved on both NHMD 164741 (Fig. 3.12) and NHMD 164758 (Fig. 3.13). The postorbital is a triradiate, Y-shaped bone, forming the posterodorsal margin of the orbit, the anterior margin of the infratemporal fenestra and the anterolateral margin of the supratemporal fenestra. The anterodorsal process of the postorbital is oriented anteromedially and dorsally. It is lateromedially broader than dorsoventrally tall. The medial margin of the anterodorsal process is bifurcated to embrace the posterolateral process of the frontal, as in *Macrocollum* and *Plateosaurus*. In NHMD 164741, the anteroposterior length of the anterodorsal process of the postorbital is slightly longer than the anteroposterior length of the posterodorsal process of the postorbital. This feature cannot be observed

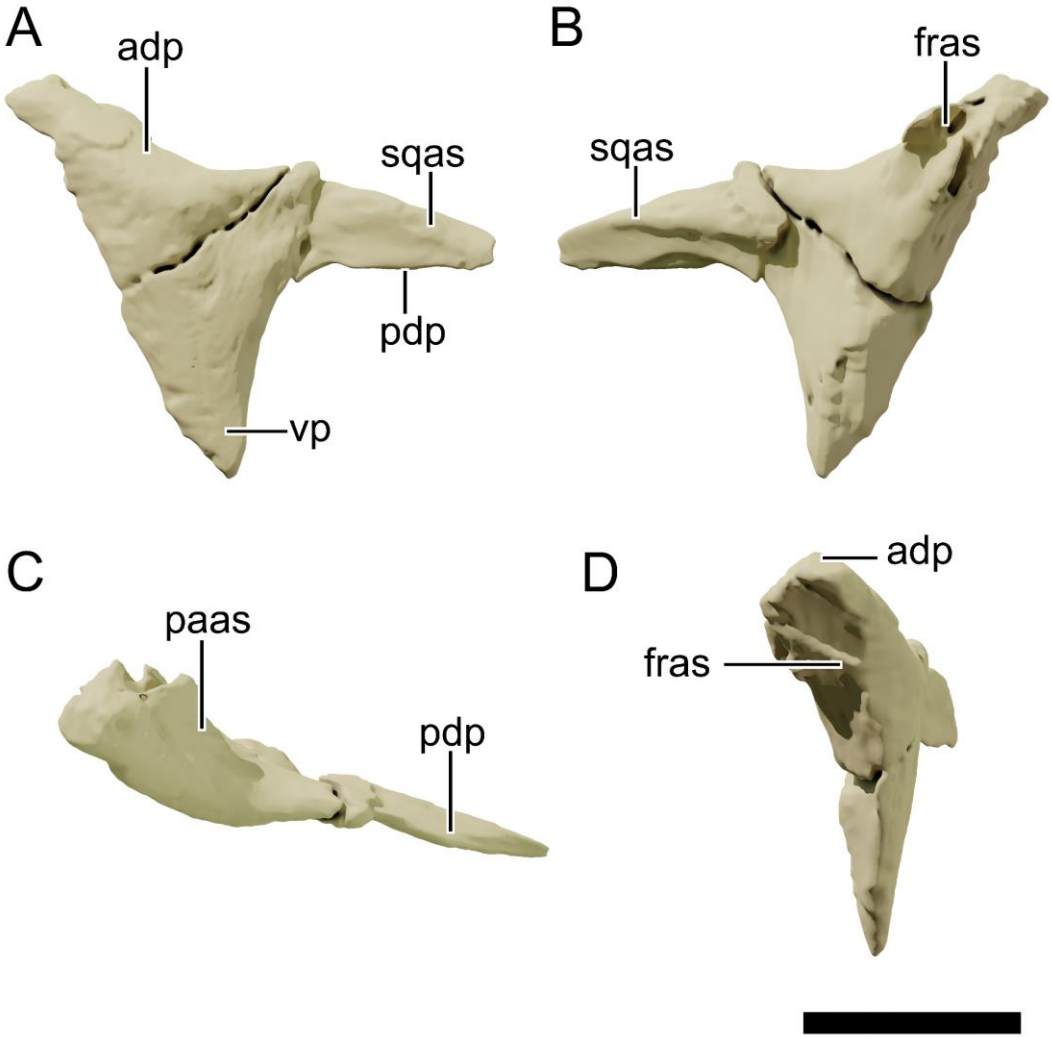

Figure 3.11 - NHMD 164741 left postorbital. Digital model of the left postorbital of NHMD 164741 in lateral view (A), medial view (B), dorsal view (C), and anterior view (D). Abbreviations: adp, anterodorsal process; fras, articular surface for the frontal; paas, articular surface for the parietal; pdq, posterodorsal process; sqas, articular surface for the squamosal; vp, ventral process. Scale bar = 20 mm.

in NHMD 164758. In *Plateosaurus*, the anteroposterior process of the postorbital is the shortest postorbital process.

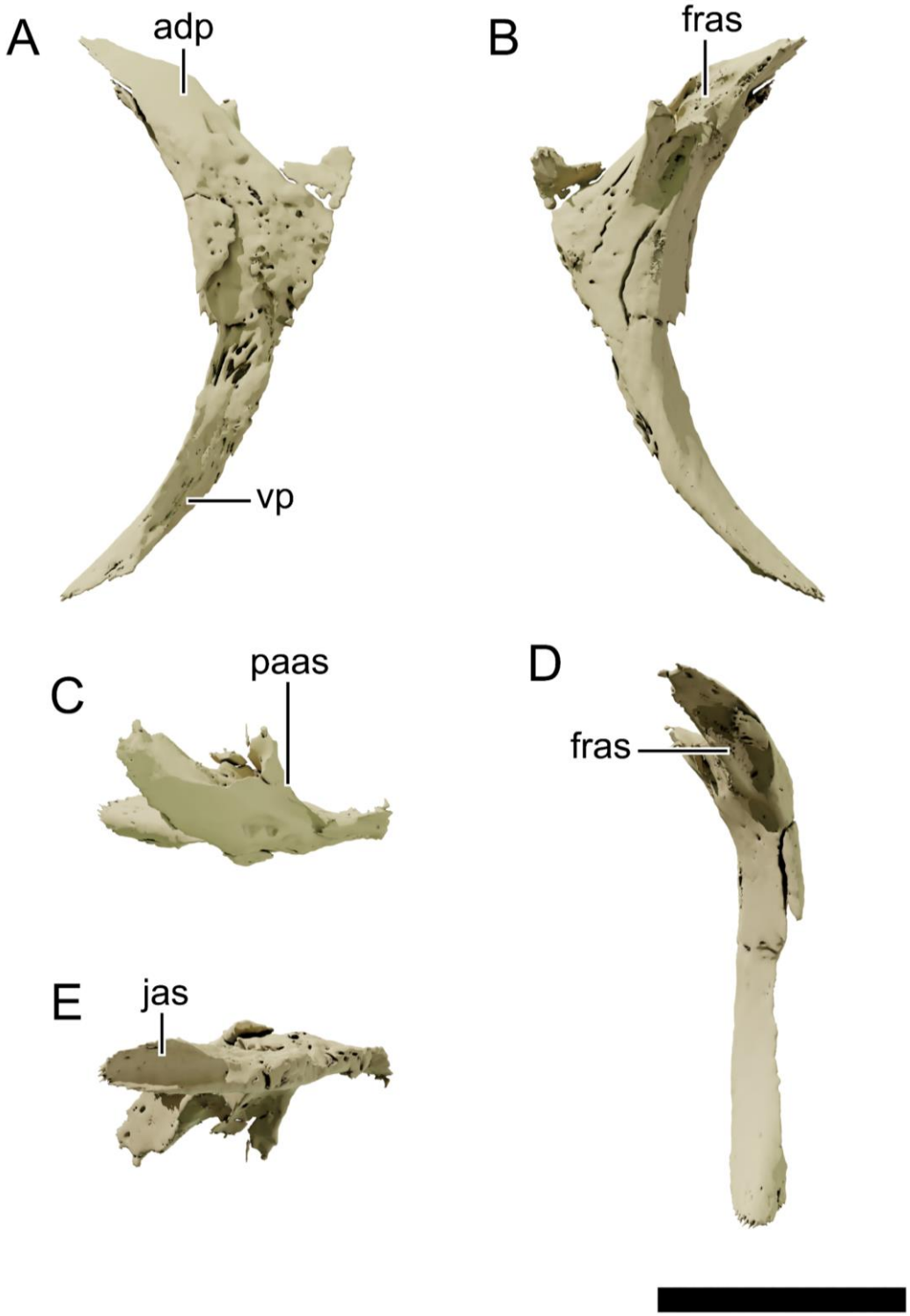

Figure 3.12 - NHMD 164758 left postorbital. Digital model of the left postorbital of NHMD 164758 in lateral view (A), medial view (B), dorsal view (C), ventral view (D) and anterior view (E). Abbreviations: adp, anterodorsal process; fras, articular surface for the frontal; jas, articular surface for the jugal; paas, articular surface for the parietal; vp, ventral process. Scale bar = 20 mm.

The posterior process of the postorbital is only preserved in NHMD 164741. This process is lateromedially slender and dorsally convex. It articulates dorsally and medially to the anterior process of the squamosal, with the dorsolateral surface partially covered by the squamosal. The posterior process of the postorbital forms an angle to the anterior process of 149º in NHMD 164741 and 134º in NHMD 164758. In *Plateosaurus* these angles vary between 160º in AMNH FARB 6810 and MSF 11.4, and 110º in MSF 12.3. This latter is thought to be closer to the original condition, as the former were mediolaterally compressed. The ventral process of the postorbital is best preserved in NHMD 164758 and is the longest process of the postorbital. This process is strongly concave anteriorly bounding the posterior surface of the orbit. It contacts the dorsal process of the jugal posteroventrally and excludes the jugal from the posterior margin of the orbit.

3.6.8 Squamosal

Only the left squamosal of NHMD 164741 is preserved (Fig. 3.14). The squamosal is a tetraradiate bone that bound the dorsoposterior margin of the infratemporal fenestra and the dorsolateral margin of the supratemporal fenestra. The anterolateral (=postorbital) process of the squamosal sheets the posterior process of the postorbital and forms the posteromedial margin of the supratemporal fenestra. The anteromedial (=parietal) process is slightly laterally compressed, diverging from the anterolateral process at an angle of 45º. In *P. trossingensis* MSF 12.3 this divergence is 60º and possibly closer to the *in vivo* state (Lallensack *et al.*, 2021). This process marginates the posterior margin of the supratemporal fenestra laterally and contacts the posterior process of the parietal medially. The posterior process of the squamosal is 1.33 times longer than the anterior process, comprising over half the total dorsal length of the squamosal. In *Plateosaurus* and *Macrocollum*, the posterior process of the squamosal is shorter than the anterior process in all other described specimens (see Table 3). Ventrally, this process encapsulates the dorsalmost region of the quadrate head. This process is slightly ventrolaterally oriented, with a concave median margin that contacts part of the posterior process of the parietal and the distal surface of the paroccipital process of the otoccipital.

Table 3 - Relative length of the posterior to the anterolateral processes of the squamosal across basal sauropodomorphs. Measurements were taken on the 3D models when available.

Squamosal - posterior process length to anterolateral process length		
Greenland specimen	NHMD 164741	1.31
P. trossingensis	AMNH FARB 6810	0.55
P. trossingensis	MSF 16.1	0.41
P. trossingensis	NAAG_00011238	0.48
P. trossingensis	MSF 12.3	0.53
P. trossingensis	MSF 15.4	0.83

Macrocollum	CAPPA/UFSM 0001b	0.77
M. carinatus	BP/1/5241	0.86
Buriolestes	CAPPA/UFSM 0035	0.88

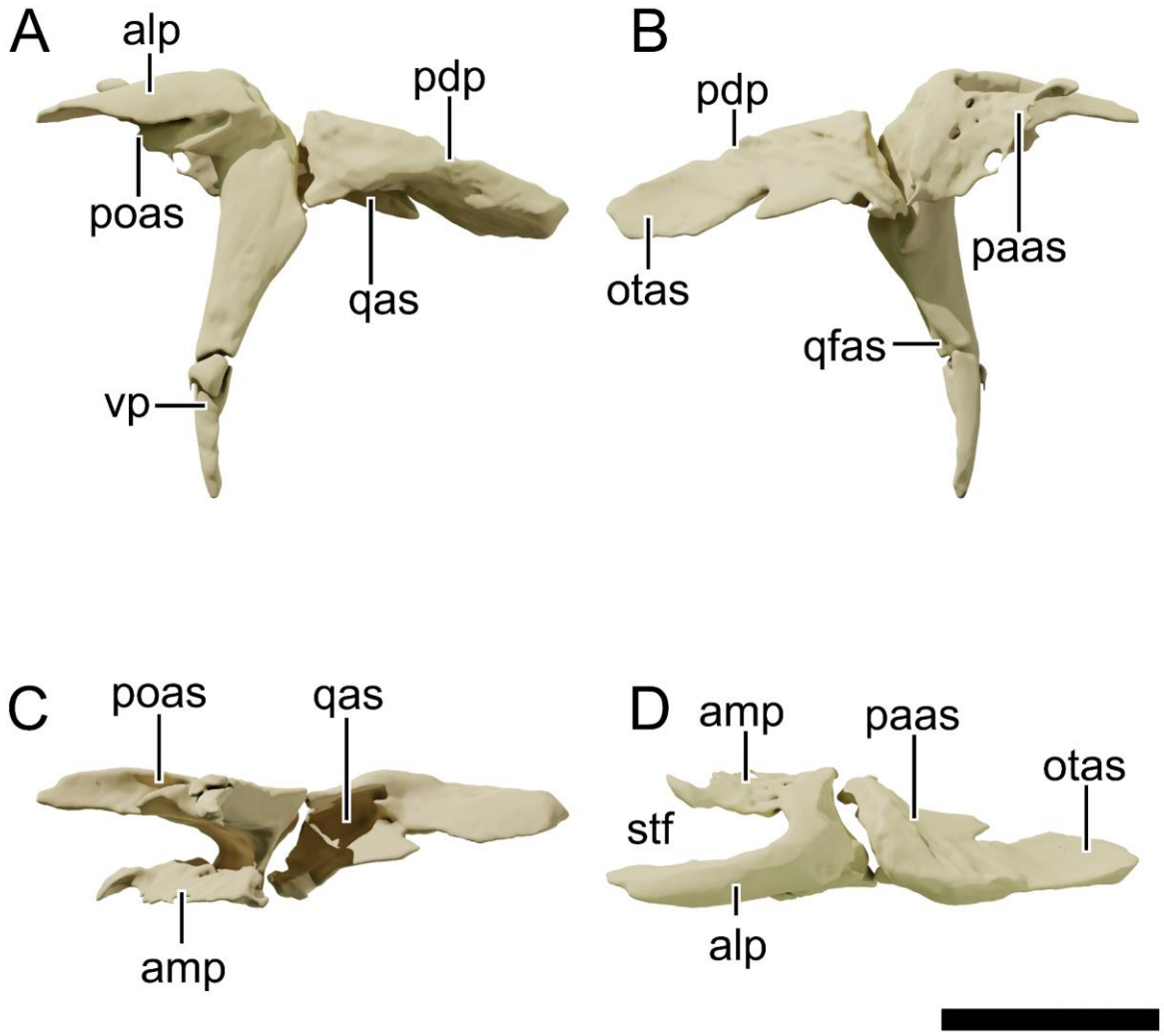

Figure 3.13 - NHMD 164741 left squamosal. Digital model of the left squamosal of NHMD 164741 in lateral view (A), medial view (B), ventral view (C), and dorsal view (D). Abbreviations: alp, anterolateral process; amp, anteromedial process; otas, articular surface for the otoccipital; paas, articular surface for the parietal; pdt, posterodorsal process; poas, articular surface for the postorbital; qas, articular surface for the quadrate; qfas, articular surface for the quadrate flange; stf, supratemporal fenestra. Scale bar = 20 mm.

The ventral (=quadrate) process of the squamosal is the longest of the processes, tapering distally and comprising the dorsoposterior margin of the infratemporal fenestra. It extends ventrally to about 60% of the infratemporal fenestra dorsoventral height. The distal end is deflected posteriorly as in *Plateosaurus*. The articular facet to the squamosal ramus of the quadratojugal is exposed laterally, meaning that it contacted the quadratojugal medially.

3.6.9 Jugal

The left jugal of NHMD 164758 is the best-preserved jugal among the specimens (Fig. 3.15), only missing the posteroventral process. This bone forms the ventral margin of the orbit and is concave dorsally and straight ventrally.

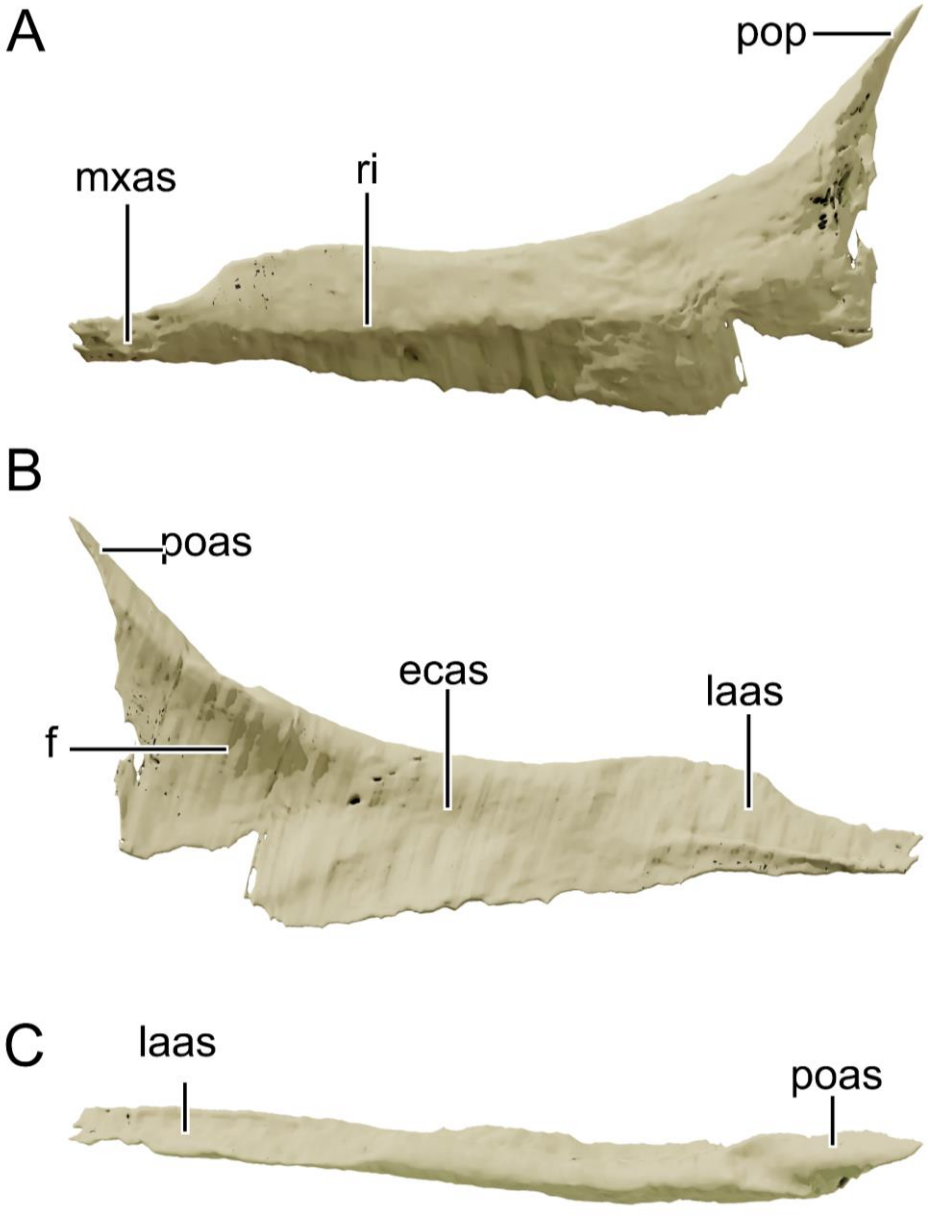

Figure 3.14 - NHMD 164758 left jugal. Digital model of the left jugal of NHMD 164741 in lateral view (A), medial view (B) and dorsal view (C). Abbreviations: ecas, articular surface for the ectopterygoid; f, fossa; laas, articular surface for the lacrimal; mxas, articular surface for the maxilla; poas, articular surface for the postorbital; pop, postorbital process; ri, ridge. Scale bar = 20 mm.

The anterior process of the jugal is five times anteroposteriorly longer than dorsoventrally tall, as in *P. trossingensis*, being relatively taller than in *Macrocollum* and *Efraasia.* A dorsoventrally high jugal was found to a derived feature of *P. trossingensis* (Yates, 2003). The anterior process of the jugal is laterally concave and divided in the mid-height by a longitudinal ridge. This process articulates to the maxilla beneath this ridge, at its anteroventral half, and medially to the lacrimal anteriorly and the ectopterygoid posterior to it. The posterodorsal (=postorbital) process of the jugal is deflected posteriorly, forming an angle of 137º to the anterior process. It contacts the ventral process of the postorbital anteriorly and bounds the anteroventral margin of the infratemporal fenestra. Medioventrally to this process is the jugal fossa. The posterior process of the jugal is disarticulated to the main body in NHMD 164741. This process is slender and anteroposteriorly long and articulates with the quadratojugal lateroventrally.

3.6.10 Quadratojugal

The left quadratojugal of NHMD 164741 is preserved (Fig. 3.2-3.3), however the distal ends of the anteroventral (=jugal) and posterodorsal (=squamosal) processes are missing. The quadratojugal delimits the posteroventral corner of the infratemporal fenestra. The main body of the quadratojugal is posteriorly convex and slightly posteroventrally oriented. The anteroventral and posterodorsal processes are almost perpendicular, being separated by an 84º angle. In some specimens of *P. trossingensis*, this angle is less than 45º or subparallel, however, these acute angles are possibly the result of plastic deformation and were originally close to 70º (Galton & Upchurch, 2004; Lallensack *et al.*, 2021). The anteroventral process is laterally convex and articulates to the posteroventral process of the jugal both medially and ventrally, as observed by a ventral fossa in this process. The posterodorsal process is inclined medially to contact the lateral margin of the quadrate.

3.6.11 Quadrate

NHMD 164741 preserves the only complete quadrate (left quadrate, Fig. 3.16), whereas both quadrates of NHMD 164758 have only the distal part preserved (Fig. 3.17). The main shaft of the quadrate is gently concave posteriorly and forms an angle of 153º to the quadrate head. The anterolateral and dorsal surfaces of the quadrate head are obscured by the ventral process of the squamosal. The head is anteroposteriorly expanded with a ridge at its lateral surface that continues ventrally to the lateral flange of the quadrate, which is poorly preserved in NHMD 164741. In anterior view, the quadrate is straight for most of its length, but slightly laterally oriented distally. The lateral medial condyle of the quadrate is ventrally positioned in relation to the lateral condyle, and it is lateromedially inflated distally. The

quadrate in NHMD 164741 is relatively tall when compared to the rostrum height. This ratio is also higher in NHMD 164741 than in other sauropodomorphs (Table 4). The medial (=pterygoid) flange of the quadrate is poorly preserved in NHMD 164741 but is in articulation to the posterolateral process of the pterygoid in the right element of NHMD 164758. This articulation occurs at the medial surface of this flange.

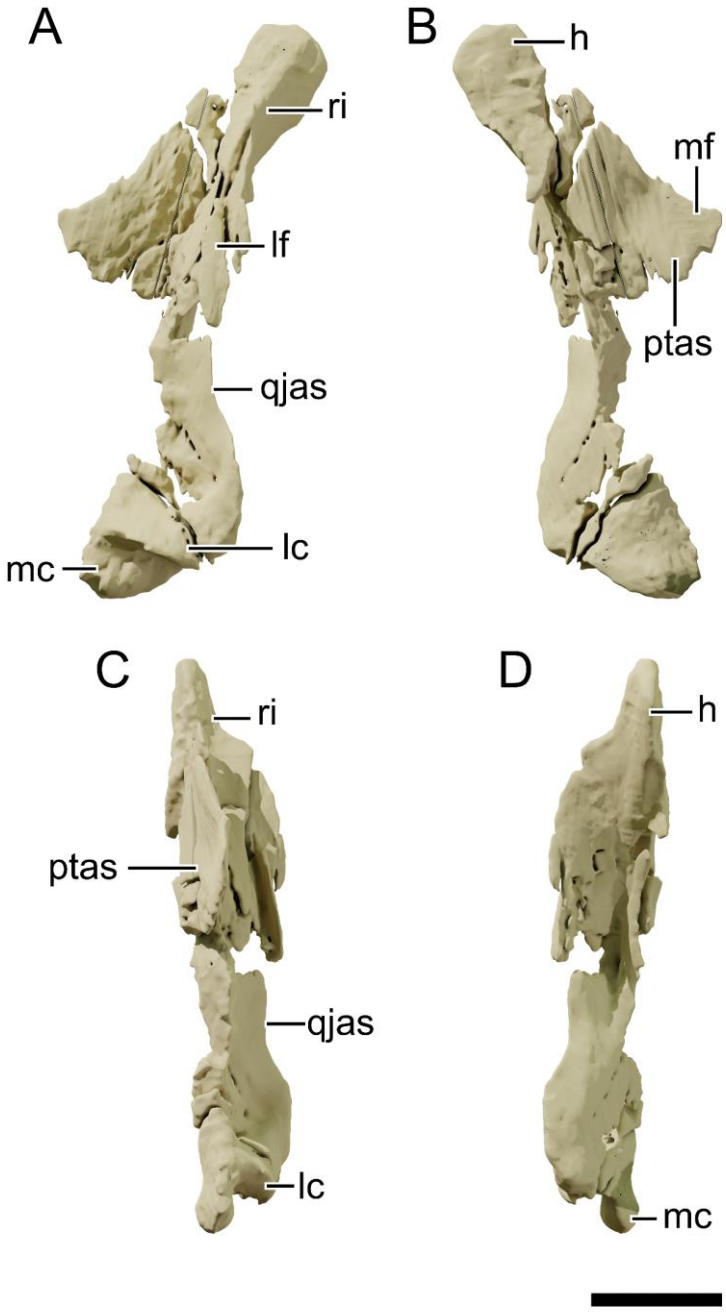

Figure 3.15 - NHMD 164741 left quadrate. Digital model of the left quadrate of NHMD 164741 in lateral view (A), medial view (B), anterior view (C), and posterior view (D). Abbreviations: h, head; lc, lateral condyle; lf, lateral flange; mc, medial condyle; mf, medial flange; ptas, articular surface for the pterygoid; qjas, articular surface for the quadratojugal; ri, ridge. Scale bar = 20 mm.

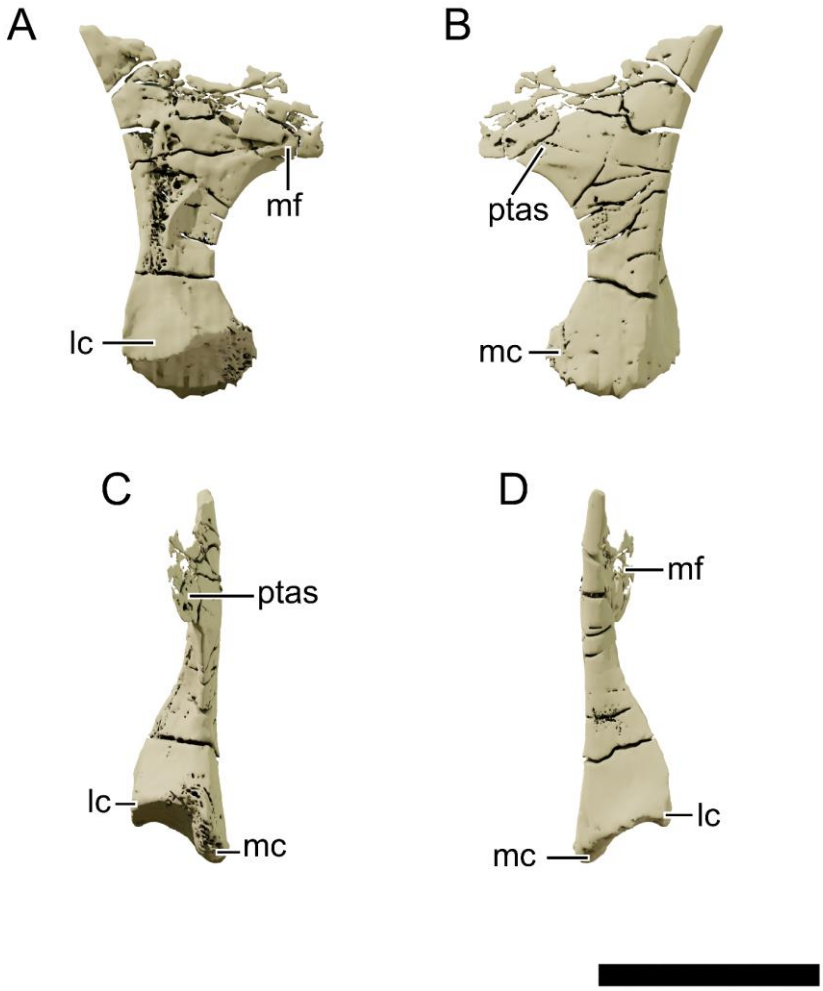

Figure 3.16 - NHMD 164758 right quadrate. Digital model of the right quadrate of NHMD 164758 in lateral view (A), medial view (B), anterior view (C), and posterior view (D). Abbreviations: lc, lateral condyle; mc, medial condyle; mf, medial flange; ptas, articular surface for the pterygoid. Scale bar = 20 mm.

Table 4 - Quadrate dorsoventral height to rostrum dorsoventral height ratio. The rostrum height is measured at the posterior margin of the external naris, from the ventral tip of the maxilla to the dorsal tip of the nasal. Measurements were taken on the 3D models when available.

Quadrate - dorsoventral height to rostrum dorsoventral height		
Greenland specimen	NHMD 164741	1.57
P. trossingensis	AMNH FARB 6810	1.18
P. trossingensis	NAAG_00011238	1.30
P. trossingensis	MSF 11.4	1.27
P. trossingensis	MSF 15.4	1.13
Macrocollum	CAPPA/UFSM 0001a	1.28
Buriolestes	CAPPA/UFSM 0035	1.40
M. carinatus	BP/1/5241	1.12
Ngwevu	BP/1/4779	1.11

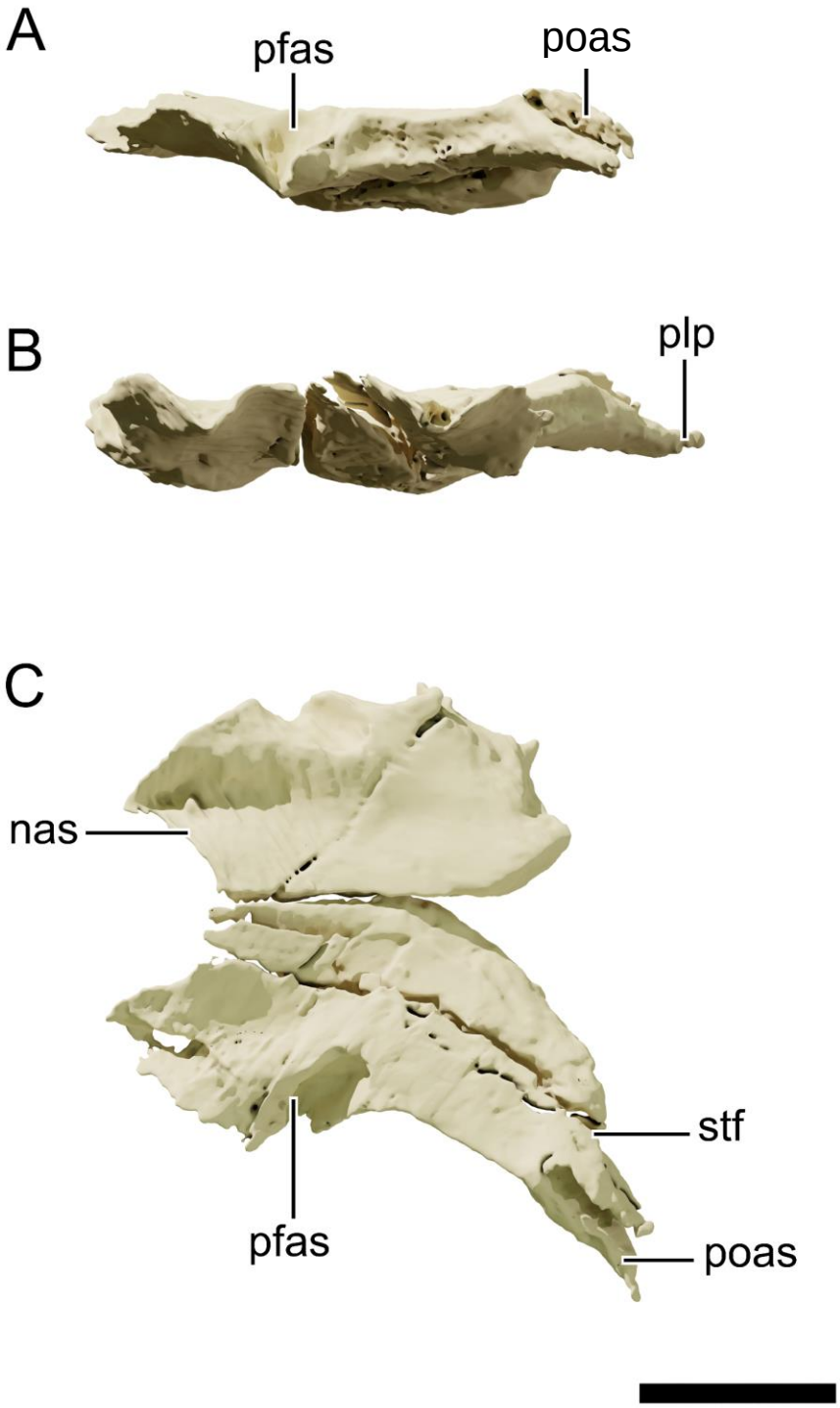

Figure 3.17 - NHMD 164741 frontals. Digital model of the frontals of NHMD 164741 in lateral view (A), anterior view (B), and dorsal view (C). Abbreviations: nas, articular surface for the nasal; pfas, articular surface for the prefrontal; poas, articular surface for the postorbital; plp, posterolateral process; stf, supratemporal fossa. Scale bar = 20 mm.

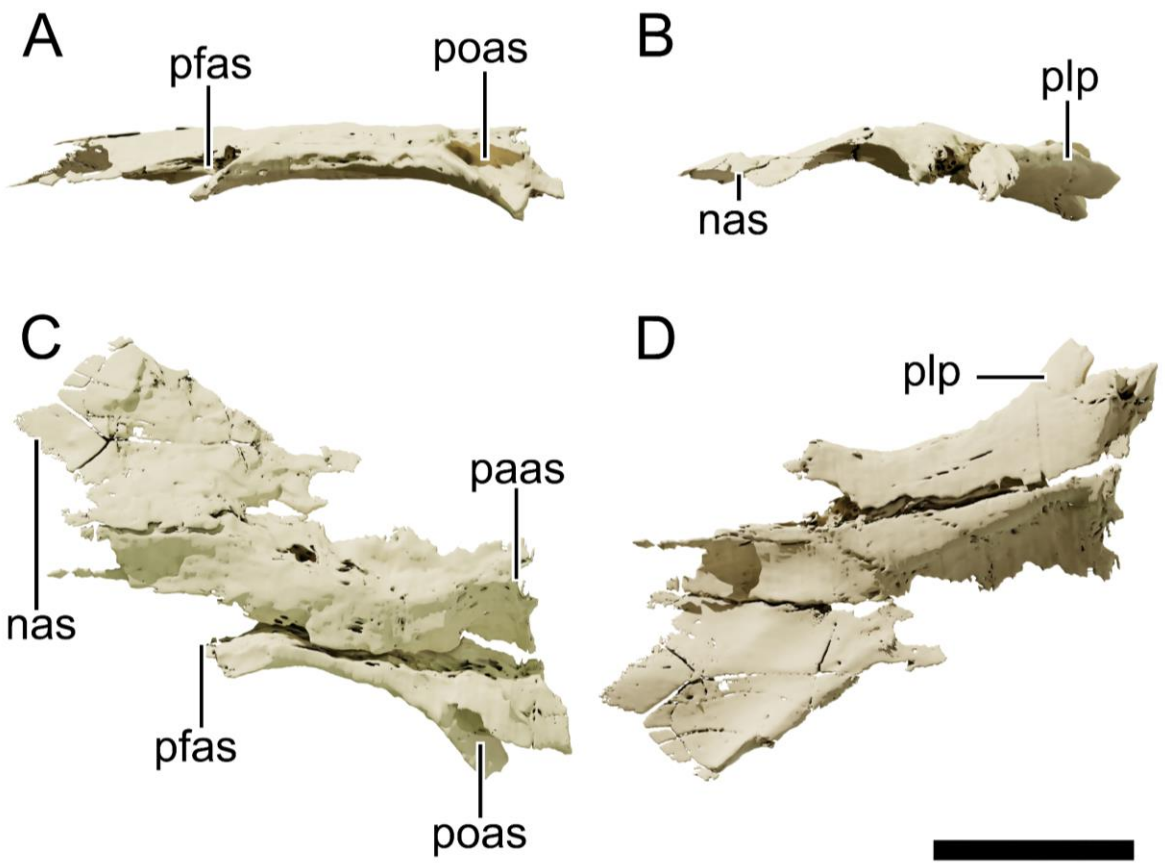

Figure 3.18 - NHMD 164758 frontals. Digital model of the frontals of NHMD 164758 in lateral view (A), anterior view (B), dorsal view (C), and ventral view. Abbreviations: nas, articular surface for the nasal; paas, articular surface for the parietal; pfas, articular surface for the prefrontal; poas, articular surface for the postorbital; plp, posterolateral process; stf, supratemporal fossa. Scale bar = 20 mm.

3.6.12 Frontal

Both frontals of NHMD 164741 are displaced, with the left frontal preserving most of its total length (Fig. 3.18), whereas in NHMD 16758 only the left frontal is preserved (Fig. 3.19). The frontal delimits the orbit lateroventrally but is excluded from the supratemporal fenestra by the parietal. The dorsal margin of the frontal is slightly concave in lateral view. The anterodorsal margin of the frontal forms a depression at its mid-width, raising the lateral and medial margins of the bone. Lateral to this depression, an indentation encapsulates the posterior process of the prefrontal, as in *Plateosaurus*. In dorsal view, directly behind this indentation, the lateral margin of the frontal broadens, forming the posterolateral (=postorbital) process of the frontal. This process is well developed and extends further laterally in NHMD 164741, but not as much in NHMD 164758. The distal end of the process forms a groove for the insertion of the anterodorsal process of the postorbital. The medioventral margin of this process is bound by the parietal in NHMD 164758. The lateral half of the posterior margin of the posterolateral process is excavated, forming the anterior margin of the supratemporal fossa, as in *Macrocollum* and *Plateosaurus* but absent in *Coloradisaurus* and *Massospondylus*.

3.6.13 Parietal

Only the anterior part of the left parietal is preserved in NHMD 164758 (Fig. 3.20), and the posterolateral process of the left parietal in NHMD 164741 (Fig. 3.2-3.3). The anterolateral process of the parietal articulates to the mediodorsal process of the postorbital, excluding the frontal from the supratemporal fenestra. This process of the parietal bounds the anteromedial margin of the

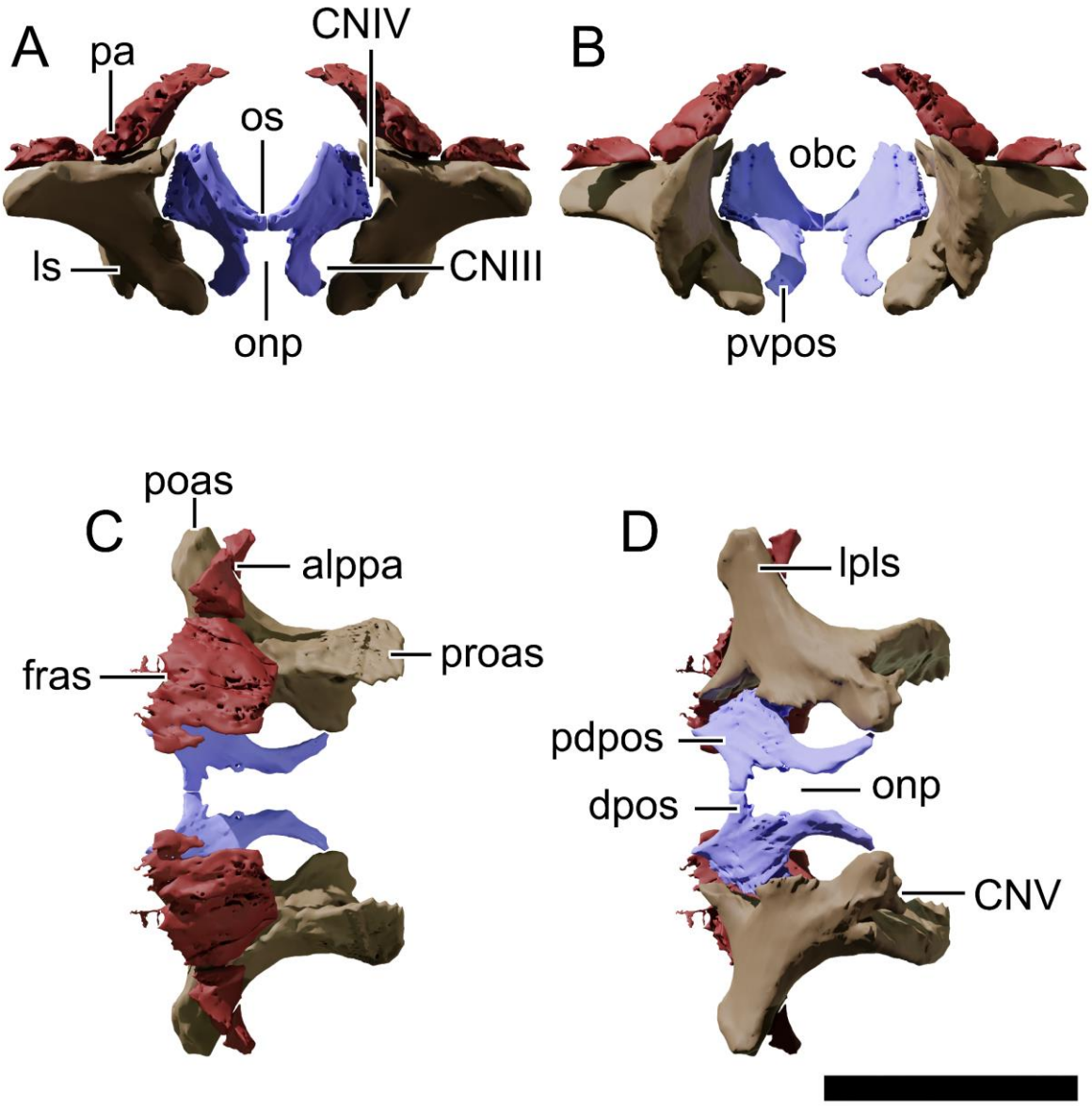

Figure 3.19 - NHMD 164758 braincase elements. Digital reconstruction of the mirrored braincase elements of NHMD 164758 in anterior view (A), posterior view (B), dorsal view (C), and ventral view (D). Abbreviations: alppa, anterolateral process of the parietal; CN, cranial nerve; dpos, dorsal process of the orbitosphenoid; fras, articular surface for the frontal; lpls, lateral process of the laterosphenoid; ls, laterosphenoid; obc, olfactory bulb canal; onp, optic nerve passage; os, orbitosphenoid; pa, parietal; pdpos, posterodorsal process of the orbitosphenoid; poas, articular surface for the postorbital; proas, articular surface for the prootic; pvpos, posteroventral process of the orbitosphenoid. Scale bar = 20 mm

supratemporal fenestra. The frontal-parietal suture is rugose and slightly elevated medially, as in *P. trossingensis*. The posterolateral process of the parietal is gently convex laterally, anteroposteriorly longer than dorsoventrally tall and mediolaterally flat. The lateral surface contacts the anteromedial and the proximal half of the posterior processes of the squamosal, and contacts medially the lateral surface of the paroccipital process of the otoccipital. The distal end of this process slopes ventrally.

3.6.14 Orbitosphenoid

The orbitosphenoid is a thin sheet of bone and only preserved in NHMD 164758 (Fig. 3.20). When articulated at its original position, the orbitosphenoid forms the anterior wall of the braincase and contacts the laterosphenoid in three points. The orbitosphenoid contains three processes, one on the anterior surface (dorsal process) that contacts its counterpart medially, and two (posterodorsal and posteroventral processes) on the posterior surface, articulating with the laterosphenoid. The dorsal process forms the anteroventral margin of the olfactory bulb and contacts its counterpart. The posteroventral process of the orbitosphenoid is the longest process. It differs from the condition in *M. carinatus* BP/1/5241where the posterodorsal process is the longest. The distal half of this process is laterally deflected and contacts the laterosphenoid laterally. The medial surface of this process forms with its counterpart the dorsolateral margins of the optic nerve passage.

The contacts between the laterosphenoid and the orbitosphenoid were digitally recreated. These contacts forms two lateral foramina, a dorsal foramen that is smaller in diameter than the ventral foramen. This is another feature that distinguishes NHMD 164758 from *M. carinatus* BP/1/5241, as the dorsal foramen is the largest in the latter. The dorsal foramen would have formed the passage to the cranial nerve IV (CNIV), whereas the ventral would have formed the passage to the cranial nerve III (CNIII).

3.6.15 Laterosphenoid

The laterosphenoids of both NHMD 164741 and NHMD 164758 are disarticulated and displaced. When articulated in its original position in NHMD 164758 (Fig. 3.20), the laterosphenoid contacts the orbitosphenoid anteriorly, the frontal anterodorsally, the parietal dorsally, the postorbital laterally. However, it remains unclear if the condition of *P. trossingensis* of a ventral contact to the basisphenoid occurs. The anterodorsal ramus of the laterosphenoid is a finger-like anterior projection that contacts the frontal distally and dorsally, and the orbitosphenoid medially. The lateral (=postorbital) process extends laterodorsally and has a distal inflated articular surface for the postorbital. This process is dorsoventrally robust and contacts the medial surface of the anterodorsal process of the postorbital. In

P. trossingensis AMNH FARB 6810, the postorbital process is proportionally much longer, slender and curving anterodorsally than in NHMD 164758 (Prieto-Márquez & Norell, 2011, fig. 26). In this sense, NHMD 164758 laterosphenoid is closer to the condition observed in *M. carinatus* and *Ngwevu*. The posterior region of the laterosphenoid articulates with the prootic and contains a deep notch that forms the anterior margin of the large trigeminal foramen (CNV), as in *Coloradisaurus* and *Plateosaurus*, but differing from the gently concave condition in *Ngwevu* and *M. carinatus*.

3.6.16 Otoccipital

The paroccipital process of NHMD 164741 (Fig. 3.2-3.3) is lateromedially flattened and dorsoventrally expanded. Distally it is laterally deflected and contacts the posterior process of the squamosal. Anteriorly the process expands to create the basioccipital articular surface. A deep, oval groove is present at the ventral surface of the proximal part of the paroccipital process, as in *P. trossingensis* AMNH FARB 6810.

3.6.17 Basioccipital

Only a small fragment of the occipital condyle is preserved in NHMD 164741 (Fig. 3.2-3.3), and part of the occipital condyle and the right basal tubera in NHMD 164758 (Fig. 3.4-3.5). The occipital condyle is convex ventrally and concave dorsally at the foramen magnum exit. The basal tubera is separated from the occipital condyle by a deep lateral fossa. This condition is not as extreme as in *P. gracilis* GPIT 18318a. Due to its disarticulated preservation, it is not possible to discern if the basioccipital is located dorsally to the basisphenoid.

3.6.18 Basisphenoid

The main body of the basisphenoid is missing on NHMD 164758 but preserved disarticulated in NHMD 164741 (Fig. 3.21). Both specimens preserve the basipterygoid process of the right basisphenoid, and the parasphenoid process (Fig. 3.22). As this element is disarticulated in both specimens, the autapomorphic feature of a high interbasipterygoid septum with a median process of *P. trossingensis* cannot be assessed. The basipterygoid process is wrapped by the median "hook-like" process of the pterygoid. This feature was considered to be autapomorphic for *P. trossingensis* (Galton & Kermack, 2010), but was also described for *Massospondylus* BP/1/5241 (Chapelle & Choiniere, 2018), possibly being generally variable in basal sauropodomorphs Lallensack *et al.*, 2021. In NHMD 164758, the basipterygoid process extends anteroventrally, as in the juvenile *M. carinatus* BP/1/4376, whereas in NHMD 164741 the basipterygoid process appears to extend ventrally and only slightly anteriorly, as in

the adult *M. carinatus* BP/1/5241, *Unaysaurus* UFSM11069 and *Thecodontosaurus* YPM 2192. In *P. trossingensis* MSF 15.8.1043 and MSF 07.M this process is posteroventrally oriented. The parasphenoid process is a long and slender anteriorly oriented process. In lateral view, the parasphenoid is smooth and does not feature the lateral deep groves observed in *P. trossingensis* MSF 07.M, MSF 08.M, and MSF 15.8.1043. In lateral view, the ventral margin of the parasphenoid is straight and the dorsal margin is gently convex distally. The dorsal surface of the parasphenoid is composed of a deep

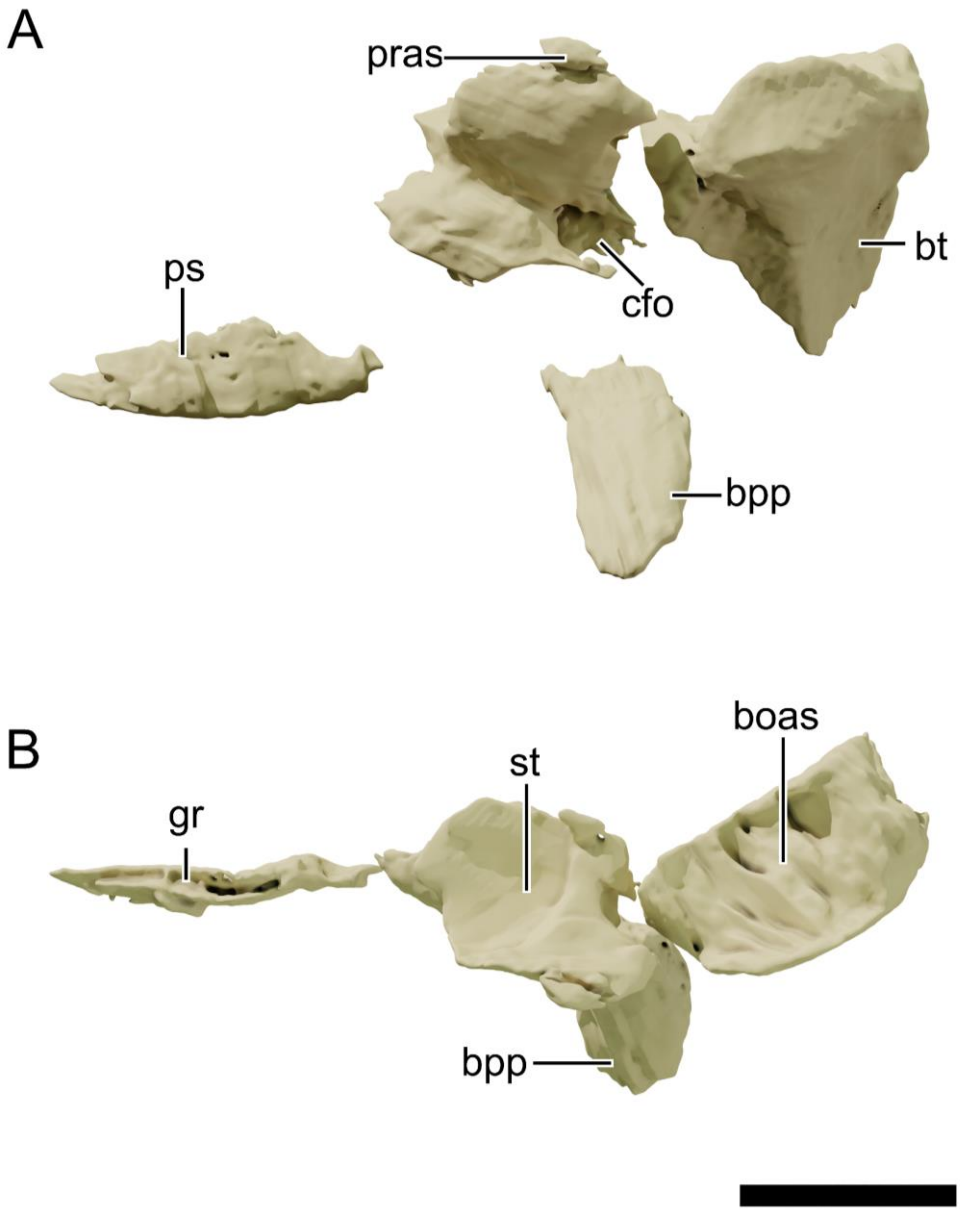

Figure 3.20 - NHMD 164741 basisphenoid. Digital model of the basisphenoid of NHMD 164741 in lateral view (A), and dorsal view (B). Abbreviations: boas, articular surface for the basioccipital; bpp, basipterygoid process; bt, basal tubera; cfo, carotid foramen; gr, groove; pras, articular surface for the prootic; ps, parasphenoid; st, sella turcica. Scale bar = 20 mm.

groove, making the cross-section of this bone U-shaped. This feature is similar to the one observed in *M. carinatus* BP/1/5241 and appears to be so in *P. trossingensis* MSF 15.8.1043.

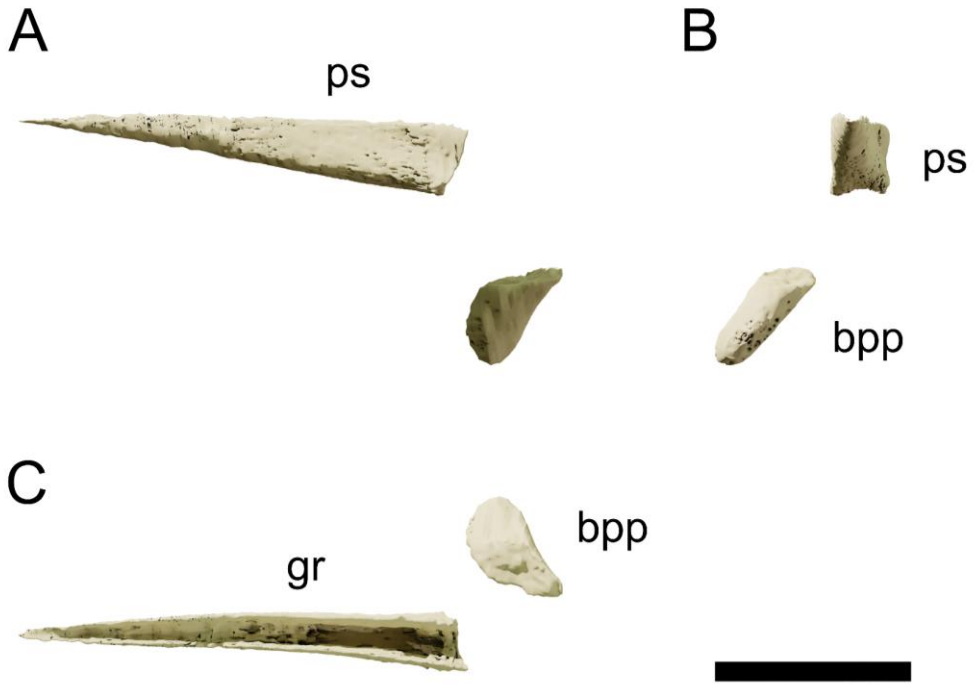

Figure 3.21 - NHMD 164758 basisphenoid. Digital model of the basisphenoid of NHMD 164758 in lateral view (A), anterior view (B), and dorsal view (C). Abbreviations: bpp, basipterygoid process; gr, groove; ps, parasphenoid. Scale bar = 20 mm.

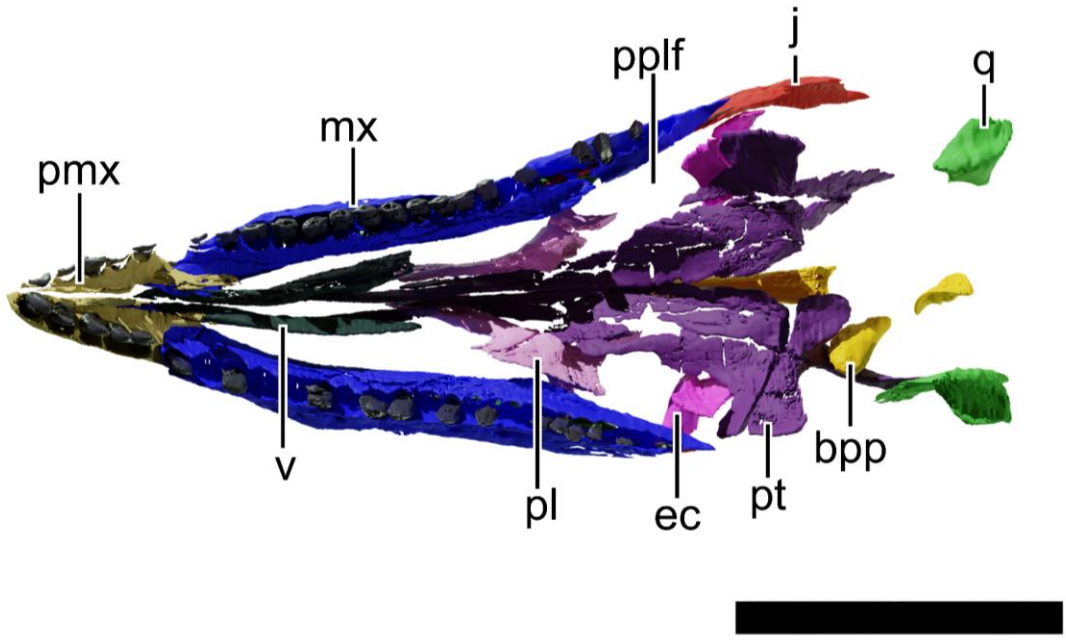

Figure 3.22 - NHMD 164758 palatal region of the skull. Digital reconstruction of the palatal region of NHMD 164758 in ventral view. Abbreviations: bpp, basipterygoid process; ec, ectopterygoid; j, jugal; mx, maxilla; pl, palatine; pmx, premaxilla; pplf, postpalatine fenestra; pt, pterygoid; q, quadrate; v, vomer. Scale bar = 50 mm.

3.6.19 Palate

The palate is best preserved in NHMD 164758, with all the composing elements partially articulated, almost complete and in anatomical position. NHMD 164741 preserves both pterygoids, the left ectopterygoid, fragments of both palatines and fragments of the left vomer. NHMD 164758 preserves both pterygoids, both ectopterygoids, both palatines and both vomers (Fig. 3.23-3.24). The postpalatine fenestra is bound anteriorly by the palatine, laterally by the maxilla, medially by the pterygoid and

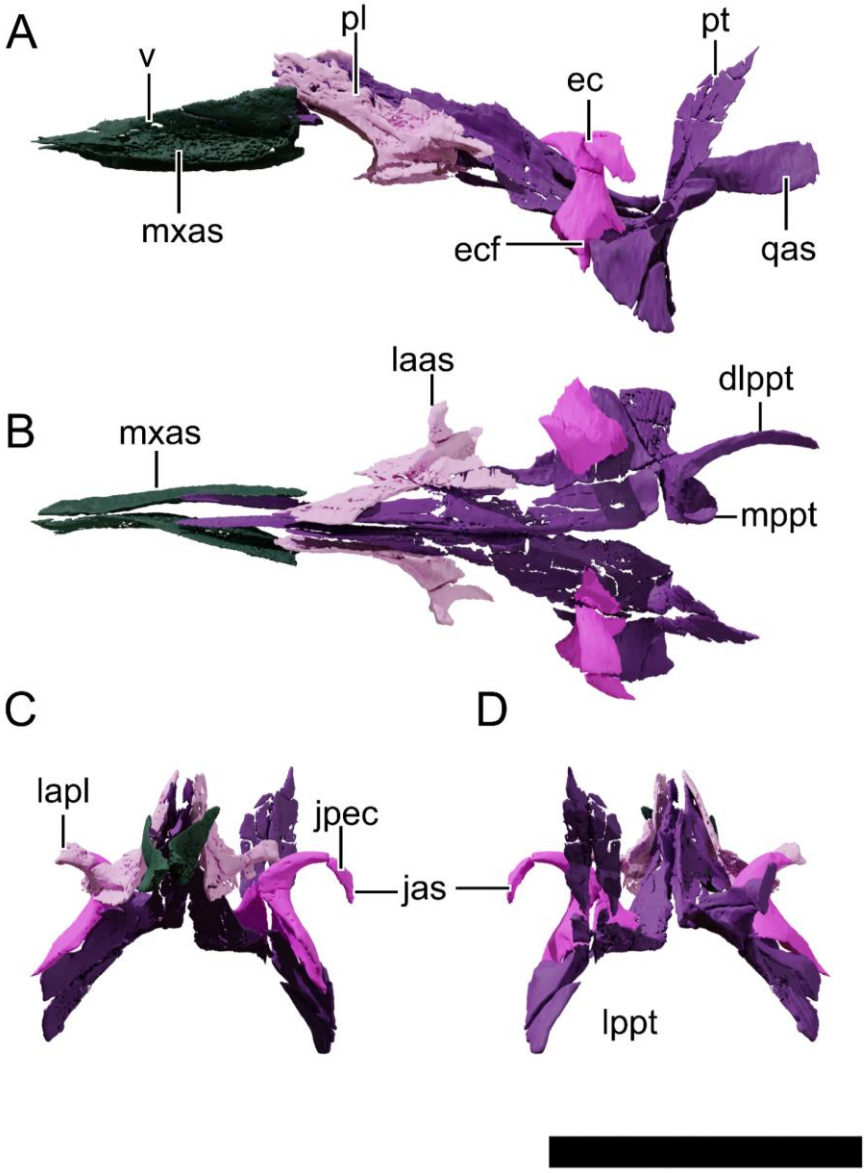

Figure 3.23 - NHMD 164758 palate. Digital reconstruction of the palate of NHMD 164758 in left lateral view (A), dorsal view (B), anterior view (C), and posterior view (D). Abbreviations: dlppt, dorsolateral process of the pterygoid; ec, ectopterygoid; ecf, ectopterygoid fossa; jas, articular surface for the jugal; jpec, jugal process of the ectopterygoid; laas, articular surface for the lacrimal; lapl, lateral process of the palatine; lppt, lateral process of the pterygoid; mppt, posteromedial process of the pterygoid; mxas, articular surface for the maxilla; pl, palatine; pt, pterygoid; qas, articular surface for the quadrate; v, vomer. Scale bar = 20 mm.

posteriorly by the ectopterygoid. This fenestra is slightly anteroposteriorly longer than lateromedially wide (Fig. 3.23).

3.6.20 Pterygoid

None of the pterygoids are complete, but the best-preserved are the left element in NHMD 164741 (Fig. 3.25) and the right one in NHMD 164758 (Fig. 3.26). The pterygoid is the largest component of the palate. It is a tetraradiate bone that composes the posterolateral area of the palate. The anterior process of the pterygoid is the longest and subdivided into two areas, a distal half that contacts the vomer

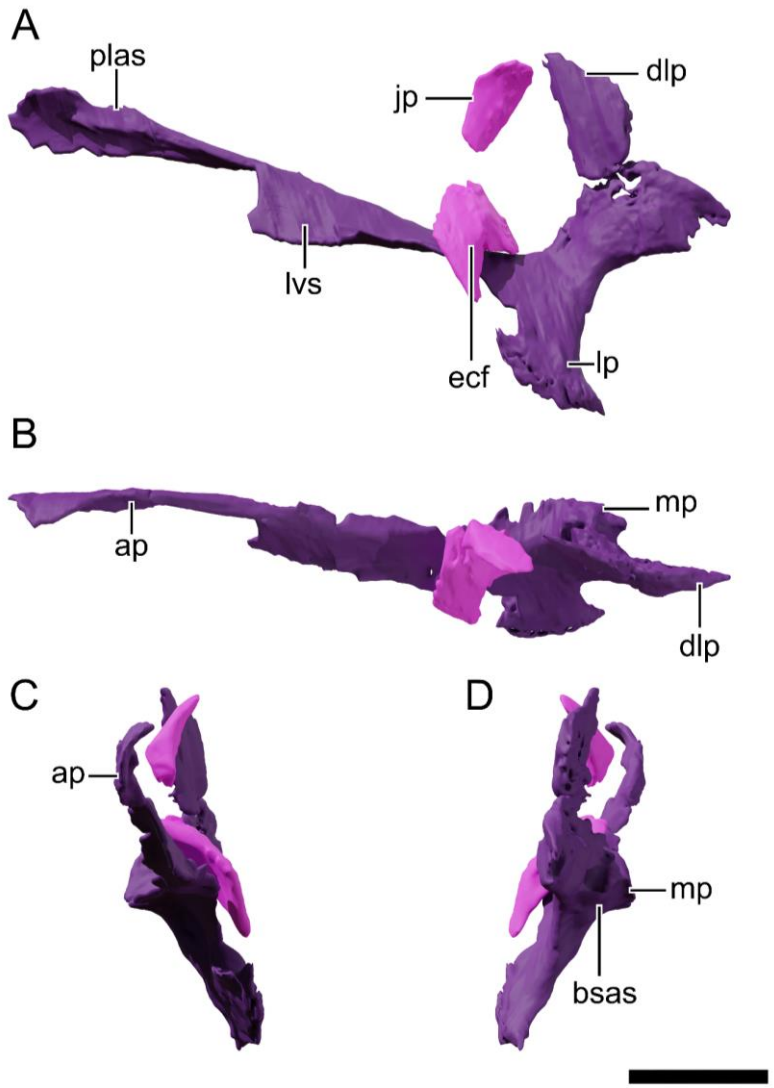

Figure 3.24 - NHMD 164741 pterygoid and ectopterygoid. Digital model of the left pterygoid and ectopterygoid of NHMD 164741 in lateral view (A), dorsal view (B), anterior view (C), posterior view (D). Abbreviations: ap, anterior process; bass, articular surface for the basisphenoid; dlp, dorsolateral process; ecf, ectopterygoid fossa; jp, jugal process; lp, lateral process; lvs, lateroventral sheet of bone; mp, medial process; plas, articular surface for the palatine. Scale bar = 20 mm.

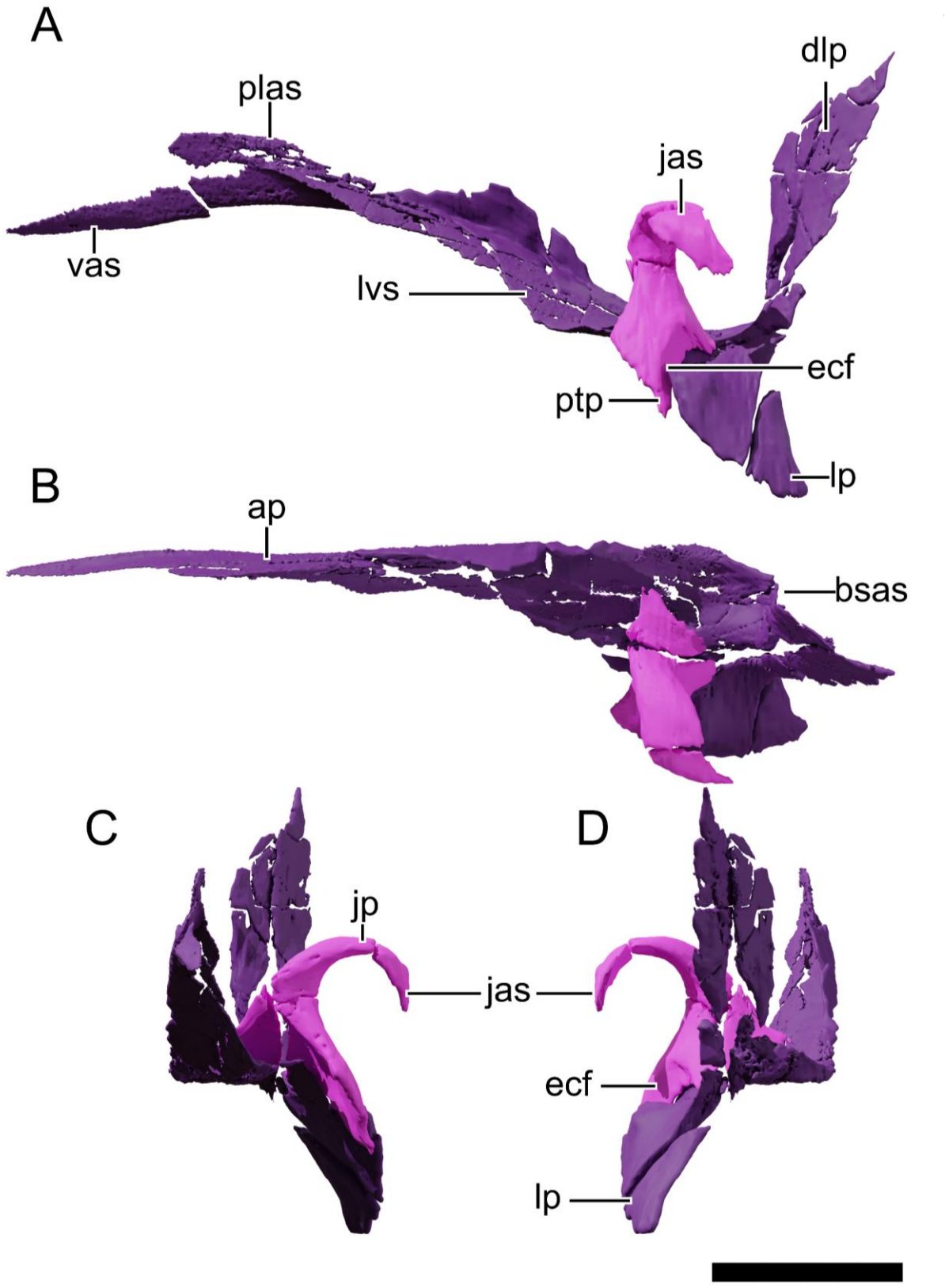

Figure 3.25 - NHMD 164758 pterygoid and ectopterygoid. Digital model of the left pterygoid and ectopterygoid of NHMD 164758 in lateral view (A), dorsal view (B), anterior view (C), posterior view (D). Abbreviations: ap, anterior process; bsas, articular surface for the basisphenoid; dlp, dorsolateral process; ecf, ectopterygoid fossa; jas, articular surface for the jugal; jp, jugal process; lp, lateral process; lvs, lateroventral sheet of bone; mp, medial process; plas, articular surface for the palatine. Scale bar = 20 mm.

of the pterygoid is slender and terminates in a sharp tip in NHMD 164758 and a spatulated tip in NHMD 164741. However, the distalmost part seems to be broken in the latter. The proximal half of the anterior process is lateroventrally expanded forming a dorsoventrally high lamina.

The lateral process of the pterygoid is anteroposteriorly expanded and dorsoventrally flattened. This process is separated from the anterior process by an almost 90º angle in lateral view. The medial surface that separates both processes is highly dorsoventrally concave. The distal area of the lateral process is inflated both anteroposteriorly and dorsoventrally. This process contacts the ectopterygoid laterally and anteriorly.

The dorsolateral (=quadrate) process of the pterygoid is broken on both specimens. This process curves lateroposteriorly and contacts the pterygoid flange of the quadrate laterally. Medially at the proximal surface of this process, it contacts the lateral surface of the basipterygoid process. As mentioned before, the medial process of the pterygoid is hook-shaped and wraps the basipterygoid laterally.

3.6.21 Ectopterygoid

The left ectopterygoid of NHMD 164758 is the best preserved (Fig. 3.26). This bone is divided into two processes, a dorsal (=jugal) and a ventral (=pterygoid). The dorsal process is hook-shaped and expands dorsolaterally in the proximal half and ventrally in the distal half. The distal half contacts laterally the posteroventral half of the jugal. This contact forms the posterior margin of the postpalatine fenestra in dorsal view. The contact margin of the dorsal process of the ectopterygoid is similar to that of *Macrocollum*, contrasting with the anteriorly projected, T-shaped tip of *P. trossingensis* AMNH FARB 6810.

The ventral process of the ectopterygoid is dorsoventrally elongated, expanding over the lateral surface of the pterygoid. The distal tip of the ventral process of the ectopterygoid is dorsally obscured by the distal expansion of the lateral process of the pterygoid. Posteriorly, the ectopterygoid is concave, forming the articular surface to the pterygoid (Fig. 3.25-3.26).

3.6.22 Palatine

Both palatines are preserved in NHMD 164758 (Fig. 3.27) as well as in NHMD 164741, but are fragmented in the latter. The palatine is anteroposteriorly elongated and lateromedially flattened. The anterior process of the palatine expands anterodorsally and slightly laterally. This process contacts the posterior margin of the vomer distally and the anterior process of the pterygoid medially. Ventral to the contact with the pterygoid, the palatine expands medially and posteriorly. This expansion forms a

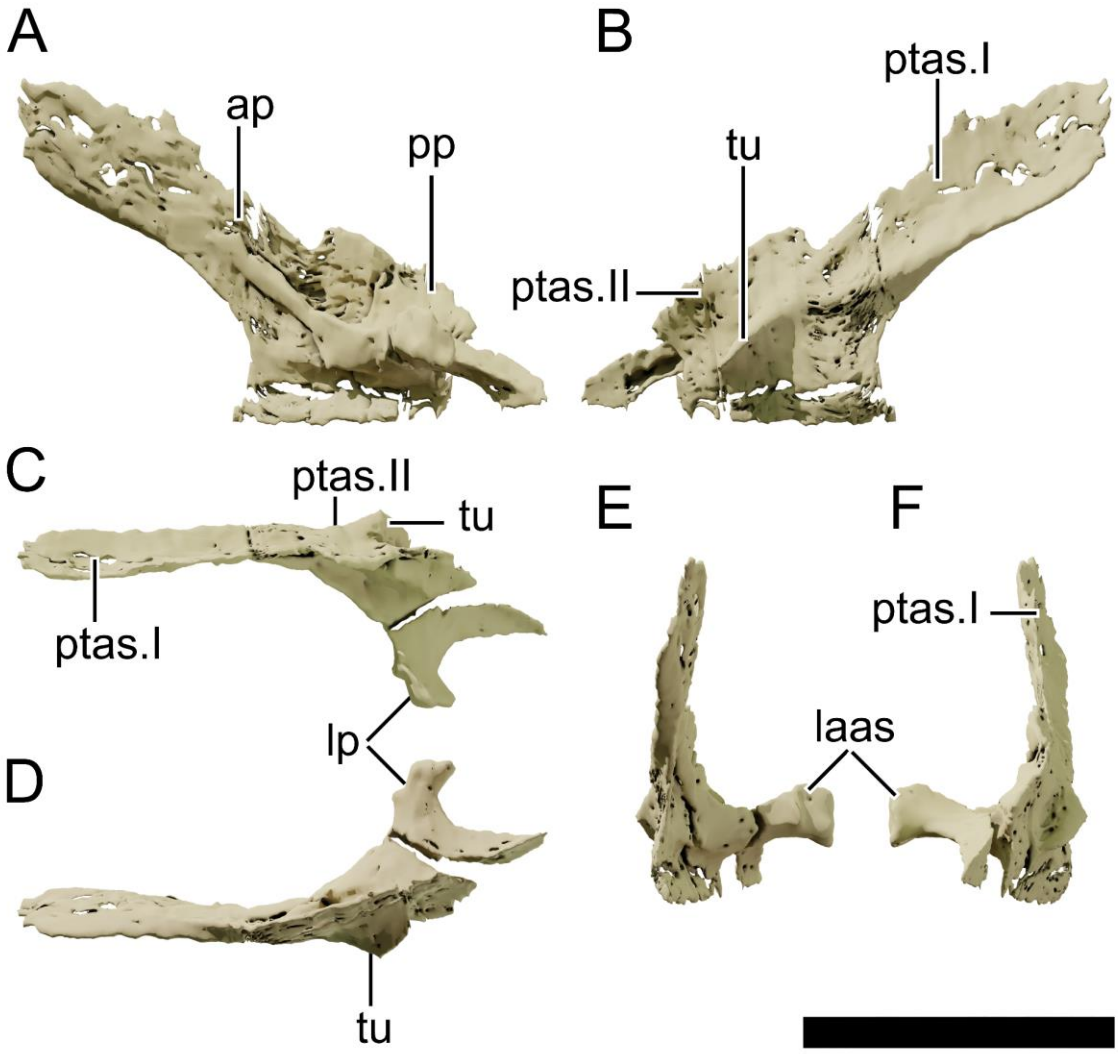

Figure 3.26 - NHMD 164758 left palatine. Digital model of the left palatine of NHMD 164758 in lateral view (A), medial view (B), dorsal view (C), ventral view (D), anterior view (E), and posterior view (F). Abbreviations: ap, anterior process; laas, articular surface for the lacrimal; lp, lateral process; pp, posterior process; ptas, articular surface for the pterygoid; tu, tubercle.

medial ridge and posteriorly a small tubercle. This tubercle, however, does not show the autapomorphic peg-like morphology of *P. trossingensis* observed by Galton and Upchurch (2004) and Prieto-Márquez and Norell (2011). The lateral process of the palatine forms the anterior and anteromedial margins of the postpalatine fenestra. This process contacts the ventral process of the lacrimal laterally. Ventral to this process, the palatine contacts the maxilla laterally. The posterior process of the palatine contacts the proximal half of the anterior process of the pterygoid dorsomedially.

3.6.23 Vomer

The vomers are better preserved in NHMD 164758 and form the anterior region of the palate (Fig. 3.23-3.24). This bone is anteroposteriorly elongated and triangular in shape in lateral view, with a tapered

anterior margin and a perpendicular and dorsoventrally tall posterior margin. The anteroposterior length of the vomer is slightly over 0.25 of the total skull anteroposterior length. This ratio is around 0.18 in *P. trossingensis* AMNH FARB 6810, 0.22 in *Ngwevu* BP/1/4779 and 0.31 in *M. carinatus* BP/1/5241. The vomer is laterally convex in anterior view, having a ventral lateral expansion that articulates with the ventromedial surface of the maxilla. The medial surface of the vomer contacts the anterior process of the pterygoid over a shallow medial ridge in the vomer. The posterior surface contacts the anterior process of the palatine in an almost straight margin.

3.6.24 Dentary

The specimen NHMD 164741 preserves both dentaries but lacks the anteriormost region of both (Fig. 3.28). NHMD 164758 preserves both complete dentaries partially in articulation (the right mandible is slightly ventrally deflected) (Fig. 3.29). The dentary is the largest bone in the mandible. The dentary articulates posteromedially with the splenial, dorsomedially with the coronoid, posteroventrally with the angular and posterodorsally with the surangular. Posteriorly, the dentary bounds the anterior margin of the mandibular fenestra. The dentary is slender and long, being over six times longer than tall, and over twice taller than wide (see Table 5 for measurements). In lateral view, the dorsal margin of the dentary is straight, and the ventral margin is slightly concave, as in *Unaysaurus*, *Macrocollum* and *Plateosaurus*, and different from the straight condition of basal sauropodomorphs such as *Buriolestes*. The symphysis in NHMD 164758 is straight at the medial contact surface to its counterpart. Posterior to the symphysis, the dentary is laterally deflected. The lateral and medial surfaces are parallel for most of the dentary extent, tapering posterolaterally to the last alveoli. The lateral surface of the anteriormost region of the left dentary in NHMD 164741 is missing, exposing three dentary teeth roots. In both NHMD 164741 and 164758, the dentary preserved a maximum of 18 alveoli, but this number might be underestimated in NHMD 164741 due to the lack of the anteriormost region. However, the anteriormost medial margin of the dentary in NHMD 164741 already represents the posterior surface of the symphysis, meaning that it is not missing much of the anterior area, having a possible maximum of 20 dentary teeth.

Table 5 - Mandible measurements of the Greenland specimens NHMD 164741 and NHMD 164758. * indicates maximum preserved measurement.

Measurements (in mm)	**NHMD 164741**	**NHMD 164758**
Mandible maximum length	210.1*	167.1
Mandible maximum height	45.6	33.8
Dentary maximum length	118.0*	100.1
Dentary maximum height	34.4	22.1

Surangular maximum length	118.1	79.8
Surangular maximum height	44.8	25.5

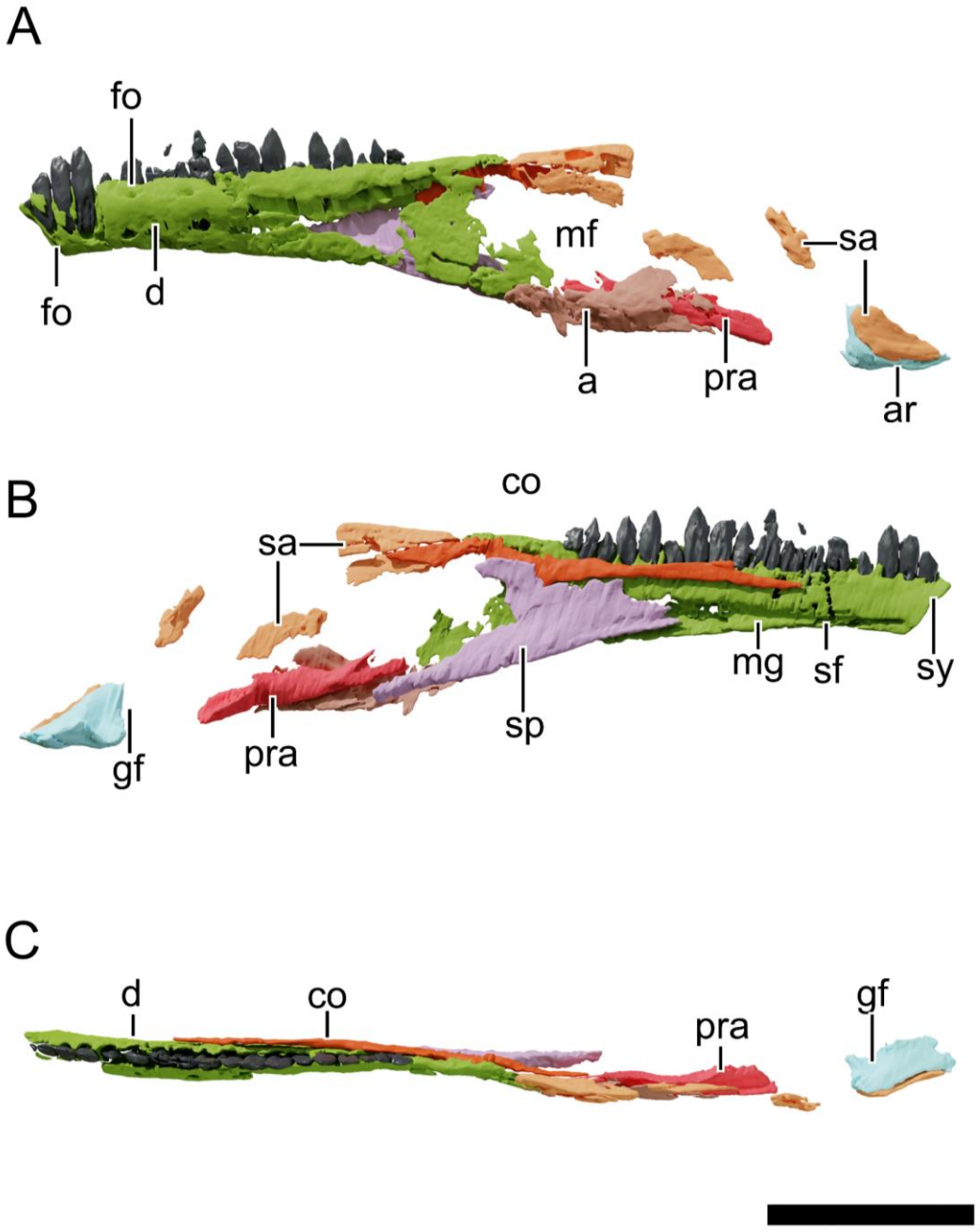

Figure 3.27 - NHMD 164741 left mandible. Digital model of the left mandible of NHMD 164741 in lateral view (A), medial view (B), and dorsal view (C). Abbreviations: a, angular; ar, articular; co, coronoid; d, dentary; fo, foramen; gf, glenoid fossa; mf, mandibular fenestra; mg, Meckelian groove; pra, prearticular; sa, surangular; sf, secondary fossa; sp, splenial; sy, symphysis. Scale bar = 50 mm.

A row of foramina is present at the first half of the dorsolateral surface, just below the alveolar margin, as in *Unaysaurus*, *Macrocollum* and *Plateosaurus*. Different from the 9-12 foramina in *P. trossingensis* AMNH FARB 6810, MSF 01 and MSF 16.1, both Greenland specimens only preserve 3-4 foramina. In NHMD 164741 these foramina are large and opened anterodorsally, whereas in NHMD 164758 these foramina are smaller and opening dorsally. Both dentaries of NHMD 164758 preserved a small

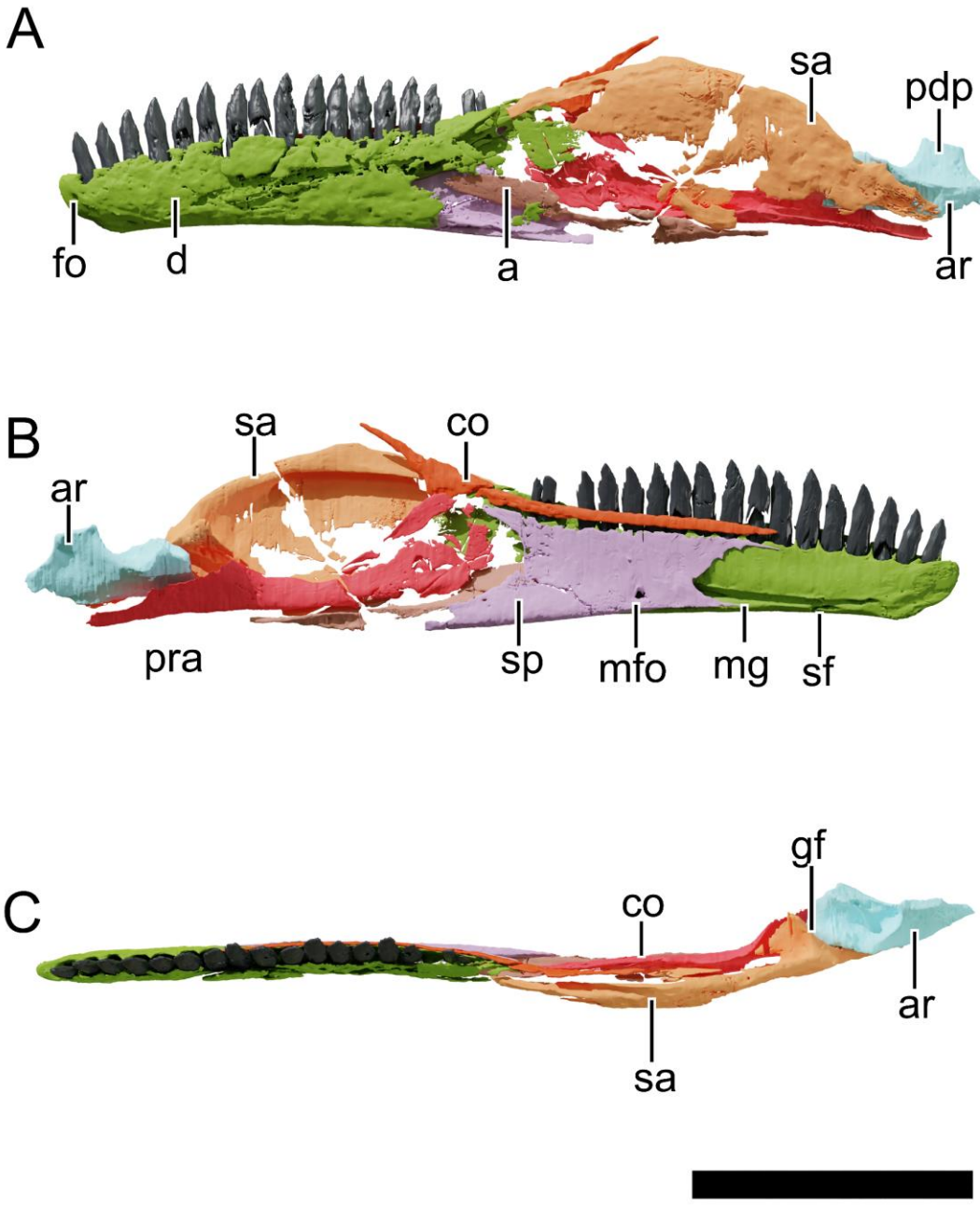

Figure 3.28 - NHMD 164758 left mandible. Digital model of the left mandible of NHMD 164758 in lateral view (A), medial view (B), and dorsal view (C). Abbreviations: a, angular; ar, articular; co, coronoid; d, dentary; fo, foramen; gf, glenoid fossa; mf, mandibular fenestra; mfo, mylohyoid foramen; mg, Meckelian groove; pdp, posterodorsal process; pra, prearticular; sa, surangular; sf, secondary fossa; sp, splenial; sy, symphysis. Scale bar = 50 mm.

anteroventral foramen at the lateral surface near the ventral corner of the dentary. This foramen was not reported for any other plateosaurid (*Macrocollum*, *Unaysaurus* and *Plateosaurus*), however, this might be caused by poorer preservation of this area in most specimens. In NHMD 164741 this feature cannot be assessed with confidence due to damage in this area. In *Pampadromaeus* ULBRA-PVT016 this foramen is situated dorsally.

The Meckelian groove extends longitudinally along the ventral part of the medial surface of the dentary. Anteriorly, this groove is constricted, and posteriorly dorsoventrally expanded and covered by the splenial medially. An anterior sheet of bone expands posteroventrally posterior to the symphysis, covering the anteriormost region of the Meckelian groove. This condition was observed in *Macrocollum* and *Unaysaurus*, on the latter, however, this sheet of bone is more developed. A deep, secondary fossa is present ventral to the anterior region of the Meckelian groove, as in *Unaysaurus*, and different from the single fossa condition of *Macrocollum*.

3.6.25 Splenial

The specimen NHMD 164758 preserves both complete splenials (Fig. 3.29), and NHMD 164741 only the left element (Fig. 3.28). The splenial is a rectangular sheet of bone that obscures the posteromedial surface of the dentary. Two processes extend anteriorly and posteriorly, one dorsally and one ventrally, making the anterior and posterior margins of the splenial concave in lateral view. The medial surface of the splenial is gently concave and contains a mylohyoid foramen ventrally at its anterior third. In *Buriolestes* CAPPA/UFSM 0035, this foramen is located at the midpoint dorsoventrally. In *Plateosaurus*, this foramen is not visible in medial view. The lateral surface contains a ventral sheet of bone that lies on the dorsal margin of the ventral region of the dentary. This sheet of bone continues posteriorly, forming the elongated posteroventral process. This process accommodates the anteroventral margin of the prearticular dorsally and the anteroventral margin of the angular ventrally. The dorsal margin of the splenial contacts the coronoid dorsally.

3.6.26 Intercoronoid/Coronoid

The intercoronoid is preserved on both mandibles of NHMD 164758 (Fig. 3.29) and in the left mandible of NHMD 164741 (Fig. 3.28). It is a slender and elongated bone that marginates the lingual surface of the dentary teeth. It extends anteriorly to the first third of the dentary. The coronoid is posterodorsally oriented and contacts the surangular laterally. The ventral margin of the coronoid is anteroposteriorly expanded and ventrally deflected, forming a triangular base for the coronoid as in *P. trossingensis* AMNH FARB 6810. The coronoid tappers in a more dorsal position *Ngwevu*.

3.6.27 Surangular

The left surangular in NHMD 164758 (Fig. 3.29) is the best-preserved surangular among the specimens. The surangular composes most of the posterolateral surface of the mandible and bounds the posterior margin of the mandibular fenestra. The surangular is sigmoid in lateral view, with the anterior half being more dorsoventrally expanded compared to the posterior half. The anterior (=dentary) process of the surangular is dorsally convex. It covers the posterodorsal corner of the dentary and is partially covered anteromedially by the coronoid. The anterior process is medioventrally expanded, forming a ventral groove that covers the dorsal corner of the adductor fossa. The lateral surface of the anterior process is slightly convex in anterior view and extends ventrally to contact the angular at its ventral margin. A medial expansion of the surangular is present posterior to the anterior process of the surangular. This expansion forms a mediolaterally wide flange that articulates anteroventrally to the prearticular and posterodorsally forms the surangular contribution to the glenoid fossa. This contribution is marked laterally by a deep transverse groove, as in *Pampadromaeus*, but is not as deep and marked in *P. trossingensis*. Posterior to the glenoid the surangular tappers dorsoventrally, marginating the lateral surface of the articular.

3.6.28 Angular

The left angular of NHMD 164741 is the best-preserved, although being broken at its posterior half (Fig. 3.28), whereas in NHMD 164758 both angular bones are fragmented (Fig. 3.29). It is a lateromedially flat bone with a medial concavity in anterior view. It contacts the posteroventral process of the dentary medially, the prearticular medially and the surangular dorsally. Anterodorsally it contributes to the posteroventral corner of the mandibular fenestra.

3.6.29 Prearticular

Both prearticulars are present in NHMD 164758 (Fig. 3.29), but only the main shaft of the left prearticular of NHMD 164741 is preserved (Fig. 3.28). Anteriorly, the prearticular is dorsoventrally expanded and lateromedially flat. This anterior region contacts the splenial anteriorly and the surangular dorsally and is sub-circular in lateral view. The main shaft is constricted dorsoventrally and concave laterally. Medially it bounds the ventral corner of the interior mandibular fenestra. The posteromedial process expands dorsally to contact the medial process of the surangular anteriorly and the medial surface of the articular laterally.

3.6.30 Articular

The anterior part of NHMD 164741 left articular is preserved (Fig. 3.28), and both articulars of NHMD 164758 are preserved and in articulation (Fig. 3.29-3.30). The anterior process of the articular forms the posterior half of the glenoid fossa dorsally. It is bound by a dorsolaterally oriented ridge and a well-developed medial pyramidal process, as in *P. trossingensis* AMNH FARB 6810. In *Macrocollum*, this medial expansion is less developed. The lateral surface of the articular is concave in anterior view and contacts the posterior process of the surangular, whereas medially the articular is slightly convex and contacts the posterior process of the prearticular. The articular of NHMD 164758 has a peculiar dorsoposterior process, situated posterior to the glenoid fossa (Fig. 3.30). This process is as tall as anteroposteriorly long, being more prominent dorsoventrally than in other plateosaurids, such as *Plateosaurus* and *Macrocollum*. This process tapers lateromedially dorsally, being triangular in cross-section. The retroarticular process tapers posteriorly and ends posterior to this dorsal process.

3.6.31 Dentition

The premaxillae of NHMD 164758 preserved a total of five premaxillary tooth alveoli each. The premaxillary teeth roots comprise around two-thirds of the total tooth height on the most complete preserved teeth. The premaxillary tooth crown is conical and slightly bent distally. A constriction separates the crown from the root. The mesial carina is convex and lacks denticles, as in most sauropodomorphs. The distal carina is concave and preserves coarse denticles perpendicular to the margin. These denticles start after the first third of the crown height and end just before reaching the apex. Both premaxillae contain replacement teeth erupting from the lingual side of the descended teeth. By the time the root of the replacement tooth starts to form, the crown and its denticles are fully developed, as observed in NHMD 164758 (Fig. 3.31).

The anteriormost teeth (i.e., anterior left premaxilla, anterior right maxilla, anterior left and right dentaries) are missing in NHMD 164741. The left premaxilla preserves the two caudal-most teeth in NHMD 164741. Both teeth are descended teeth with the replacement teeth still contained inside the alveoli. NHMD 164741 and NHMD 164758 preserve a maximum of 24 and 23 maxillary teeth alveoli on the left maxilla, respectively, and 18 dentary teeth alveoli on the left dentary. Both on the maxilla and dentary, the tooth size decreases at the caudal-most part of these bones. As preserved, the left dentary teeth occlude the left maxillary teeth in NHMD 164741, whereas the right maxillary teeth occlude the right dentary teeth.

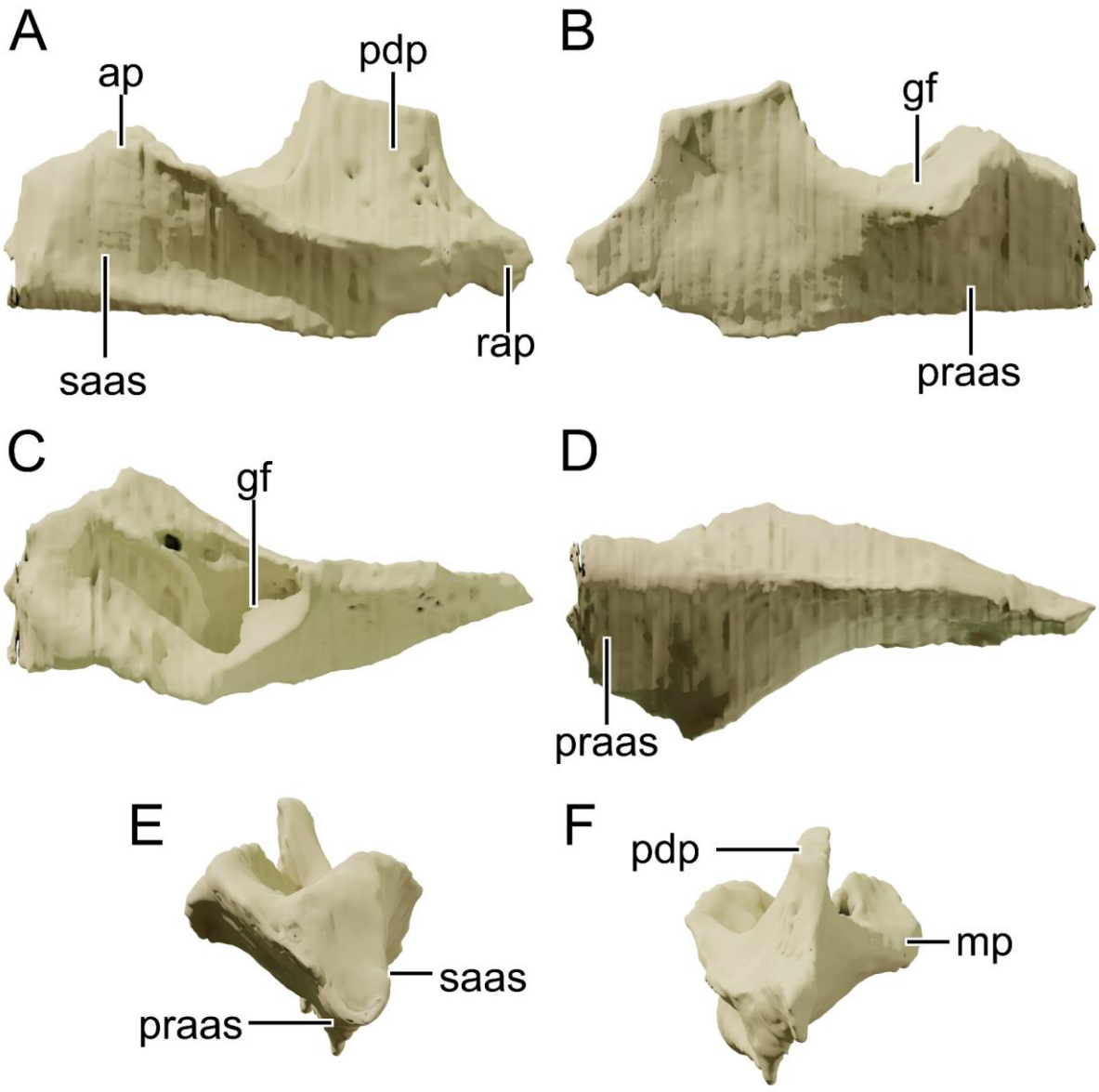

Figure 3.29 - NHMD 164758 left articular. Digital model of the left articular of NHMD 164758 in lateral view (A), medial view (B), dorsal view (C), ventral view (D), anterior view (E), and posterior view (F). Abbreviations: ap, anterior process; gf, glenoid fossa; mp, medial process; pdp, posterodorsal process; praas, articular surface for the prearticular; rap, retroarticular process; saas, articular surface for the surangular. Scale bar = 10 mm.

The maxillary and dentary teeth crowns are leaf-shaped, with both labial and lingual surfaces slightly convex and the mesial and distal carinas covered with coarse denticles. The denticles are deflected apically and are more abundant on the distal carina. As in the premaxillary teeth, the denticles start after the first third of the crown (Fig. 3.31 C-D). The apex of the teeth lacks denticles. The tooth root is slender and comprises most of the tooth height (average root height = 14.2 mm; average crown height = 8.6 mm in NHMD 164741). The labial surface of the root is slightly convex, whereas the lingual surface of the root is marked by a shallow groove, making the root overall B-shaped in cross-section (Fig. 3.32).

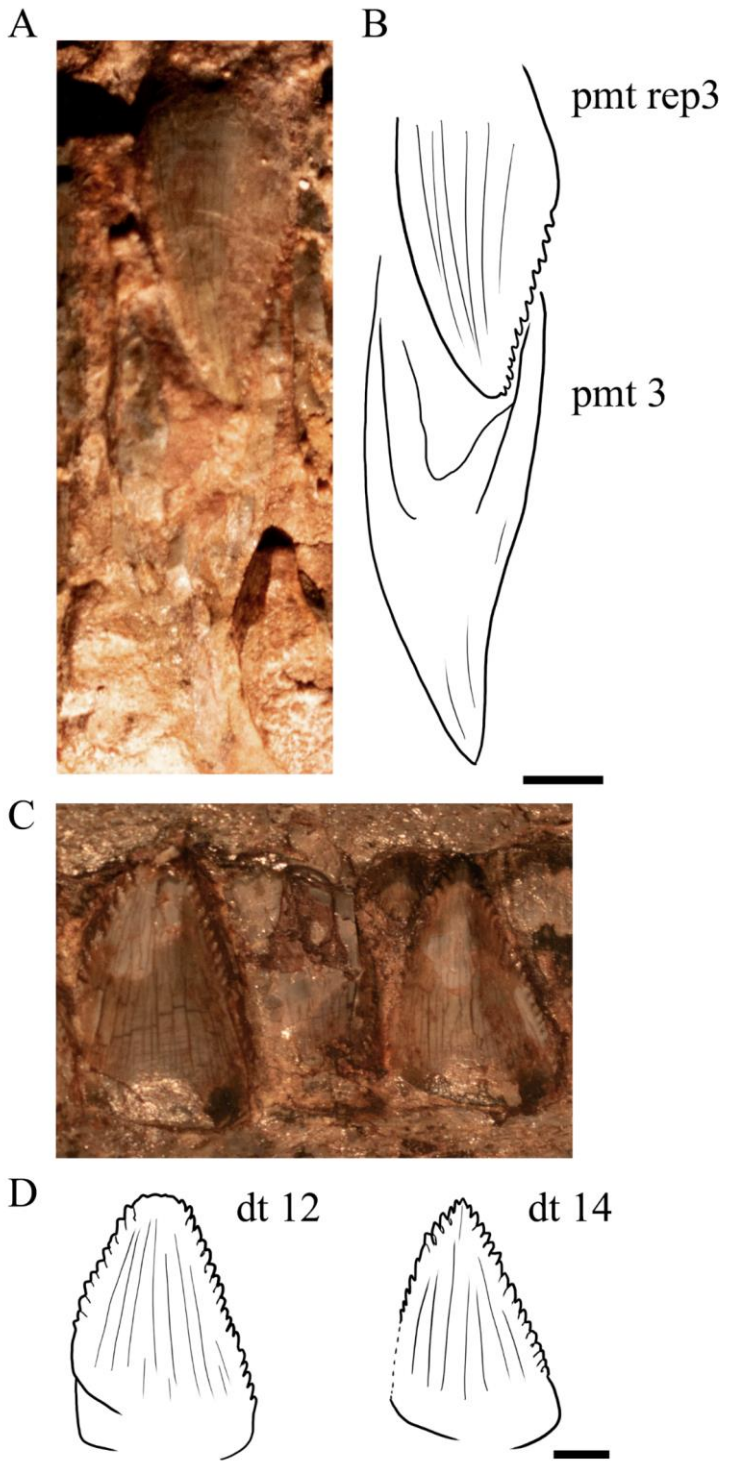

Figure 3.30 - NHMD 164741 and NHMD 164758 dentition. Left premaxillary replacement tooth in the third position of NHMD 164758 in labial view (photo A and line drawing B); Left dentary teeth in the 12th to 14th positions of NHMD 164741 in labial view (photo C and line drawing D). Scale bar = 2 mm.

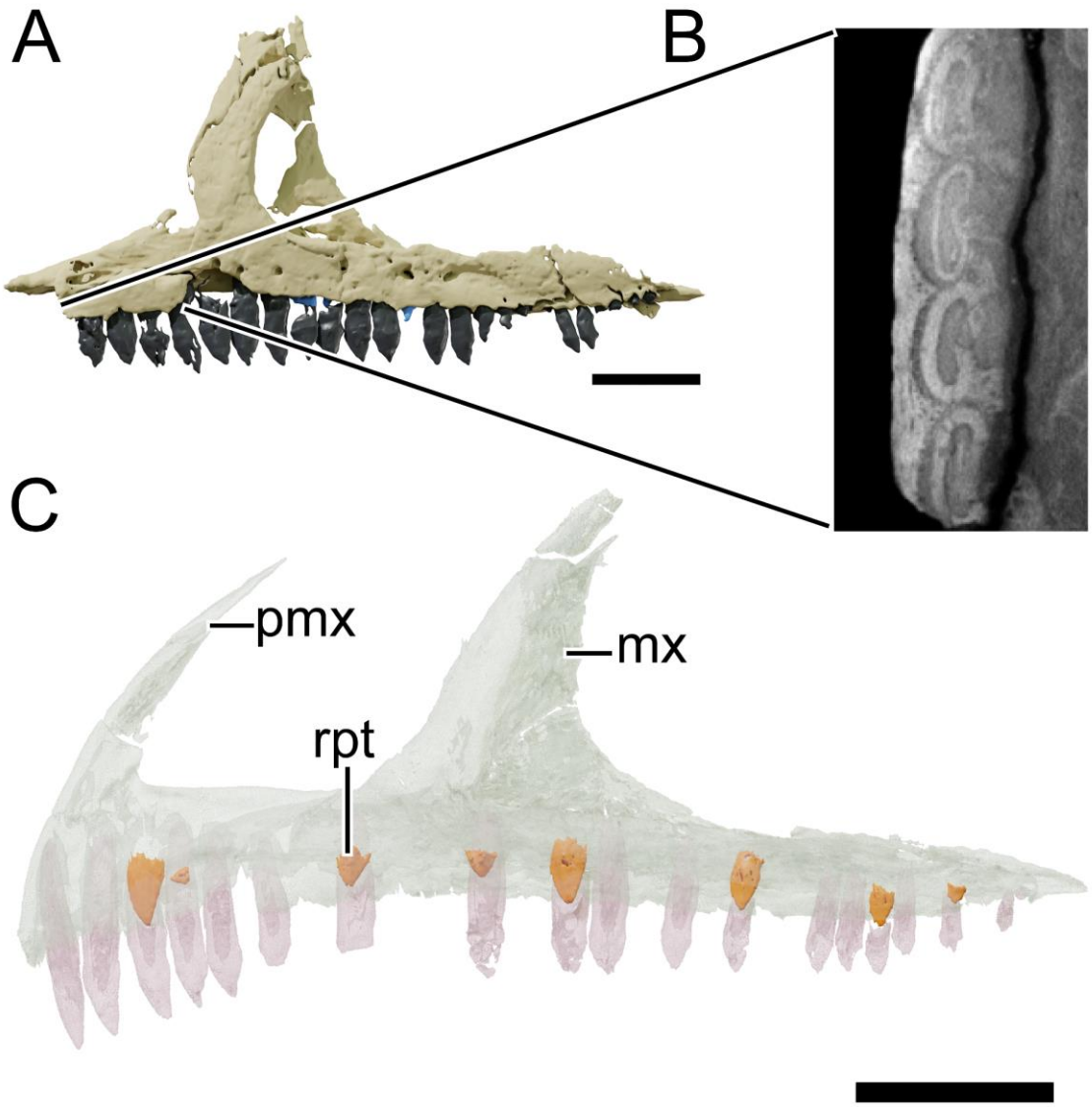

Figure 3.31 - NHMD 164741 and NHMD 164758 dentition. Digital model of the left maxilla of NHMD 164741 (A), slice of the anterior teeth of the maxilla of NHMD 164741 showing the teeth roots in cross-section (B), and mirrored reconstruction of the upper jaw of NHMD 164758 (C). Abbreviations: mx, maxilla; pmx, premaxilla; rpt, replacement tooth. Scale bar = 50 mm.

3.6.32 Hyoid

Four long and slender bone fragments pertaining to the hyoid apparatus are preserved in NHMD 164758. One of these rod-like bones is thicker and longer than the other three fragments (Fig. 3.4-3.5). It is sigmoid in lateral view, with a convex dorsal margin at its anterior half and a concave dorsal margin at its posterior half. This bone has an anterior round and blunt edge and ends posteriorly in an expanded and lateromedially flattened process. The posterior process is laterally depressed. The three slender fragments are located behind the left articular and are equal in diameter. These elements are arched anteroposteriorly but only preserved in the mid-shaft region.

3.6.33 Sclerotic Ring

A total of 18 lateromedially thin and square-shaped plates are partially in articulation in NHMD 164758 left orbit (Fig. 3.33). These plates form a circular arrangement, but the identification of the positive and negative plates cannot be fully assessed, nor is it possible to determine if the 18 plates constitute the whole sclerotic ring.

3.7 Skull reconstruction

Ontogenetic differences are thought to be consistent both in the cranial and post-cranial skeleton, and may not play a large role in the variation between skulls (Nau *et al.*, 2020; Lallensack *et al.*, 2021). Therefore, duplicating, and rescaling bones from one specimen to the other can help in building an accurate reconstruction. However, caution is advised, because the digital reconstruction shows minor changes in the proportions between NHMD 164741 and NHMD 164758 (Fig. 3.34-3.37, Table 6). For example, the orbit in NHMD 164758 is proportionally longer than in NHMD 164741 due to a slender ventral process of the postorbital in NHMD 164758 and a bulkier laterally expanded frontal in NHMD 164741. The skulls of both Greenland specimens are relatively longer than wide when compared to other plateosaurids, such as *Macrocollum* CAPPA/UFSM 0001b (skull length to width ratio = 2.0) and *P. trossingensis*, which was suggested to be between 1.95 and 2.2 (Lallensack *et al.*, 2021). When articulated, the quadrate proportions in NHMD 164758 are possibly closer to NHMD 164741 (quadrate height to rostrum height ratio = 1.6 in NHMD 164758).

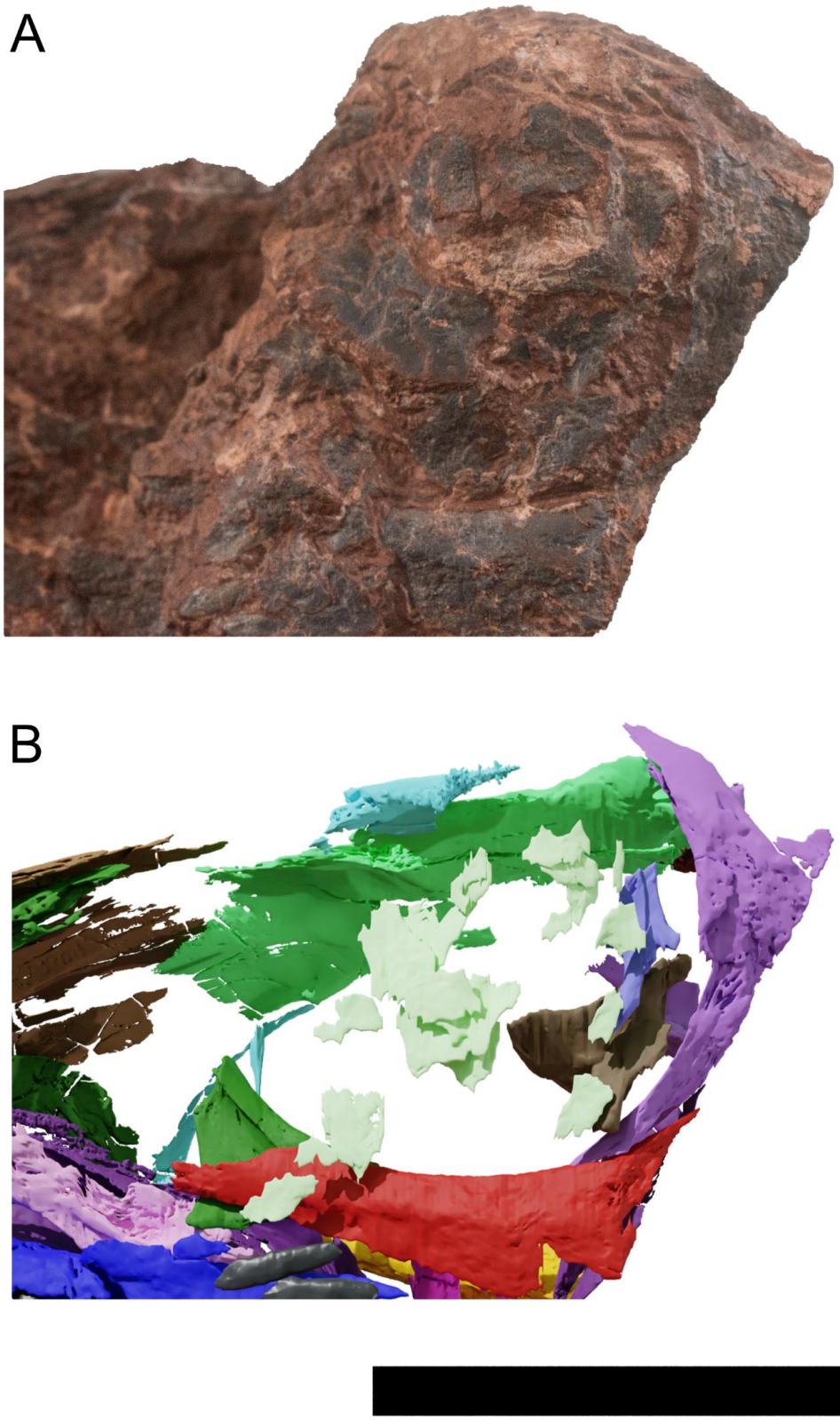

Figure 3.32 - NHMD 164758 orbit region. Photograph of the left lateral orbit region of NHMD 164758 (A) and digital model of the orbit region of NHMD 164758 (B). Scale bar = 50 mm.

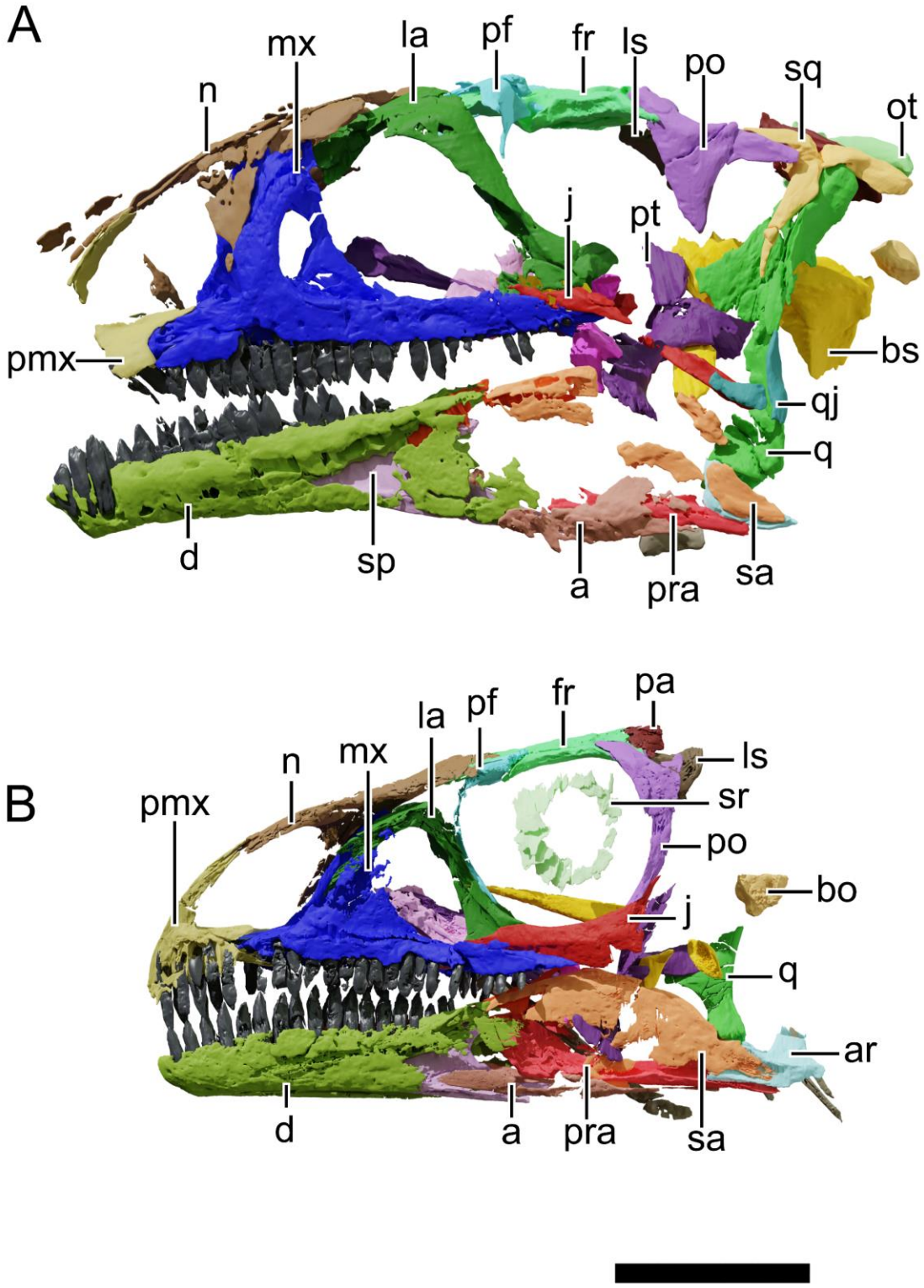

Figure 3.33 - NHMD 164741 and NHMD 164758 skull reconstruction. Digital manipulation of preserved bone elements of NHMD 164741 (A) and NHMD 164758 (B) in left lateral view. Abbreviations: ar, articular; bo, basioccipital; bs, basisphenoid; d, dentary; fr, frontal; j, jugal; la, lacrimal; ls, laterosphenoid; mx, maxilla; n, nasal; ot, otoccipital; pf, prefrontal; pmx, premaxilla; po, postorbital; pra, prearticular; pt, pterygoid; q, quadrate; qj, quadratojugal; sa, surangular; sp, splenial; sq, squamosal; sr, sclerotic ring. Scale bar = 50 mm.

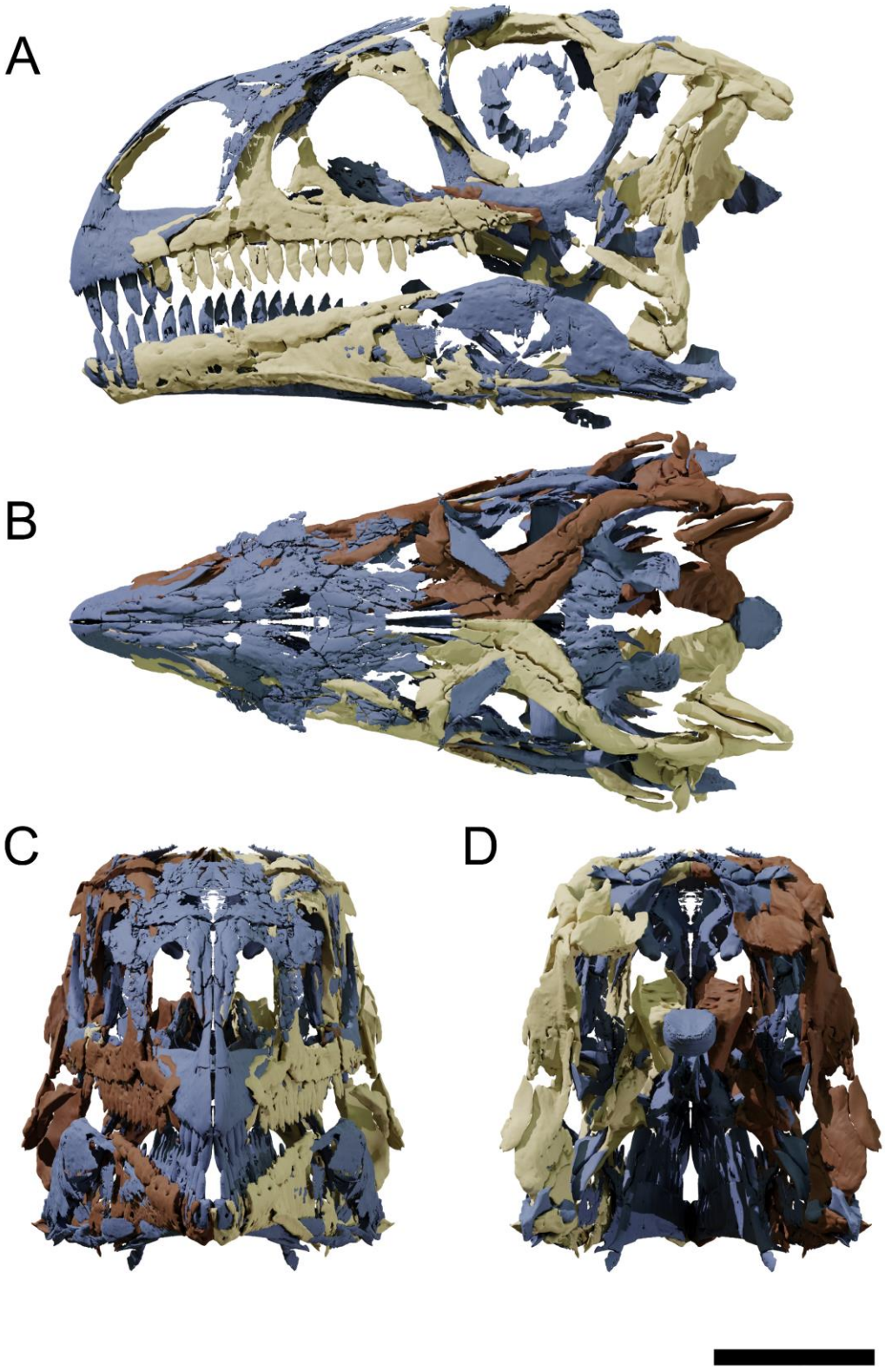

Figure 3.34 - NHMD 164741 skull reconstruction. Digital reconstruction of the skull NHMD 164741 in left lateral view (A), dorsal view (B), anterior view (C), and posterior view (D). Preserved bones in beige, mirrored elements in brown and scaled elements from the skull 164758 in blue. Scale bar = 50 mm.

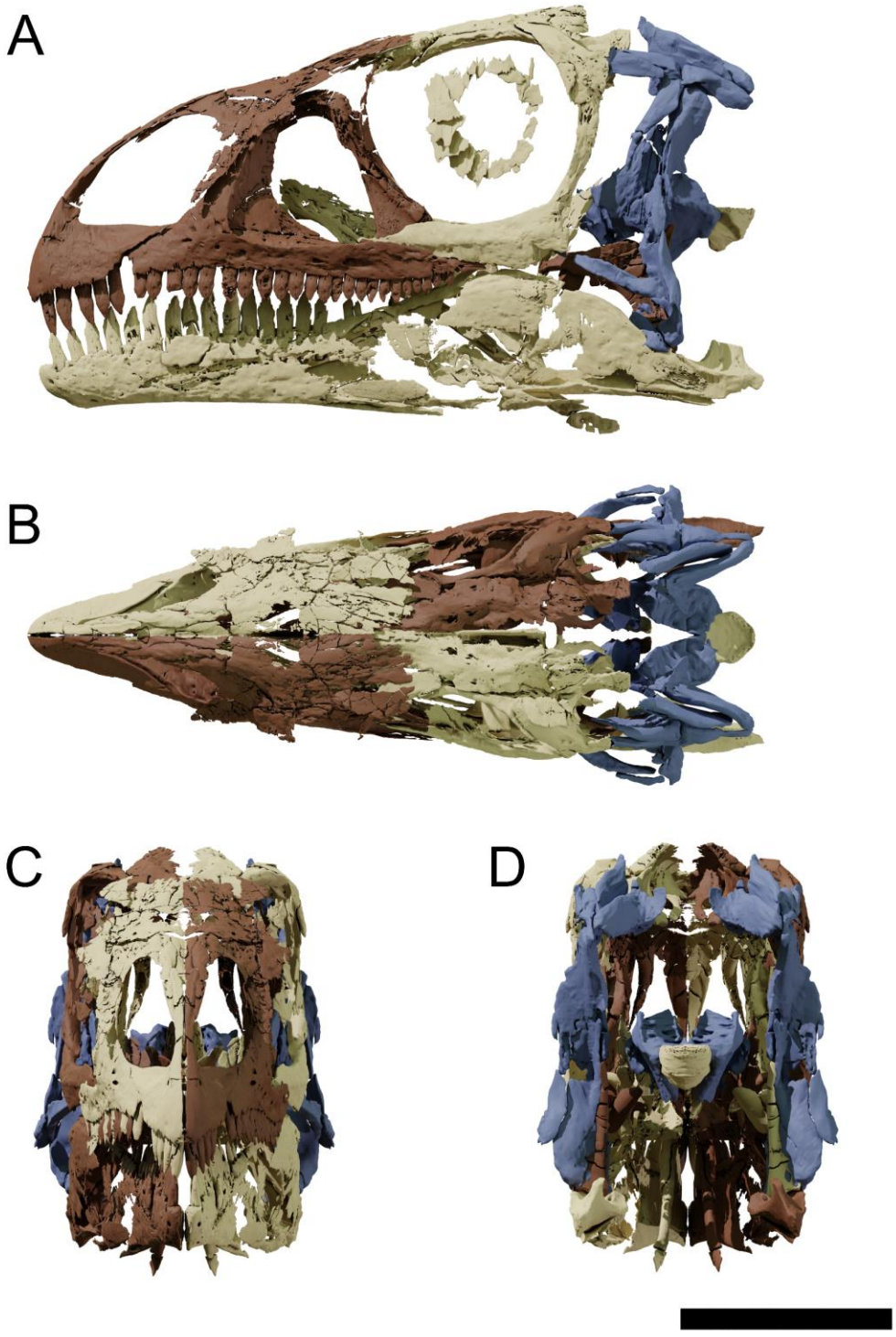

Figure 3.35 - NHMD 164758 skull reconstruction. Digital reconstruction of the skull NHMD 164758 in left lateral view (A), dorsal view (B), anterior view (C), and posterior view (D). Preserved bones in beige, mirrored elements in brown and scaled elements from the skull 164741 in blue. Scale bar = 50 mm.

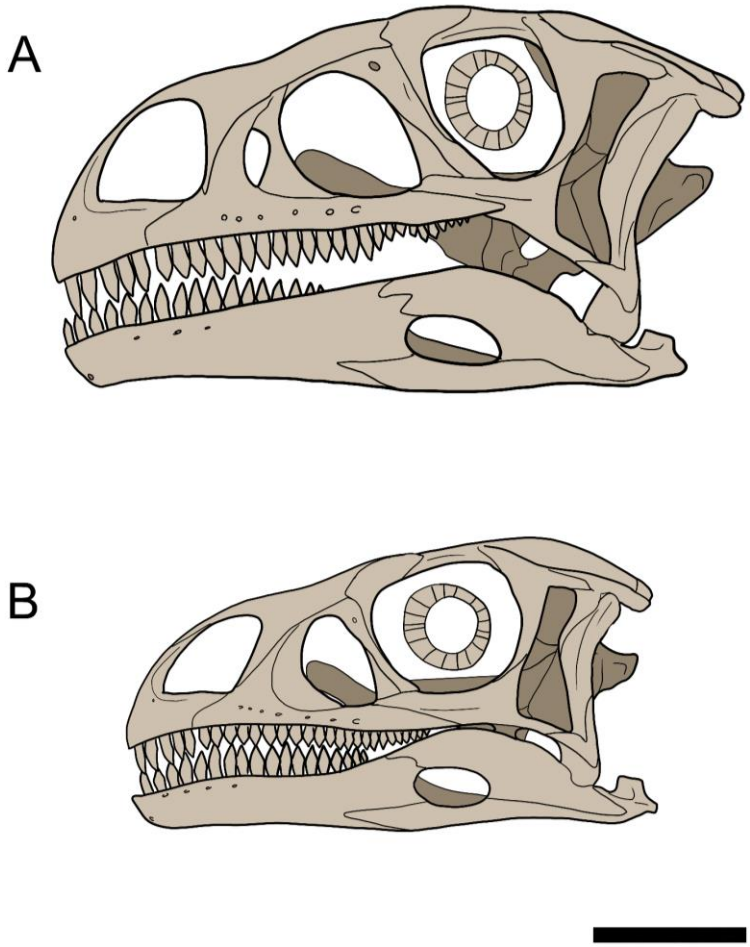

Figure 3.36 - NHMD 164741 and NHMD 164758 skull reconstruction. Schematic illustration of the skull NHMD 164741 (A) and NHMD 164758 (B) in left lateral view. Scale bar = 50 mm.

Table 6 - Measurements for the digitally reconstructed skulls of NHMD 164741 and NHMD 164758.

Measurements (in mm)	**NHMD 164741**	**NHMD 164758**
Skull anteroposterior length (from the anterior tip of the premaxilla to posterior margin of occipital condyle)	228.2	178.8
Skull dorsoventral height at orbit	66.6	58.6
Rostrum dorsoventral height	52.9	40.7
Skull lateromedial width	94.6	69.2
Orbit length	50.2	50.1
Orbit height	46.5	44.3
Skull length to width ratio	2.4	2.6
Skull length to height at the orbit ratio	3.4	3.1
Orbit length to skull length	0.22	0.28
Quadrate height	91.0	66.3
Quadrate height to rostrum height	1.7	1.6

3.8 Phylogenetic Analysis

Phylogenetic analysis following the dataset of Rauhut *et al.*, (2020) recovered a total of 400 MPTs of 1582 steps, with consistency index (CI) of 0.286 and retention index of 0.657. The strict consensus tree with Bremer Support is found below (Fig. 3.38). The Greenland sauropodomorphs were nested together as in the first analysis as a sister clade of *P. trossingensis* and *P. gracilis*. This clade is characterized by four unambiguous cranial synapomorphies: the postorbital rim of the orbit raised and projecting laterally [54, (1)], shared with Massospondylidae; the presence of a central tubercle on the ventral surface of the palatine [90, (1)], also shared with Massospondylidae; vomer anteroposterior length over 0.25 of the skull total length [92, (1)], shared with *Melanorosaurus*; and five or more premaxillary teeth [106, (1)].

The specimens NHMD 164741 and NHMD 164758 form a clade supported by six unambiguous synapomorphies: weakly developed narial fossa [character 10, state (0)], shared with *Macrocollum* and other more derived sauropodomorphs; small subnarial foramen [12, (1)], shared with *Sarahsaurus*; anterior margin of the external naris anterior to the mid-length of the premaxilla [17, (0)], a plesiomorphic feature for Sauropodomorpha; anteroposterior length of the antorbital fossa being less than the orbit [28, (1)], shared with Massopoda (*sensu* Yates, 2007a); antorbital fossa ending before the ventral process of the lacrimal [41, (1)], shared with *Yunnanosaurus*; the strongly curved jugal process of the ectopterygoid [86, (1)], shared with *Pantydraco, Leyesaurus* and *Sarahsaurus*.

The genus *Plateosaurus* (i.e., *P. trossingensis* and *P. gracilis*) was recovered by three unambiguous cranial synapomorphies: point contact of the posterolateral process of the premaxilla and the anteroventral process of the nasal [7, (1)], shared with *Efraasia* and *Unaysaurus*; a depression behind the naris at the dorsal profile of the skull [19, (1)], shared with Massospondylidae (*sensu* Yates, 2007a); the length of the posterior process of the prefrontal equal to that of the orbit [42, (1)], shared with Massopoda.

The clade Plateosauridae is supported by two cranial and two post-cranial synapomorphies: basipterygoid processes and the parasphenoid rostrum below the level of the basioccipital condyle and the basal tuberae [80, (1)], not visible in the Greenland sauropodomorphs and *Macrocollum*; strongly ventrally curved of the dentary symphyseal end [98, (1)], also shared with Massospondylidae; ventrolateral twisting of the transverse axis of the distal end of the first phalanx of manual digit one relative to its proximal end of 60º [244, (2)], not preserved on NHMD 164741, NHMD 164758 and *P. gracilis*; transverse width of the conjoined distal ischial expansions being less than their sagittal depth [292, (1)], only observed in *Macrocollum* and *P. trossingensis*.

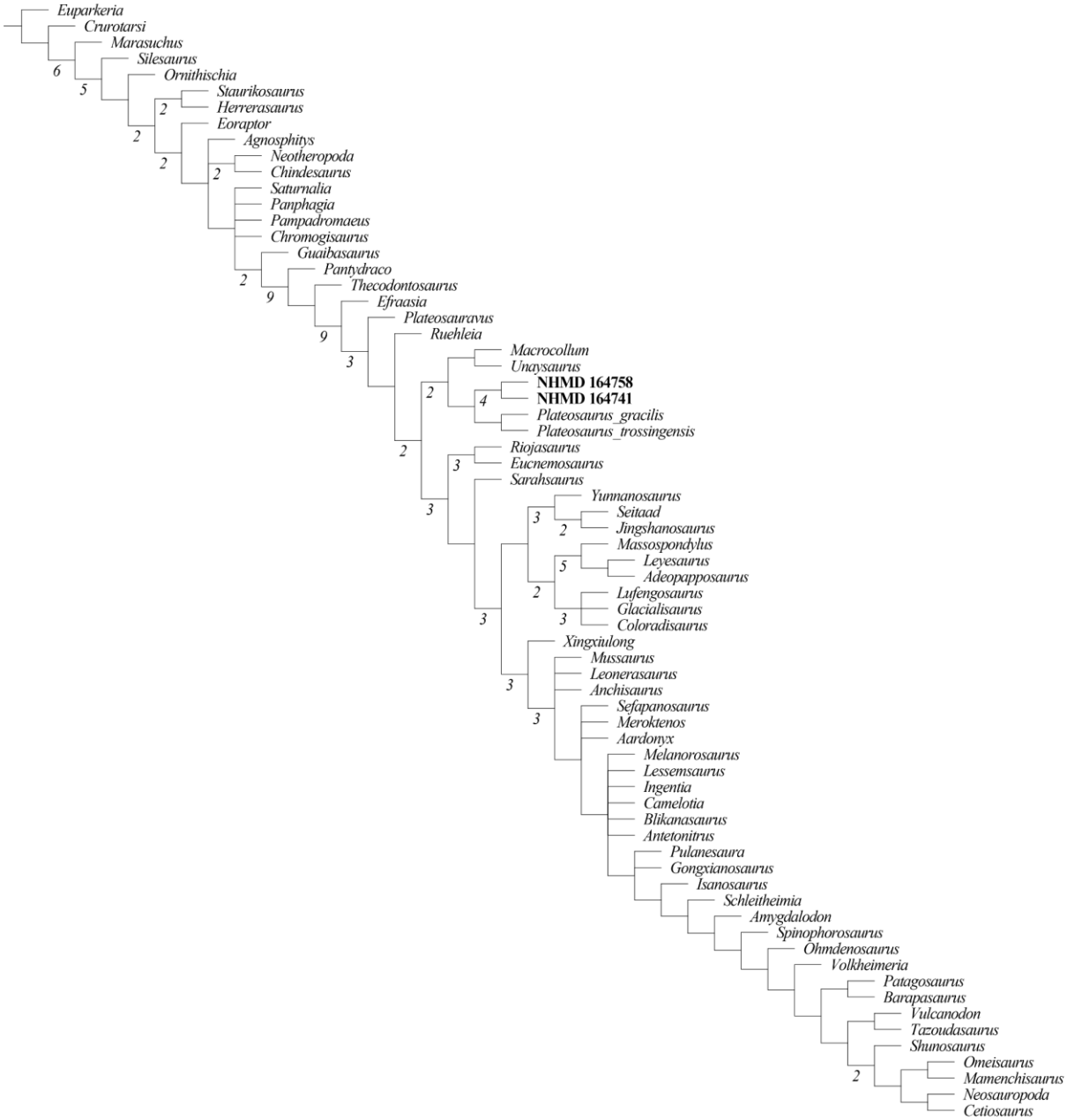

Figure 3.37 - Strict consensus tree of the Greenland specimens. Bremer support number (>1) are found under the nodes.

However, in contrast to the analysis of Müller, (2020), *Macrocollum* forms a clade with *Unaysaurus* at the base of Plateosauridae. This clade is supported by four unambiguous post-cranial synapomorphies: absence of ventral keels on the cervical vertebrae [132, (0)]; transverse width of the distal humerus over 0.33 of the length of the total length of the humerus [217, (1)]; the first phalanx of manual digit one shorter than the first metacarpal [245, (1)]; femoral length between 200 and 399 mm [379, (1)].

4 Discussion

4.1 Arguments for a new taxon

The taxonomy of early sauropodomorphs, and plateosaurids specifically, is still under investigation. Therefore, any attempt to erect a new taxon of plateosaurid sauropodomorphs should be done carefully and be well-grounded. The Greenland sauropodomorphs were recovered from rocks of similar age to the central European *Plateosaurus* (Kent & Clemmensen, 2021), therefore age separation cannot be used as an argument for the validity of a separate taxon for the Greenland sauropodomorphs. NHMD 164741 and NHMD 164758 suffered some degree of lateral deformation, with NHMD 164741 right side bones either fragmented, missing or presenting a higher degree of distortion (i.e., the anterior process of the right maxilla, the posterodorsal process of the postorbital, the mediodorsal process of the squamosal and the parasphenoid process), whereas in NHMD 164758 the bones were partially dislocated ventrally and compressed, but show little deformation. At least some of the disarticulation in NHMD 164741, however, may originate from an early diagenetic stage, as some bones were disarticulated to a larger degree than expected from taphonomical deformation alone, i.e., ventral deflection of the jaws and disarticulation of the skull roof. However, none of these deformations can explain most of the differences observed between the Greenland specimens and other sauropodomorphs.

As mentioned above, there are six synapomorphies shared between NHMD 164741 and NHMD 164758 and three synapomorphies supporting *Plateosaurus* as the sister clade for the Greenland specimens. While these features cannot be caused by taphonomic deformation alone, some of these synapomorphies could indeed be attributed to intraspecific variation. The developmental plasticity of the closely related *Plateosaurus* was noted for specimens from Trossingen (Sander & Klein, 2005) and Frick (Lallensack *et al.*, 2021). This plasticity ranges from the total size and proportions of individuals to more intrinsic skull characters usually coded on most phylogenetic studies. Phylogenetic characters such as the shape and size of the narial and antorbital fossae or the position of the external naris in the premaxilla found as synapomorphic for the Greenland specimens are highly variable among *P. trossingensis* specimens (Lallensack *et al.*, 2021). Therefore, the scoring of these characters should be revised in future phylogenetic analysis, as there is potentially a slight, but insignificant uncertainty regarding the interpretation of these characters in this thesis. Nevertheless, some synapomorphies of the Greenland specimens, such as the weakly development of the narial fossa and the strongly curved jugal ramus of the ectopterygoid, differ clearly from the condition observed in the described specimens of *Plateosaurus* (Galton, 1984, 1985; Yates, 2003; Prieto-Márquez & Norell, 2011; Lallensack *et al.*, 2021).

Furthermore, the three abovementioned synapomorphies supporting the clade *Plateosaurus* are different from the conditions observed in the Greenland specimens.

The Greenland specimens possess a unique combination of traits that cannot be observed in other basal sauropodomorphs. NHMD 164741 and NHMD 164758 share a foramen in the medial surface of the premaxilla (Fig. 4.1), not observed on the disarticulated or exposed medial surface of the premaxillae of the plateosaurids *Unaysaurus* UFSM11069 (McPhee *et al.*, 2020, fig. 1B) and *P. trossingensis* AMNH FARB 6810 (Prieto-Márquez & Norell, 2011, figs 3A and D), MSF 16.1 (Lallensack *et al.*, 2021, figs 3A1-2) and MSF 15.8.935 (Lallensack *et al.*, 2021, fig. 9A), nor the derived massospondylid *M. carinatus* BP/1/5241 (Chapelle & Choiniere, 2018, figs 4A and D). However, the saturnaliid sauropodomorph *Pampadromaeus* ULBRA-PVT016 preserved a similar foramen at the medial surface of the premaxilla, although more posteriorly and ventrally located (Langer *et al.*, 2019, figs 1B and 2C-D). NHMD 164741 squamosal preserves a uniquely elongated posterior process. This process is relatively anteroposteriorly longer than in other basal sauropodomorphs, being 1.31 the length of the anterolateral process (Fig. 4.2 and see Table 3). In *P. trossingensis* this ratio is usually around 0.5, except for the specimen MSF 15.4, whose posterior process is slightly longer (posterior process to anterolateral process ratio = 0.83). NHMD 164741 also preserved a dorsoventrally elongated and mediolaterally slender quadrate that differs from all other closely related sauropodomorphs (Fig. 3.16 and see Table 4). This makes the skull of NHMD 164741 dorsoventrally taller at its posterior half than other sauropodomorphs such as *P. trossingensis*, *Macrocollum*, *Buriolestes*, *Ngwevu* and *M. carinatus*. NHMD 164758 preserves a unique morphology of the articular for basal sauropodomorphs (Fig. 4.3). The dorsoposterior process of the articular is well-developed and dorsally tall, forming a squared blade in lateral view. This morphology differs from the dorsoventrally short, anteroposteriorly elongated and gently dorsally convex dorsoposterior process of the articular in *Macrocollum* CAPPA/UFSM 0001b (Müller *et al.*, 2021, fig. 15A), the short and posteriorly convex dorsoposterior process of *P. trossingensis* AMNH FARB 6810 (Prieto-Márquez & Norell, 2011, figs 31–32), and this process is absent in *Buriolestes* CAPPA/UFSM 0035 (Müller *et al.*, 2018a, fig. 16).

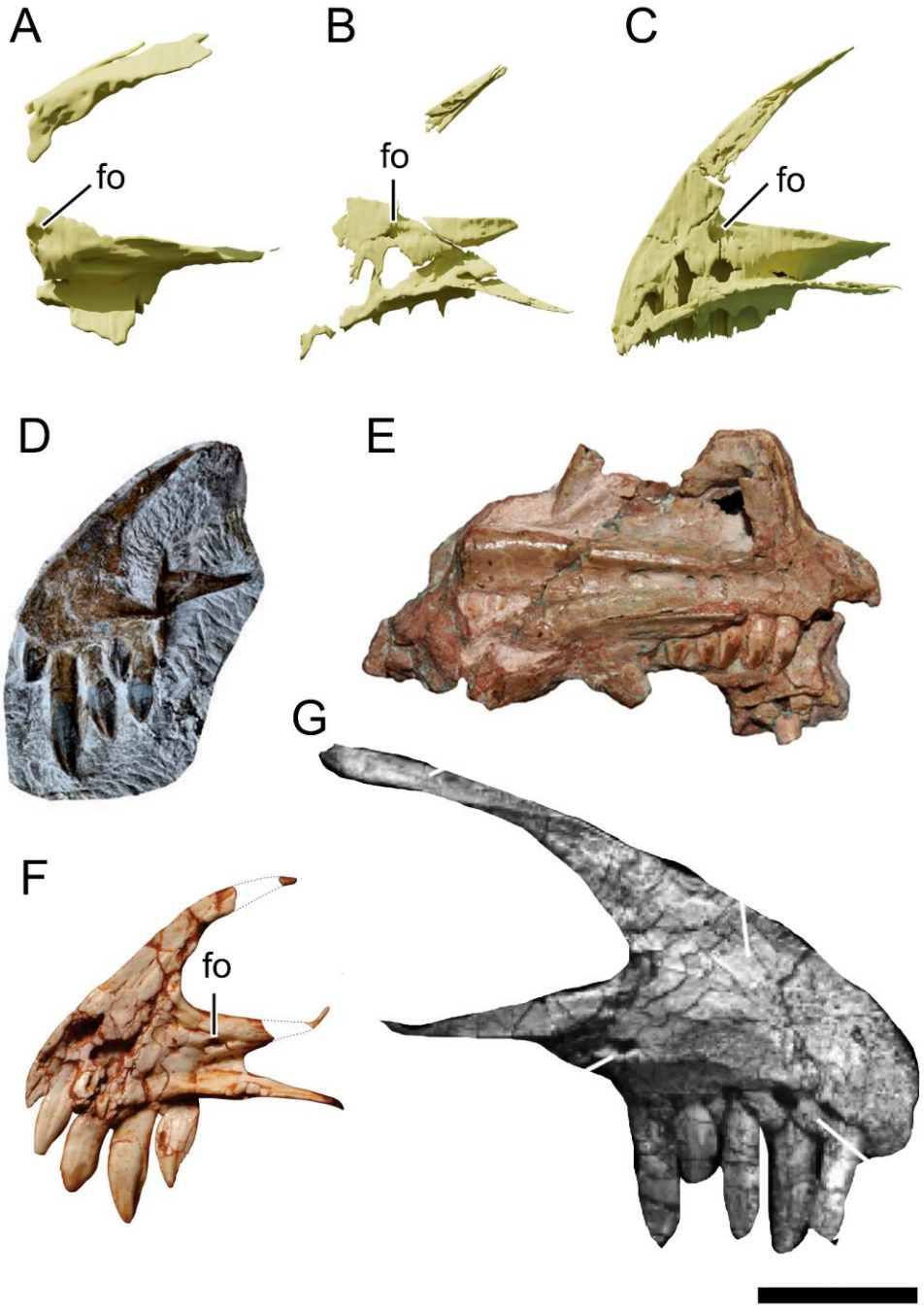

Figure 4.1 - Medial surface of the premaxilla. Comparison of the medial premaxillary foramen (fo) across basal sauropodomorphs. Mirrored left premaxilla of NHMD 164741 (A), mirrored left premaxilla of NHMD 164758 (B), right premaxilla of NHMD 164758 (C), right premaxilla of *P. trossingensis* MSF 15.8.935 (D), left premaxilla of *Unaysaurus* UFSM11069 (E), right premaxilla of *Pampadromaeus* ULBRA-PVT016 (F), and left premaxilla of *P. trossingensis* AMNH FARB 6810 (F). Scale bar = 20 mm.

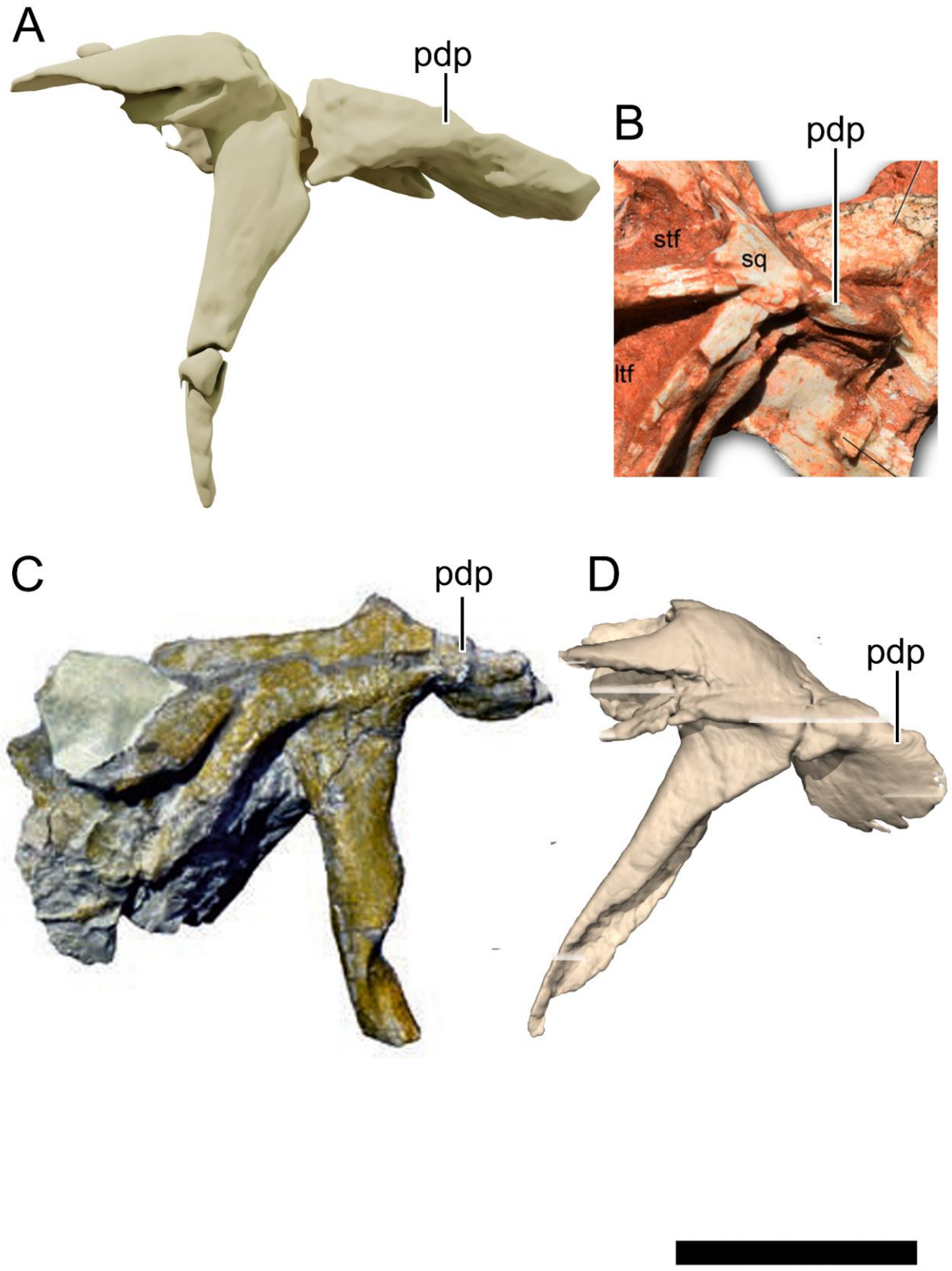

Figure 4.2 - Comparison of the posterodorsal process of the squamosal (pdp) across basal sauropodomorphs. Left squamosal of NHMD 164741 (A), left squamosal of *Macrocollum* CAPPA/UFSM 0001b (B), left squamosal of *P. trossingensis* MSF 15.8.935 (C), and left squamosal of *M. carinatus* BP/1/5241 (D). Scale bar = 20 mm.

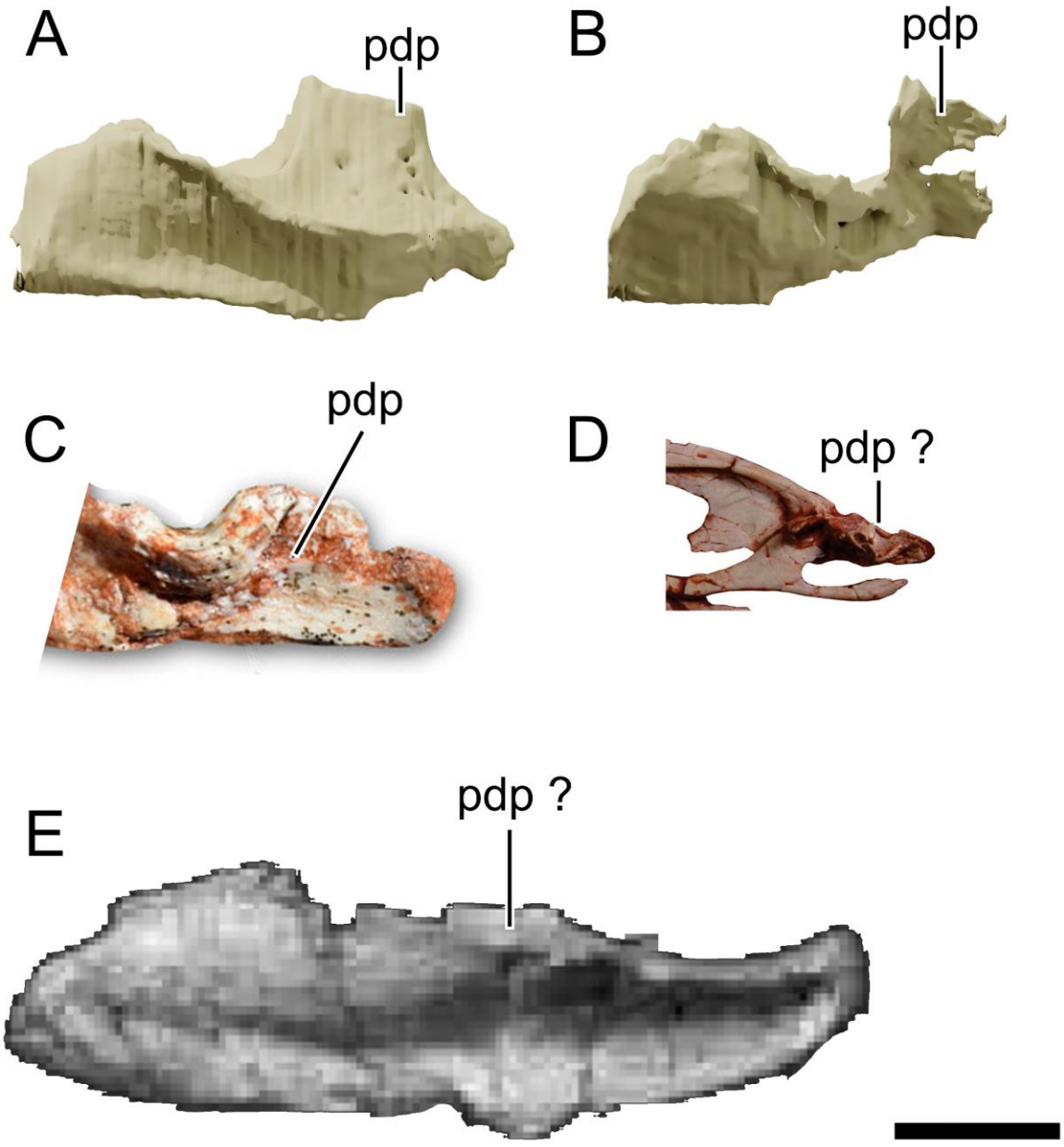

Figure 4.3 - Comparison of the posterodorsal process of the articular (pdp) across basal sauropodomorphs. Left articular of NHMD 164758 (A), right articular of NHMD 164758 (B), right articular of *Macrocollum* CAPPA/UFSM 0001b (C), right articular of *Pampadromaeus* ULBRA-PVT016 (D), and right articular of *P. trossingensis* AMNHD FARB 6810 (E). Scale bar = 10 mm.

A combination of additional features further differentiates the Greenland specimens from *Plateosaurus*. NHMD 164741 and NHMD 164758 nasals occupy 0.41 and 0.48, respectively, of the total skull roof length, whereas in *Plateosaurus* the nasal occupies over 0.5 of the skull roof length (Galton & Upchurch, 2004; Prieto-Márquez & Norell, 2011; Lallensack *et al.*, 2021). The lateral process of the laterosphenoid is elongated and arches laterally in *P. trossingensis* AMNH FARB 6810 (Prieto-Márquez & Norell, 2011, fig. 26), whereas in NHMD 164758 this process is short and straight, as is the condition to other sauropodomorphs such as *Macrocollum*, *Ngwevu* and *M. carinatus*. The autapomorphic feature of a ventrally located, central peg-like process of the palatine of *P. trossingensis* is absent in both NHMD 164741 and NHMD 164758. Only two of the autapomorphic features for *P. trossingensis* are present in the Greenland specimens. The lateral sheet of bone in the lacrimal is present in NHMD 164741, although differing from *P. trossingensis* in having a foramen in the dorsolateral margin of this sheet of bone and being concave anteriorly in the Greenland specimens. The dorsoventrally high jugal of *P. trossingensis* is visible in NHMD 164758 left jugal. This bone is morphologically similar to most *P. trossingensis* specimens.

4.2 Are these specimens of Greenland sauropodomorphs monospecific?

The specimens NHMD 164741 and NHMD 164758 are almost complete skulls of different sizes, varying only slightly in their morphology. Both were recovered from the same locality, i.e., the Macknight Bjerg site of Malmros Klint Formation, Fleming Fjord Group, Jameson Land, central East Greenland, meaning that both specimens were coeval. When coded in the data matrix of Rauhut *et al*., 2020, both specimens received the same scores for every coded bone, falling together as the sister clade of *Plateosaurus*. However, due to the lack of completeness, a problem arises when comparing the single shared autapomorphy of NHMD 164741 and NHMD 164758 (the medial foramen of the premaxilla). The squamosal and dorsal half of the quadrates are missing in NHMD 164758 and the posterior half of the articular is missing in NHMD 164741, rendering the assessment of these autapomorphies impossible. NHMD 164741 differs from NHMD 164758 in having a promaxillary fenestra in the antorbital fossa (Fig. 3.8), the shape of the anterodorsal process of the lacrimal (which is distally broken in NHMD 164741, fig. 3.10) and the bulkier frontals and postorbital in NHMD 164741 (Fig. 3.12 and 3.18). The presence of a promaxillary fenestra was recovered as a synapomorphy for the Brazilian "unaysaurids" *Macrocollum* and *Unaysaurus* (Müller *et al.*, 2018b; McPhee *et al.*, 2020; Müller, 2020). However, this feature is plastic and can even be present in one element and absent in the other for the same individual (Müller, 2020, fig. 5B). Therefore, the presence of a promaxillary fenestra does not support a separation of both Greenland specimens. The difference in the anterodorsal process of the lacrimal and the bulkier postorbital in NHMD 164741 could be attributed to ontogeny or even

intraspecific variation, as is the case of the main body of the postorbital in *P. trossingensis* (Lallensack *et al.*, 2021). Due to the lack of features distinguishing both Greenland specimens, NHMD 164741 and NHMD 164758 are regarded as a single taxon.

4.3 Ontogeny

Although representing the same taxon, NHMD 164741 and NHMD 164758 differ in size and some of the skull proportions. However, size is not a good correlation for the ontogenetic stage in the closely related *P. trossingensis* (Sander & Klein, 2005; Klein & Sander, 2007). NHMD 164741 measures 1.45 the anteroposterior length of NHMD 164758, even with the anteriormost region of the skull missing. However, the orbit size is estimated to be only slightly anteroposteriorly longer (Fig. 3.37 and Table 6). The orbit length to skull length is higher in NHMD 164758. A longer orbit relative to the skull length is supposed to be a juvenile feature, as shown by the late-stage juvenile of *P. trossingensis* MSF 12.3 proportionally larger orbit (Lallensack *et al.*, 2021, fig. 8). A reduced dentary teeth count (<20 tooth position) is also a feature related to the ontogeny in plateosaurids such as *Macrocollum, Unaysaurus* and *P. trossingensis* (Lallensack *et al.*, 2021). NHMD 164758 shows only 18 tooth positions in its dentary, and NHMD 164741 preserves a maximum of 18 tooth positions. In the latter this number might be underestimated, as the anterior region of the dentary is missing in this specimen. However, the posterior margin of the symphysis is preserved in NHMD 164741 left dentary, meaning that the tooth count could be of a maximum of 20 teeth. The reduced gap between the first premaxillary tooth and the anterior tip of the premaxilla is observed in NHMD 164758, representing another juvenile feature for this specimen (Lallensack *et al.*, 2021). The orientation of the basipterygoid process of the basisphenoid can also be an indicative of ontogenetic stage in some sauropodomorphs, such as in *M. carinatus* (Chapelle & Choiniere, 2018). Therefore, the differences between the slightly anteriorly deflected basipterygoid process of NHMD 164758 (Fig. 3.21) and the sub-perpendicular basipterygoid process of NHMD 164741 (Fig. 3.22) may be caused by their ontogenetic stage. All these discussed features places NHMD 164758 in an earlier stage of development than NHMD 164741, the former being regarded as an early-stage juvenile and the latter as a possible late-stage juvenile or young adult specimen.

4.4 Paleobiogeographic and chronological implications

Plateosaurid specimens have been recovered from the Late Triassic (Norian) of Brazil, Germany, France, Switzerland and Norway (Sander, 1992; Moser, 2003; Galton & Upchurch, 2004; Hurum *et al.*, 2006; Mallison, 2010b; Prieto-Márquez & Norell, 2011; Müller, 2020; Nau *et al.*, 2020), and are now confidently reported for Greenland. The Greenland sauropodomorph and the Central European

Plateosaurus share some features, as was discussed above. These features correlate these taxa, as would be expected by the similar age and closeness of both localities. However, the Greenland sauropodomorph also shares features with the mid-Norian Brazilian plateosaurids. These correlation to the Brazilian plateosaurids may be explained by a dispersion event that is yet unclear. Fossils from plateosaurids are yet unknown for both Africa and North America. Therefore, the exact route and timing of the evolution of this clade cannot be assessed in the present work. Nevertheless, the Greenland sauropodomorph is the first sauropodomorphs to reach paleolatitudes of over 40º N, and the first non-*Plateosaurus* plateosaurid for Laurasia.

5 Conclusion

Two skulls of a new basal sauropodomorph (plateosaurid) dinosaur taxon from the Late Triassic (Norian) of Jameson Land, central East Greenland were here described based on new imaging methods (CT-Scanning and Photogrammetry). Specimen NHMD 164741 was briefly mentioned before, but lacked a thorough description. NHMD 164741 and NHMD 164758 were recovered from the same site, and due to strong morphological similarities and no robust distinguishing features between both, are here regarded as a single taxon. The smaller NHMD 164758 represents an early-stage juvenile, due to the larger orbit, a low number of teeth positions in the dentary and an anteriorly deflected basipterygoid process of the basisphenoid. The Greenland sauropodomorph differs from all other basal sauropodomorphs in four observed diagnostic features: 1) the presence of a small foramen at the medial surface of the premaxilla at the base of the lateral process of the premaxilla; 2) an anteroposteriorly elongated dorsoposterior process of the squamosal; 3) a quadrate relatively tall in comparison to the rostrum height; 4) a well-developed, square-shaped in lateral view posterodorsal process of the articular.

Six unambiguous synapomorphies position the Greenland sauropodomorph as the sister clade to *Plateosaurus* (*P. trossingensis* and *P. gracilis*). The clade Unaysauridae was not recovered in the phylogenetic analysis, with the Brazilian sauropodomorphs recovered at the base of Plateosauridae and forming the sister clade to the clade containing the Greenland sauropodomorph and *Plateosaurus*. The correlation with Brazilian taxa is briefly discussed, however, the dispersion routes and evolutionary timing for plateosaurids is yet unclear. The Greenland sauropodomorph is the first non-*Plateosaurus* plateosaurid for the North Pangea and was recovered for the same age as the Central European *Plateosaurus*.

6 References

Apaldetti, C., Martinez, R. N., Alcober, O. A., & Pol, D. (2011). A New Basal Sauropodomorph (Dinosauria: Saurischia) from Quebrada del Barro Formation (Marayes-El Carrizal Basin), Northwestern Argentina. *PLoS ONE*, *6*(11), e26964. https://doi.org/10.1371/journal.pone.0026964

Apaldetti, C., Martinez, R. N., Pol, D., & Souter, T. (2014). Redescription of the Skull of *Coloradisaurus brevis* (Dinosauria, Sauropodomorpha) from the Late Triassic Los Colorados Formation of the Ischigualasto-Villa Union Basin, northwestern Argentina. *Journal of Vertebrate Paleontology*, *34*(5), 1113–1132. https://doi.org/10.1080/02724634.2014.859147

Bachmann, G. H., & Kozur, H. W. (2004). Die Germanische Trias: Korrelation mit der internationalen chronostratigraphischen Gliederung, numerische Altersdaten und Milankovitch-Zyklizität. *Hallensches Jarbuch Für Geowissenschaften*, *26*, 17–62.

Bakker, R. T. (1977). Tetrapod Mass Extinctions: A Model of the Regulation of Speciation Rates and Immigration by Cycles of Topographic Diversity. In *Developments in Palaeontology and Stratigraphy* (Vol. 5, pp. 439–468). Elsevier. https://doi.org/10.1016/S0920-5446(08)70334-0

Ballell, A., King, J. L., Neenan, J. M., Rayfield, E. J., & Benton, M. J. (2020a). The braincase, brain and palaeobiology of the basal sauropodomorph dinosaur *Thecodontosaurus antiquus*. *Zoological Journal of the Linnean Society*, 1–22. https://doi.org/10.1093/zoolinnean/zlaa157

Ballell, A., Rayfield, E. J., & Benton, M. J. (2020b). Osteological redescription of the Late Triassic sauropodomorph dinosaur *Thecodontosaurus antiquus* based on new material from Tytherington, southwestern England. *Journal of Vertebrate Paleontology*, *40*(2), e1770774. https://doi.org/10.1080/02724634.2020.1770774

Barrett, P. M. (2009). A New Basal Sauropodomorph Dinosaur from the Upper Elliot Formation (Lower Jurassic) of South Africa. *Journal of Vertebrate Paleontology*, *29*(4), 1032–1045.

Barrett, P. M., Butler, R. J., & Nesbitt, S. J. (2010). The roles of herbivory and omnivory in early dinosaur evolution. *Earth and Environmental Science Transactions of the Royal Society of Edinburgh*, *101*(3–4), 383–396. https://doi.org/10.1017/S1755691011020111

Barrett, P. M., & Upchurch, P. (2007). The evolution of feeding mechanisms in early sauropodomorph dinosaurs. *Special Papers in Palaeontology*, *77*, 91–112.

Barrett, P. M., Upchurch, P., & Xiao-Lin, W. (2005). Cranial osteology of *Lufengosaurus huenei* Young (Dinosauria: Prosauropoda) from the Lower Jurassic of Yunnan, People's Republic of China. *Journal of Vertebrate Paleontology*, *25*(4), 806–822. https://doi.org/10.1671/0272-4634(2005)025[0806:COOLHY]2.0.CO;2

Benton, M. J. (1983). Dinosaur success in the Triassic: A noncompetitive ecological model. *The Quarterly Review of Biology*, *58*(1), 29–55. https://doi.org/10.1086/413056

Benton, M. J., Juul, L., Storrs, G. W., & Galton, P. M. (2000). Anatomy and systematics of the prosauropod dinosaur *Thecodontosaurus antiquus* from the Upper Triassic of southwest England. *Journal of Vertebrate Paleontology*, *20*(1), 77–108. https://doi.org/10.1671/0272-4634(2000)020[0077:AASOTP]2.0.CO;2

Bonaparte, J. F. (1978). *Coloradia brevis* n. G. Et n. Sp. (Saurischia, Prosauropoda), a plateosaurid dinosaur from the Los Colorados Formation, Upper Triassic of La Rioja, Argentina. *Ameghiniana*, *15*(3–4), 7.

Brochu, C. A. (1996). Closure of neurocentral sutures during crocodilian ontogeny: Implications for maturity assessment in fossil archosaurs. *Journal of Vertebrate Paleontology*, *16*(1), 49–62. https://doi.org/10.1080/02724634.1996.10011283

Bronzati, M., Müller, R. T., & Langer, M. C. (2019). Skull remains of the dinosaur *Saturnalia tupiniquim* (Late Triassic, Brazil): With comments on the early evolution of sauropodomorph feeding behaviour. *PLOS ONE*, *14*(9), e0221387. https://doi.org/10.1371/journal.pone.0221387

Bronzati, M., & Rauhut, O. W. M. (2018). Braincase redescription of *Efraasia minor* Huene, 1908 (Dinosauria: Sauropodomorpha) from the Late Triassic of Germany, with comments on the evolution of the sauropodomorph braincase. *Zoological Journal of the Linnean Society*, *182*, 173–224.

Bronzati, M., Rauhut, O. W. M., Bittencourt, J. S., & Langer, M. C. (2017). Endocast of the Late Triassic (Carnian) dinosaur *Saturnalia tupiniquim*: Implications for the evolution of brain tissue

in Sauropodomorpha. *Scientific Reports*, *7*(1), 11931. https://doi.org/10.1038/s41598-017-11737-5

Brusatte, S. L., Nesbitt, S. J., Irmis, R. B., Butler, R. J., Benton, M. J., & Norell, M. A. (2010). The origin and early radiation of dinosaurs. *Earth-Science Reviews*, *101*(1–2), 68–100. https://doi.org/10.1016/j.earscirev.2010.04.001

Button, D. J., Barrett, P. M., & Rayfield, E. J. (2016). Comparative cranial myology and biomechanics of *Plateosaurus* and *Camarasaurus* and evolution of the sauropod feeding apparatus. *Palaeontology*, *59*(6), 887–913. https://doi.org/10.1111/pala.12266

Button, D. J., Barrett, P. M., & Rayfield, E. J. (2017). Craniodental functional evolution in sauropodomorph dinosaurs. *Paleobiology*, *43*(3), 435–462. https://doi.org/10.1017/pab.2017.4

Cabreira, S. F., Kellner, A. W. A., Dias-da-Silva, S., Roberto da Silva, L., Bronzati, M., Marsola, J. C. de A., Müller, R. T., Bittencourt, J. de S., Batista, B. J., Raugust, T., Carrilho, R., Brodt, A., & Langer, M. C. (2016). A Unique Late Triassic Dinosauromorph Assemblage Reveals Dinosaur Ancestral Anatomy and Diet. *Current Biology*, *26*(22), 3090–3095. https://doi.org/10.1016/j.cub.2016.09.040

Cabreira, S. F., Schultz, C. L., Bittencourt, J. S., Soares, M. B., Fortier, D. C., Silva, L. R., & Langer, M. C. (2011). New stem-sauropodomorph (Dinosauria, Saurischia) from the Triassic of Brazil. *Naturwissenschaften*, *98*(12), 1035–1040. https://doi.org/10.1007/s00114-011-0858-0

Chapelle, K. E. J., Barrett, P. M., Botha, J., & Choiniere, J. N. (2019). *Ngwevu intloko*: A new early sauropodomorph dinosaur from the Lower Jurassic Elliot Formation of South Africa and comments on cranial ontogeny in *Massospondylus carinatus*. *PeerJ*, *7*, e7240. https://doi.org/10.7717/peerj.7240

Chapelle, K. E. J., & Choiniere, J. N. (2018). A revised cranial description of *Massospondylus carinatus* Owen (Dinosauria: Sauropodomorpha) based on computed tomographic scans and a review of cranial characters for basal Sauropodomorpha. *PeerJ*, *6*, e4224. https://doi.org/10.7717/peerj.4224

Clemmensen, L. B. (1980). Triassic lithostratigraphy of East Greenland between Scoresby Sund and Kejser Franz Josephs Fjord. *Grønlands Geologiske Undersøgelse Bulletin*, *139*, 56.

Clemmensen, L. B., Kent, D. V., & Jenkins, F. A. (1998). A Late Triassic lake system in East Greenland: Facies, depositional cycles and palaeoclimate. *Palaeogeography, Palaeoclimatology, Palaeoecology*, *140*(1–4), 135–159. https://doi.org/10.1016/S0031-0182(98)00043-1

Clemmensen, L. B., Kent, D. W., Mau, M., Mateus, O., & Milàn, J. (2020). Triassic lithostratigraphy of the Jameson Land Basin (central EastGreenland), with emphasis on the new Fleming Fjord Group. *Bulletin of the Geological Society of Denmark*, *68*, 95–132. https://doi.org/10.37570/bgsd-2020-68-05

Clemmensen, L. B., Milàn, J., Adolfssen, J. S., Estrup, E. J., Frobøse, N., Klein, N., Mateus, O., & Wings, O. (2016). The vertebrate-bearing Late Triassic Fleming Fjord Formation of central East Greenland revisited: Stratigraphy, palaeoclimate and new palaeontological data. *Geological Society, London, Special Publications*, *434*(1), 31–47. https://doi.org/10.1144/SP434.3

Decou, A., Andrews, S. D., Alderton, D. H. M., & Morton, A. (2017). Triassic to Early Jurassic climatic trends recorded in the Jameson Land Basin, East Greenland: Clay mineralogy, petrography and heavy mineralogy. *Basin Research*, *29*(5), 658–673. https://doi.org/10.1111/bre.12194

Ezcurra, M. D. (2010). A new early dinosaur (Saurischia: Sauropodomorpha) from the Late Triassic of Argentina: a reassessment of dinosaur origin and phylogeny. *Journal of Systematic Palaeontology*, *8*(3), 371–425. https://doi.org/10.1080/14772019.2010.484650

Fraas, E. (1913). Die neuesten Dinosaurierfunde in der schwäbischen Trias. *Naturwissenschaften*, *1*(45), 1097–1100. https://doi.org/10.1007/BF01493265

Galton, P. M. (1976). Prosauropod Dinosaurs (Reptilia: Saurischia) of North America. *Postilla*, *169*, 98 p.

Galton, P. M. (1984). Cranial anatomy of the prosauropod dinosaur Plateosaurus from the Knollenmergel (Middle Keuper, Upper Triassic) of Germany. I. Two complete skulls from Trossingen/Württ. With comments on the diet. *Geologica et Palaeontologica*, *18*, 139–171.

Galton, P. M. (1985). Cranial anatomy of the prosauropod dinosaur *Plateosaurus* from the Knollenmergel (Middle Keuper, Upper Triassic) of Germany. 2. All the cranial material and details of soft-part anatomy. *Geologica et Palaeontologica*, *19*, 119–159.

Galton, P. M. (1986). Prosauropod dinosaur *Plateosaurus* (= *Gresslyosaurus*)(Saurischia: Sauropodomorpha) from the Upper Triassic of Switzerland. *Geologica et Palaeontologica*, *20*, 167–183.

Galton, P. M. (2000). The prosauropod dinosaur *Plateosaurus* Meyer, 1837 (Saurischia: Sauropodomorpha). 1. The syntypes of *P. engelhardti* Meyer1,837 (Upper Triassic, Germany), with notes on other European prosauropods with 'distally straight' femora. *Neues Jahrbuch Für Geologie Und Paläontologie-Abhandlungen*, *216*(2), 233–275.

Galton, P. M. (2001). The prosauropod dinosaur Plateosaurus Meyer, 1837 (Saurischia: Sauropodomorpha; Upper Triassic). II. notes on the referred species. *Revue de Paléobiologie*, *20*(2), 435–502.

Galton, P. M. (2012). Case 3560 *Plateosaurus engelhardti* Meyer, 1837 (Dinosauria, Sauropodomorpha): Proposed replacement of unidentifiable name-bearing type by a neotype. *The Bulletin of Zoological Nomenclature*, *69*(3), 203–212. https://doi.org/10.21805/bzn.v69i3.a15

Galton, P. M., & Kermack, D. (2010). The anatomy of *Pantydraco caducus*, a very basal sauropodomorph dinosaur from the Rhaetian (Upper Triassic) of South Wales, UK. *Revue de Palóbiologie*, *29*(2), 341–404.

Galton, P. M., & Upchurch, P. (2004). 12. Prosauropoda. In *The Dinosauria, second edition* (pp. 232–258). University of California Press.

Goloboff, P. A., & Catalano, S. A. (2016). TNT version 1.5, including a full implementation of phylogenetic morphometrics. *Cladistics*, *32*(3), 221–238. https://doi.org/10.1111/cla.12160

Hatcher, J. B. (1901). *Diplodocus* (Marsh): Its osteology, taxonomy, and probable habits, with a restoration of the skeleton. *Memoirs of the Carnegie Museum*, *1*(1), 90. https://doi.org/10.5962/bhl.title.46734

Hofmann, R., & Sander, P. M. (2014). The first juvenile specimens of *Plateosaurus engelhardti* from Frick, Switzerland: Isolated neural arches and their implications for developmental plasticity in a basal sauropodomorph. *PeerJ*, *2*, e458. https://doi.org/10.7717/peerj.458

Huene, F. F. von. (1905). Über die Trias-Dinosaurier Europas. *Zeitschrift Der Deutschen Geologischen Gesellschaft*, *57*, 345–349.

Huene, F. F. von. (1908). *Die Dinosaurier der europäischen Triasformation mit Berücksichtigung der aussereuropäischen Vorkommnisse* (Vol. 1). G. Fischer.

Huene, F. F. von. (1926). *Vollständige Osteologie eines Plateosauriden aus dem schwäbischen Keuper*. Fischer (Gustav).

Huene, F. F. von. (1932). *Die fossile Reptil-Ordnung Saurischia, ihre Entwicklung un Geschichte* [Monographien zur Geologie und Palaeontologie].

Hurum, J. H., Bergan, M., Müller, R., Nystuen, J. P., & Klein, N. (2006). A Late Triassic dinosaur bone, offshore Norway. *Norwigian Journal of Geology*, *86*, 117–123.

ICZN. (2019). Opinion 2435 (Case 3560) – Plateosaurus Meyer, 1837 (Dinosauria, Sauropodomorpha): New type species designated. *The Bulletin of Zoological Nomenclature*, *76*(1), 144–145. https://doi.org/10.21805/bzn.v76.a042

Jaekel, O. (1910). Die Fußstellung und Lebensweise der großen Dinosaurier. *Zeitschrift Der Deutschen Geologischen Gesellschaft*, 270–277.

Jenkins, F. A., Shubin, N. H., Amaral, W. W., Gatesy, S. M., Schaff, C. R., Clemmensen, L. B., Downs, W. R., Davidson, A. R., Bonde, N., & Osbaeck, F. (Eds.). (1994). *Late Triassic continental vertebrates and depositional environments of the Fleming Fjord Formation, Jameson Land, East Greenland*. Geografforl.

Kent, D. V., & Clemmensen, L. B. (2021). Northward dispersal of dinosaurs from Gondwana to Greenland at the mid-Norian (215–212 Ma, Late Triassic) dip in atmospheric pCO_2. *Proceedings of the National Academy of Sciences*, *118*(8), e2020778118. https://doi.org/10.1073/pnas.2020778118

Kent, D. V., & Tauxe, L. (2005). Corrected Late Triassic Latitudes for Continents Adjacent to the North Atlantic. *Science*, *307*(5707), 240–244. https://doi.org/10.1126/science.1105826

Klein, N., & Sander, P. M. (2007). Bone Histology and Growth of the Prosauropod Dinosaur *Plateosaurus engelhardti* von Meyer, 1837 from the Norian Bonebeds of Trossingen (Germany) and Frick (Switzerland). *Special Papers in Palaeontology*, *77*, 169–206.

Lallensack, J. N., Klein, H., Milán, J., Wings, O., Mateus, O., & Clemmensen, L. (2017). Sauropodomorph dinosaur trackways from the Fleming Fjord Formation of East Greenland:

Evidence for Late Triassic sauropods. *Acta Palaeontologica Polonica*, *62*(4), 833–843. https://doi.org/10.4202/app.00374.2017

Lallensack, J. N., Teschner, E., Pabst, B., & Sander, P. M. (2021). New skulls of the basal sauropodomorph *Plateosaurus trossingensis* from Frick, Switzerland: Is there more than one species? *Acta Palaeontologica Polonica*, *66*(1), 1–28. https://doi.org/10.4202/app.00804.2020

Langer, M. C., Abdala, F., Richter, M., & Benton, M. J. (1999). A sauropodomorph dinosaur from the Upper Triassic (Carnian) of southern Brazil. *Académie Des Sciences*, *329*, 511–517.

Langer, M. C., Ezcurra, M. D., Bittencourt, J. S., & Novas, F. E. (2010). The origin and early evolution of dinosaurs. *Biological Reviews*, *85*(1), 55–110. https://doi.org/10.1111/j.1469-185X.2009.00094.x

Langer, M. C., McPhee, B. W., Marsola, J. C. de A., Roberto-da-Silva, L., & Cabreira, S. F. (2019). Anatomy of the dinosaur *Pampadromaeus barberenai* (Saurischia—Sauropodomorpha) from the Late Triassic Santa Maria Formation of southern Brazil. *PLoS ONE*, *14*(2), e0212543. https://doi.org/10.1371/journal.pone.0212543

Langer, M. C., Ramezani, J., & Da Rosa, Á. A. S. (2018). U-Pb age constraints on dinosaur rise from south Brazil. *Gondwana Research*, *57*, 133–140. https://doi.org/10.1016/j.gr.2018.01.005

Lautenschlager, S., Brassey, C. A., Button, D. J., & Barrett, P. M. (2016). Decoupled form and function in disparate herbivorous dinosaur clades. *Scientific Reports*, *6*(1), 26495. https://doi.org/10.1038/srep26495

Leal, L. A., Azevedo, S. A. K., Kellner, A. W. A., & Rosa, Á. A. S. da. (2004). A New Early Dinosaur (Sauropodomorpha) From The Caturrita Formation (Late Triassic), Paraná Basin, Brazil. *Zootaxa*, *690*, 1–24. https://doi.org/10.5281/ZENODO.169421

Lockley, M. G., Lucas, S. G., & Hunt, A. P. (2006a). *Eosauropus*, Anew Name Foralate Triassic Track: Further Observations on the Late Triassic ichnogenus *Tetrasauropus* and Related Forms, with Notes on the Limits of Interpretation. *New Mexico Museum of Natural History and Science, Bulletin*, *37*, 192.

Lockley, M. G., Lucas, S. G., & Hunt, A. P. (2006b). *Evazoum* and the renaming of northern hemisphere '*Pseudotetrasauropus*': Implications for tetrapod ichnotaxonomy at the Triassic-Jurassic boundary. *New Mexico Museum of Natural History and Science, Bulletin*, *37*.

Mallison, H. (2010a). The digital *Plateosaurus* I: body mass, mass distribution and posture assessed using cad and cae on a digitally mounted complete skeleton. *Palaeontologia Electronica*, *13*(2), 26.

Mallison, H. (2010b). The Digital *Plateosaurus* II: An Assessment of the Range of Motion of the Limbs and Vertebral Column and of Previous Reconstructions using a Digital Skeletal Mount. *Acta Palaeontologica Polonica*, *55*(3), 433–458. https://doi.org/10.4202/app.2009.0075

Mallison, H., & Wings, O. (2014). Photogrammetry in paleontology—A practical guide. *Journal of Paleontological Techniques*, *12*, 1–31.

Marsh, O. C. (1895). On the affinities and classification of the dinosaurian reptiles. *American Journal of Science*, *s3-50*(300), 483–498. https://doi.org/10.2475/ajs.s3-50.300.483

Martinez, R. N., & Alcober, O. A. (2009). A Basal Sauropodomorph (Dinosauria: Saurischia) from the Ischigualasto Formation (Triassic, Carnian) and the Early Evolution of Sauropodomorpha. *PLoS ONE*, *4*(2), e4397. https://doi.org/10.1371/journal.pone.0004397

Marzola, M., Mateus, O., Milàn, J., & Clemmensen, L. B. (2018). A review of Palaeozoic and Mesozoic tetrapods from Greenland. *Bulletin of the Geological Society of Denmark*, *66*, 21–46. https://doi.org/10.37570/bgsd-2018-66-02

McPhee, B. W., Bittencourt, J. S., Langer, M. C., Apaldetti, C., & Da Rosa, Á. A. S. (2020). Reassessment of *Unaysaurus tolentinoi* (Dinosauria: Sauropodomorpha) from the Late Triassic (early Norian) of Brazil, with a consideration of the evidence for monophyly within non-sauropodan sauropodomorphs. *Journal of Systematic Palaeontology*, *18*(3), 259–293. https://doi.org/10.1080/14772019.2019.1602856

McPhee, B. W., Choiniere, J. N., Yates, A. M., & Viglietti, P. A. (2015). A second species of *Eucnemesaurus* Van Hoepen, 1920 (Dinosauria, Sauropodomorpha): New information on the diversity and evolution of the sauropodomorph fauna of South Africa's lower Elliot Formation (latest Triassic). *Journal of Vertebrate Paleontology*, *35*(5), e980504. https://doi.org/10.1080/02724634.2015.980504

Meyer, H. von. (1837). Briefliche Mitteilung an Prof. Bronn über *Plateosaurus engelhardti*. *Neues Jahrbuch Für Mineralogie, Geognosie, Geologie Und Petrefakten-Kunde*, 314–316.

Meyer, H. von. (1855). *Zür Fauna der Vorwelt: Die Saurier des Muschelkalkes mit Rücksicht auf die Saurier aus buntem Sandstein und Keuper* (Vol. 2). H. Keller.

Morris, J. (1843). *A catalogue of British fossils. Comprising all the genera and species hitherto described; with references to their geological distribution and to the localities in which they have been found.* J. Van Voorst. https://doi.org/10.5962/bhl.title.112423

Moser, M. (2003). *Plateosaurus engelhardti* Meyer, 1837 (Dinosauria: Sauropodomorpha) aus dem Feuerletten (Mittelkeuper; Obertrias) von Bayern. *Zitteliana*, *24*, 3–186.

Müller, R. T. (2020). Craniomandibular osteology of *Macrocollum itaquii* (Dinosauria: Sauropodomorpha) from the Late Triassic of southern Brazil. *Journal of Systematic Palaeontology*, *18*(10), 805–841. https://doi.org/10.1080/14772019.2019.1683902

Müller, R. T., Ferreira, J. D., Pretto, F. A., Bronzati, M., & Kerber, L. (2021). The endocranial anatomy of *Buriolestes schultzi* (Dinosauria: Saurischia) and the early evolution of brain tissues in sauropodomorph dinosaurs. *Journal of Anatomy*, *238*(4), 809–827. https://doi.org/10.1111/joa.13350

Müller, R. T., & Garcia, M. S. (2020). Rise of an empire: Analyzing the high diversity of the earliest sauropodomorph dinosaurs through distinct hypotheses. *Historical Biology*, *32*(10), 1334–1339. https://doi.org/10.1080/08912963.2019.1587754

Müller, R. T., Langer, M. C., Bronzati, M., Pacheco, C. P., Cabreira, S. F., & Dias-da-Silva, S. (2018a). Early evolution of sauropodomorphs: Anatomy and phylogenetic relationships of a remarkably well-preserved dinosaur from the Upper Triassic of southern Brazil. *Zoological Journal of the Linnean Society*. https://doi.org/10.1093/zoolinnean/zly009

Müller, R. T., Langer, M. C., & Dias-da-Silva, S. (2017). Biostratigraphic significance of a new early sauropodomorph specimen from the Upper Triassic of southern Brazil. *Historical Biology*, *29*(2), 187–202. https://doi.org/10.1080/08912963.2016.1144749

Müller, R. T., Langer, M. C., & Dias-da-Silva, S. (2018b). An exceptionally preserved association of complete dinosaur skeletons reveals the oldest long-necked sauropodomorphs. *Biology Letters*, *14*(11), 20180633. https://doi.org/10.1098/rsbl.2018.0633

Nau, D., Lallensack, J. N., Bachmann, U., & Sander, P. M. (2020). Postcranial Osteology of the First Early-Stage Juvenile Skeleton of *Plateosaurus trossingensis* (Norian, Frick, Switzerland). *Acta Palaeontologica Polonica*, *65*. https://doi.org/10.4202/app.00757.2020

Nesbitt, S. J. (2011). The Early Evolution of Archosaurs: Relationships and the Origin of Major Clades. *Bulletin of the American Museum of Natural History*, *352*, 1–292. https://doi.org/10.1206/352.1

Nesbitt, S. J., Smith, N. D., Irmis, R. B., Turner, A. H., Downs, A., & Norell, M. A. (2009). A Complete Skeleton of a Late Triassic Saurischian and the Early Evolution of Dinosaurs. *Science*, *326*(5959), 1530–1533. https://doi.org/10.1126/science.1180350

Novas, F. E., Ezcurra, M. D., Chatterjee, S., & Kutty, T. S. (2010). New dinosaur species from the Upper Triassic Upper Maleri and Lower Dharmaram formations of Central India. *Earth and Environmental Science Transactions of the Royal Society of Edinburgh*, *101*(3–4), 333–349. https://doi.org/10.1017/S1755691011020093

Owen, R. (1842). *Report on British Fossil Reptiles. Part II* (Report of the British Association for the Advancement of Science No. 11).

Perch-Nielsen, K., Birkenmajer, K., Birkelund, T., & Aellen, M. (1974). Revision of Triassic stratigraphy of the Scoresby Land an d Jameson Land region, east Greenland. *Meddelelser Om Gronland*.

Pretto, F. A., Langer, M. C., & Schultz, C. L. (2019). A new dinosaur (Saurischia: Sauropodomorpha) from the Late Triassic of Brazil provides insights on the evolution of sauropodomorph body plan. *Zoological Journal of the Linnean Society*, *185*(2), 388–416. https://doi.org/10.1093/zoolinnean/zly028

Prieto-Márquez, A., & Norell, M. A. (2011). Redescription of a Nearly Complete Skull of *Plateosaurus* (Dinosauria: Sauropodomorpha) from the Late Triassic of Trossingen (Germany). *American Museum Novitates*, *3727*(3727), 1–58. https://doi.org/10.1206/3727.2

Rauhut, O. W. M., Holwerda, F. M., & Furrer, H. (2020). A derived sauropodiform dinosaur and other sauropodomorph material from the Late Triassic of Canton Schaffhausen, Switzerland. *Swiss Journal of Geosciences*, *113*(1), 8. https://doi.org/10.1186/s00015-020-00360-8

Riggs, E. S. (1903). *Brachiosaurus altithorax*, the largest known Dinosaur. *American Journal of Science (1880-1910)*, *15*(88), 299.

Rütimeyer, L. (1856). Reptilien Knochen aus dem Keuper von Liestal. *Verhandlungen Der Schweizerischen Naturforschenden Gesellschaft*, *41*, 62–64.

Sander, P. M. (1992). The norian *Plateosaurus* bonebeds of central Europe and their taphonomy. *Palaeogeography, Palaeoclimatology, Palaeoecology*, *93*(3–4), 255–299. https://doi.org/10.1016/0031-0182(92)90100-J

Sander, P. M., & Klein, N. (2005). Developmental Plasticity in the Life History of a Prosauropod Dinosaur. *Science*, *310*(5755), 1800–1802. https://doi.org/10.1126/science.1120125

Schoch, R. R., & Seegis, D. (2014). Taphonomy, deposition and pedogenesis in the Upper Triassic dinosaur beds of Trossingen. *Palaeobiodiversity and Palaeoenvironments*, *94*(4), 571–593. https://doi.org/10.1007/s12549-014-0166-8

Seeley, H. G. (1887). I. On the classification of the fossil animals commonly named Dinosauria. *Proceedings of the Royal Society of London*, *43*(258–265), 165–171. https://doi.org/10.1098/rspl.1887.0117

Sereno, P. C., Foster, C. A., Rogers, R. R., & Monetta, A. M. (1993). Primitive dinosaur skeleton from Argentina and the early evolution of Dinosauria. *Nature*, *361*(7), 64–66.

Sullivan, C., Jenkins, Farish A., F. A., Gatesy, S. M., & Shubin, N. H. (2003). A functional assessment of the foot structure in the prosauropod dinosaur *Plateosaurus*. *Journal of Vertebrate Paleontology*, *23*.

Whiteside, D. I., Duffin, C. J., Gill, P. G., Marshall, J. E. A., & Benton, M. J. (2016). The Late Triassic and Early Jurassic Fissure Faunas from Bristol and South Wales: Stratigraphy and Setting. *Palaeontologia Polonica*, *67*, 257–287.

Yates, A. M. (2003). The species taxonomy of the sauropodomorph dinosaurs from the Lowenstein Formation (Norian, Late Triassic) of Germany. *Palaeontology*, *46*(2), 317–337. https://doi.org/10.1111/j.0031-0239.2003.00301.x

Yates, A. M. (2007a). The first complete skull of the Triassic dinosaur *Melanorosaurus haughton* (Sauropodomorpha: Anchisauria). *Special Papers in Palaeontology*, *77*, 9–55.

Yates, A. M. (2007b). Solving a dinosaurian puzzle: The identity of *Aliwalia rex* Galton. *Historical Biology*, *19*(1), 93–123. https://doi.org/10.1080/08912960600866953

Yates, A. M. (2010). A Revision of the problematic sauropodomorph dinosaurs from Manchester, Connecticut and the status of *Anchisaurus* Marsh: The Taxonomic Status of *Anchisaurus*. *Palaeontology*, *53*(4), 739–752. https://doi.org/10.1111/j.1475-4983.2010.00952.x

Young, C.-C. (1941). *A Complete Osteology of* Lufengosaurus heunei *Young (gen. Et Sp. Nov.) from Lufeng, Yunnan, China*. Geol. Survey of China.

7 Appendix

7.1 Data matrix

nstates 8 ;
xread
382 69
Euparkeria
00000000?0000?0000000?000?10010000000000000000?000000000100100000000000000?0000000?00?000?000000000?10000000000000000000?000000000000???0000??000000000?00?0?00??000000000000000000000000?0?00?0?????0????0000?00200000000000000?????000000000001?0?0??0000???00?0010?000000?01100000000000010000000000?02?000??0100000??1?000?100000?0000000??0?0???0010??0000?0????0?00?1?100000000?0000[0,1]0
Crurotarsi
0000000000000?0[0,1]000000000?0000000000[0,1]00000000000000000000100000000000000000?000000000000000000000000000000000000000000000000000000000???0000??000002000?00?0?00??0000200000000000000000000000000000[0,1]00?0[0,1]0??002?00000?0000?000000000000000000000000000010000[0,1]000000010?000000?0[0,1]000000000000000000000?00?000000000000001?0000[0,1]00000?0000000??0?0??000000000?00000000?00?001000000000000[0,1]??
Marasuchus
00???????0?0?????????????0?00???????0???????????0?????????????????????????????00???00000?????????????????????????00?00000000?1?100000000010???00?0??00?000000?00???00??000?00000000?0000000000??00101000000000?000??012?1000??0000?0?????????????0?????????????????????000000000000000?0100010000000000000000100000001100000000000?000001000100010010000?000?0000000000?000??0?00?0?00?0??00???100??
Agnosphitys
?0????????0?0?????????????11?0?0001000???00?000000000???000?????????????????????????????????1100??00?????????????????????????????????????0000002010000100???10??????011000100?????0?????????????????????????????????????0???
Aardonyx
1101?00210002?11?11????1110?1011000??????1010??0?11010??10?1????????1?0???????????0??????1??0?0?1?0?????1[1,2]?00101011001?1??????00010?110100101101?0000011

?001100000000020000010?1100?0110?0000?01110?0?00??????11???????????11000??00???
???131101???1?10???10???????????????????1110100001001 1??10110?101?111100000111
000?????????1101110?0???01?????????????01201111?0?0010?0?2??00?0???00[3,4]??

Adeopapposaurus

1001100210002111011111011011111010000101101000110111111111001000102001[0,1]01100101101010101101000001011[0,1]10101021111110[0,1]1001110011110002001
000111011011002001110011000000000000000100110100100000000000010000000000010101
21100001110000011011110111201011001110000002000010003100100100011011000 10?1
100101100000011010000002101000100000111011001001111010000001110100001111000
0010200011000011000100

Amygdalodon

??
???????????????????????????????????11?21211?????????100100????????002??10??1???????
????0111?1?????????????????????????10???
????????????????????????????????????1?01[1,2]???
110[0,1]11???

Anchisaurus

10???00??0102?1??11?????111011?010?001010?10001100111101110?10??????01?
001101?1??002110??????10?10?00??1000000010 1?1[1,2]?0111?0011?0??1001001111011?
10000?010?001100?000??0000000??0100?0??00?001?00?10?0????11[0,1]?0??2?11001?01
10?0?0??0??110101101001002010100002000[0,1]101031??00000?0111100001 0011?00101
0000101101000000[0,1]1110?01000001110111?1?01?010????0?10111?0?0011????0?01?1?
00100000100101??

Antetonitrus

?1??
??????????????????????????????????1?1012000????????00?[0,1]0???????????00?000001??
00[1,2]10001010121001000???1????1000?00?01100????0?00101??32110000[0,1]0111100?
?????0011?31101???1010????????0010013??0??00020110100001????????????1110111 00
110111110011000002100111010???????????????????1211111[1,2]0100?????[1,2]1?00?0??
??03??

Barapasaurus

??
??????????????????????????????????1?111211?????????1??1?1????00??002??100101??002
0110111112012 1100?0[1,2]1001?101?1?1??1?????????1010?00?21????1???00111?????????
???0???????????????????111100310101100011111000 11???11110010???????????????????10
??1?1?????????1?1????????1?00?????????20?????????????????1?1??????15??

Blikanasaurus

??
??
??
??0000?1110111
?1?01001011001110111001201111[0,1]01?11121021100001 00?02??

Camelotia

??
???1???????????0??0??001??00210000000
0??00?0???????????1?0???0??011???
????????????????????????1???????????1??00111?1110111101 11?1??110???000002????????
?????????????????????????????????????[1,2]???000????05??

Cetiosaurus

1??11??????????????????
??2??0011121011111010010002 0?2001?10?10
20??10111020101 00???[1,2]?????101011??00100????0111110103211001?0000?111???????
1?????????????????????????1111003?010210?0110?1?0011??1101?00???21111 2??0???110?1
110?2101002100101 11???15??

Chindesaurus

??
??1?00????????????01?0??0?1??0?1??
????000??00???????????1???0?????1?00??
??????????????????????0?????101?1????00??????????????00?0101110000000 1000???00?111
11100???01111010 0?????1?????????????????????????????????01??

Chromogisaurus

??
??
??????????????????1000??1010?0??1??????????????????????????????002????????????????
???????????0????111?0002202?????????????????????????0??????1???00110????100000[1,2]
010100010?????????????????????????????????0??0???000???100??

Coloradisaurus

?00?1002??102?111111?1??1110??011000?10??01?10?10111011100001001 00?1010
01101101?110101?????1?100101101001 1??000101010001?11?00110002001 00101?01100?
00?001?100110000000000000101????00?0001000?001????????000001012121 00011?????
??????????????????1?????????????????0?0?13110100???011?111002001100101110000011010
000002111011100000111011 00??011110?00101??????000011111101010200011000021000
200

Efraasia

100?1001?010??1?111?112?1110?100???00100100000??0?10??01?0??1??????10?000?1???
??0110100??????10010010??11?021001010100001???1?110001101001011011010000001??
001?000000000000000001100001010000 0?01100000?0?010?011201200001110100011010
12010?101000001110010001000010013100000101000010000000011001011010000111100 0
000110000010000011101?001?011010?0?10?01?111000001??0?0?01?1?00100000100002?
?

Eoraptor

0010?000?01010?00110000010100100 1?000110100000?101100101010010000010 01???0??
1??????????????000000?0?0?0?0?00?100000000??????100000101000 0?10????000??00?0
????00?000??00000001??10???1000???????????0????01??0??0011????0?001?0???????20?0
000?1?000?0?00100000110100 12?00001110??0????0?0???10?0010?10????0?100??0011??0
0?00?0?11?0110??1????0??????????????0?00??????0?0??000000000??0000??

Eucnemosaurus

??
??0???01??00110
0100000??00?0??????????1000000?01100???????????11?????????????????????????????
??????????????????????????????????110????0?????????????001101?1010?0010110????00001
110110??0[3,4]??

Glacialisaurus

??
??
??

??0??????????????0011?????????????
??0???1010[0,1]010????1101?0111111?1010??????????????0???

Gongxianosaurus

1?????0??????????12??
????????????????????????????????00???1??2121?????????????0???????????1??0??001??0???
???0?0??00000????????????0????0?0?1?0??000?011????2?110?????1????1??????????????
???????????????0?100??????0????????????????????????????[1,2]111?2??????0???110??1???
???1?0??1???0?1?1???????1?11??01?0??????1?0??2?111100002000?5??

Guaibasaurus

??
??0???01??01100
1000000??00000???????0?0101000???????01????1?00?????????????01?????????????????0???
???????1???????0????11?0?00210100010000000010?10110?0000100100000?1?10??1000
0?101111001?0?01????0???0101??0000?0??001?0??0000000000000101??

Herrerasaurus

00000000?0101000000000000?000100000000001000000100010101000001000011010
1000000101?0000000?1000?00000000?1000000000000000001010001000000100000?000
010000011??0010[0,1]10000002000000100000101100001001100100100?111?0??00110000
0000100000000120000001100000110011010010000012000000000000000010???01?01010
0100001011100000110000010000110001000100100101000000000110000010000000100000
00000000?00211

Ingentia

??
??0???111????01011?0??0????????????????????
????????????????????0??????????????????????????211000?101111[0,1]0?1?10?0011131101l0?
???????????0??
??01

Isanosaurus

??
??10??0???????????2??10??0????????
???????2?011000????????????????????????????101??0????????????????????????????????????
??211112??0???001?1?011??????????
??????????????????1??????????????????0?????????????????????311

Jingshanosaurus

1001?002??10211111100?0?111011101100?102001??1?10111011100001000????01
100000101?211001000??1?10110010??111021001012110O1????111???010??????1???1010
0??0011100?1???0000000000000??10??0100000000001000000?001?0??12120100111??0?
0??00??0011?3?100100?0101001020000100031000000020110011002??110010110?010011
0100000011110l?1010001110110?12011010?00?????????0120?1112?1?01?2000100000010
?[0,1]4??

Leonerasaurus

?0??
??????????????????????0?0???????1?110100100l1???001?0?010?1???????1100?00?0?10000
110000000??00000100?111001?????????????????????00000????1100000?????????????????
????????????????????11010311100?????????0??????11??1?1????????????????????????????
????????????????????????????????100111120????????????0??????0?00

Lessemsaurus

??

???00?011??0100???101?0000011?00[1
,2]1000000011100000???????????????????????????00001???2110000101??100???????0??
?3110?????0?00??1????0010013100000000?0111100001???1??10110?111011?10???01111?0
1??00000[0,1]1101?1???011011001201??????????1?111????1?2101??00??0???0401

Leyesaurus

?001?00?1000211??11?????1010?1101000010110 1?00?1011111111?00100010[0,2]
0011?????????01?10?110??1?00?10110??1010?11110100000 1?1??1111000200100011 1011
????0????????????????????????????????????000000?001????000?????????????????????????????
???1?00??????????????????????????????????
??????????????????????????????????????010??????????0?102000????0???0???00

Lufengosaurus

100???02???0211?1?11?11111111110100101011010000101110101100010?1????01
10??0110??01010100?011010010????0111?21011010100011?00011100020011011 1?01101
000200111001100000000000000010011010010000000000[0,1]100000000001?0111212[0,1]1
0?111?00001101111011130100101201000010200001001311010000201101100021011 0010
1100001011010000002111011101000111011001001111 0?00??001?11101[0,1]01111[0,1]10
10102000110000[1,2][0,1]0004??

Mamenchisaurus

11000113?1112011012000000010111 2??0011120101010111111101211 0000011122
1010000111?201?00?????2?11[0,1]000010010001111111112111 3?000111301210100001 10
002?11101010100201100011020121000001101111111111110110011011111 1?0003211001?
0010011011001101 1000?100011?0?1?0?1?31?1111003101011?0011111000110001 1010010
0211112??0???110?0110?21010?0??0??????10101111 1??1??????1120?1????2?1??2?12111
1102??015??

Massospondylus

10011002100021111111112110111110100001011010001100110111100010001 02?0
1?01100101101 0101??1010010010110101010210[0,1]1010110011100?1110002001001111
01101000200111001100000000000000 01011101001[0,1]000000000000000000?01[0,1]00111
21201001110000001101111011120100101211010000 20000100[0,1]310000010001101 10001
00110010111000101101000000210101010000011101100100111101 0010?01111100001111
[0,1]00?01020001000002100020 0

Melanorosaurus

1001?1031000211111101?1110101111???1010101101011001101011?00000010220
110110010??2002010011011101?00111?1000210?10021100110?010110001101101001011
1?0000001??00210000000010000000?0201001100010 0?0011000????00010??2211000?001
111?0??????00?0?2?100101[1,2]0?01001020000100131100000001011010000 1???1?010110?
111011110011000111 0?1100000[1,2]110110010211010100?0100111001[1,2]01111200001
??101110000110?03??

Meroktenos

???
???0???
???
????0??0?131?0?00001011?000001?????????????111111100?0001111101?????????????????
????????????????????????0110????????????????????0???

Mussaurus

???
???000100??????10110??0000?1?00010000000
0?00000010??111?011?01?00001110??????00110?0101100101111 1010?1?11?00101201011

01201010000200???0?0311000010?011??1?001?011??10110?10101101000000111101?100
000[1,2]1101110110110100011110??????0110111100000112001110000110003[0,1][0,1]

Neosauropoda

110001131111201101200000101011[0,2]111011120101010101011[0,1]111101211000[0,
1]10112221110010111120[0,1]20000010201110000120 1000[0,2]111111[0,2]12[0,1]112[0,1
]0000113100111101001100201210101011[0,1]020111001102012110000210011101011111[0
,1]1000[0,1]0100111?0003?110010[0,1]00001111100010100000000001100012??1?3001111
00310102100011111000110011110[0,1]10[0,1]00211012??0???110?1110121010?010000111
1101011111201101 1??11211100??2?10?20121111021101511

Neotheropoda

00[0,1]0[0,1]002[0,1]010201001100001[0,1]000000000000110000000010[0,1]100[0
,1]01000001[0,1]0001[0,1,2]010000001011000000111000100000001?0000000000000000
01011001130000010000[0,1]100001020000101011001000000100000000[1,2]1000110000
100000010010000100001 0?1100000010100001000120000000010?00010001101[1,2]010101
0130100021110101000001111100001101000 01?01100000000000000[0,1]01111111100200
10110000?00111110000??0?0000000?01000000000000102[0,1][0,1]

Ohmdenosaurus

??
??
??
???001000110?11
???[0,1]11010?11010???

Omeisaurus

1100011311112011012000001010 11?201001112010101011111010121100000112221110 01
0111???0?00???1???11100001?0?00021101111121113??001113012001101011 1002?12101
0101102011000110201211 00?021??1?10101111001 00??0111111000032110 01?0000?111??
????0100000100011000 1?001?310111100310101100011111000110001111001002110 12??0
???110?0100?210100?1?0??111?011010?11?????1????121?110??2?10?20121111102?1015?
?

Ornithischia

0010000000000?0000000?000?1011000100100?1000000100100001000000[0,1]000
10010000000001000000000010010[0,1]01[0,1]000000100111001110100001000000000000101
00[0,1]0000??010000000?00?0?00?0000000000000000[1,2]10000000000000010000[0,1]1000
010?0111[0,2]1100000010?000000000000000000000000000000000000011010210100010001
??0000?000110000000100001?0101110020000000000000[0,1]111110002?01?[0,1]10000??00
111100000?000?00?00?0[0,1]00000000000100[0,1][0,1]

Pampadromaeus

00???0021100??1?011??0???000?1000000?110?0?0?0??0?10?1??0???10????111?1?
??????????????????0???00000000??0010?100101000000?????????????????????1??????0?0?0
1??001?110?01000?000000?0??0000?1?1??0??01????00?101?0??1???????1?0????1??????
?????????????????????????00100?11??010202?????????????????????00001111100110111
00?0?00?00???????010??00??

Panphagia

?0????????1??????????0?1???????????????????0??0????????1???0???????10?1?1?1????????
??????????1?01000010000?10?0101000000????????001100100011?01100?000?01???01?10
000?0000000000?0???001?0?1000?0010000?01?001?0????????????????????????????????????
???????????????0??0?11110102101?00??0?001??11??10110???????????????????????00001
1010100???00001010???0?????????????????00?10???0???????????0???

Pantydraco
?0???0????????????[0,1]00?0???1??1????000100100000010?100001?00????????00?000?1?
10??00100011?000?00?01010??0000?1001010100001001??11[0,1]00?1010100110110 1?00
???1????1????????????????????????0??1?1?000010000?100??????11?01?00????????????
????????????????????????????0010012101100001?????????0011??10110?00??????????0?1?
0000??0000010?01?001????????????????????0000111000001 01?0000000010010???
Patagosaurus
11??
??????????????????1?00001??????0??0111012111??????1120010110000011002 0?2001010?0
0201?01111120121?00?02100111010?01?0?100????0?111??00??11001?00???111?????????
?????????????????????1111003101010000111110001100111110010?211112??0???10[0,1]
11110??10100[0,1]??0??1511
Plateosaurus_trossingensis
1001100110102011[0,1]11111211110010110000100101010110011001100011001001101101
1101101111011000101111001011010111111001010100001100111100011010 0[0,1]011011
0100020011100110000000000000010110100010000000001000000000100011111200001110
0000011011110101101001002010000001000010003110100102001010000111110010111100
0000111100000011000101000011111110010011010100110010111001011100000010110010
0000010000401
Plateosaurus_gracilis
?00??001?0102?110111?1??1110?101??00?10?1010?0??0?10001100??10??????????
????????1?????????????0??0110?????12100101010?001?????11000??01???0110110 1?00?0
01?1001100000000000000010?10100010100000000100 00?00??0????11200?01110?000?1
011?1010100100 00???100?????0?00100031?0100102001010000111110010 11??000011110
0000011?0??10000?1??0110????????????10??????????0??????????????0?0????????0[2,3]?
?
Plateosauravus
??
??1?0???0100101?01101?00[1,2]0011?
00110000000001000000??10??011????00??110?????????0????[2,3]011100?111000?0?????
????????1?????????????????00100?31??100101?01?????????11??10110?000011110000001
1000??100000111011 0??????0?????????????????????110???0?????0???????????4??
Pulanesaura
??
??????????????????????????????????10?012011????????0001?11?0100??11?????0??1??00?
0010?0120001000????????111?1111011???0?0?????????????????10???1????0?????????????
??0?11??1?11?????????????????????????0000021
20101???1?????????0???
Riojasaurus
1001?00??0102011?110??00111011011000?100001000?10010?00110001000001101
?0?100101?01011??????1?001000?1??101?2000101010000 10??111100011010010110110 10
00100111001100000000000000101110100100?000000110000??0?010?0112212101?11100
0?0111111?0111101011001010100102 0?00100?3100100102011010000110110010110010 1
101110100200110??10000011101100100110101001 0???011?0010?1110?0?01?210110000
01??10300
Ruehleia
??
??100???0????01???101?002001??0011001000

0011000000?1100001?0?0?00?0110???????0100011101200?111010?0?0100??0101101010
00???0???00???00100?31??1000020??1100001101107?10110?1010110100000021000??10?0
0?11011001?000010100??????????????????????????????????????03??

Sarahsaurus

10?1000?10?11010?11?1?1?011011010000010000101001011100011000107?0???001
000111001?110111111??1?10?10010?????011001010100001?101111?011001110111011111
100100101001011100000100000111110000 1?0?00?01001000?000100010101102100011110
010111011110110001111?011101000120210000031001101021001117?001111101101110211
100110101000111000010000[0,1]000100010001110100007?1?111101?11?11??0?01?1000?
100011100?1??

Saturnalia

10?????????????????????????1??1????00?100?0?????????????????10?????1??00???0?0??0?
0000?????????01000?????000010001000?????????000001001077?01101?0000010000110
0100000000000000000001010?????????????????1110011111100001010000?????????????
?????????????????????0??0?111100021020000000010011001001000000100110000011000107
1000001010100010010010100000000001000000000000010010000?000?0010001

Schleitheimia

??
??10?????????????01?10?0111?0????
???000??1?????????????????1?1???1??110?????????????????????00?0????????????????????????
?????????????????????1310111[0,2]002?????????????????????????????????????0?0111011???????
???0???????14??

Sefapanosaurus

??
??000??01100???0?10??00?001????1?
00000001??0000????1?????110?000??011?????0?0?01010??1?00?????11100?1011??01013
11010??10101???0?111110000??11[0,1]????
?000002??????0?00110101111000001??0?????1100??0???2?0???????????0???

Seitaad

??
??00?[0,1]?1??00
??00?001????0000?????????????????????????????0000?011??11000?111?000011?11100101
3010?00?21101??0???0?????????????????0?10000001?????????????????????????????????0
?00?11101?0???01101010??000??11?00??11????0?010???1100000010?????

Shunosaurus

11000113?1102011012000000001011?201001112010101010011010120000110111210
10001011?120020???1102001000001201000111111121211127?010112?1001?1?10010012
?1100001011021?00001?0201210000?11?00?10?01?11011001 1?111?1??00022110017?1000
0??11000?10110010?0001100002??1?3101111003101011000111117?001100?111100100211
112??0???100?011??21010?[0,1]1?0????110?101???1???1011??1121?110???2?00?2?12111?
10211015??

Silesaurus

00?0??00?0000?00100000??0?00?0?01010?????????0010??0????00?????????00?0?0
?0000??000000?????1?00?0?010???0?000001000100001?000000000000???001000000000
0010100001100000000000000??000001000000?0?0????????111??11100000 1?00000000??
????????????????????????????0000010000000000000000000000?010100?0?100001101100
0001100010100011100000000?0000000??01011?1??002???00000000?0?00???000?001010[
0,1]

Spinophorosaurus

1????1??????????????????????????????2?????????????0????01?????????0??101111110[1,2]00???????????1?????????????100111012?112?????112?11011?0?01?0002?110??11????[1,2]?11???1?1211010?0????????101???11011?001?1??111?0?03?2[1,2]0?110???[1,2]????1?1????01[1,2]0?011??001??211111110?1111??0?00?20?1002??0??11?101?0?0?01?0??????????????????????????????????????1???

Staurikosaurus

00??000000001000?00?0000000000????????000010???00?01001?000011?000?000000000200000001??01010110000?001100100????1?1??0000012010011000011 0?0010?00010?00000100001??000?0001?0000?0000011000000001????01??01??

Tazoudasaurus

11??010??1?????????[0,2]011???1???1??????????????00?00000???0??10?1111012101???000??1001010??????0002??100001??0020010001102012100 0????????1111?11?111?????11??????01?211001100?10?0????????010?2010000100?01001?310?1???0310101??0?111001?002??11??1??1??21100111001111011?00??0010020101010?111101111101??011????1?????[1,2]0?????????1??10?1????15??

Thecodontosaurus

?0???????????????????????1??1??1000??????0?0?0?0???000?????????????10?0?0?1010??011000???????00?11010??????2100101010000?1??????0000101010?1?01101?000001??0011000000000000000000?1000?0101?1000?01000???00?010?0112011000?101??00011000120100001100001010000000101000 00?210?000001???0?0?00??011??01010?0000111000000110001?1000001010110 0??011010100????????1100?0?111??0??1??000??00?0????01??

Unaysauru s

100110011010??1?111??1??1010?1011000?????????????0??00????001???000??0?10??0?10??110100??????010?10110?????02100101010000???0?1??????0?1?0???????????0??0?11?00?10000?0??00000???????????????0?0???01000??00?0101011?11200000110000 0??????1????1010????211?0??0??0??110110???011010?000??????????0???1100??????0??0???0??????01??

Volkheimeria

???3??????????????00???10??11??10201100111?2110?00??????????1?1????????1???1?1??03101010000?11?10?0111?111000010?111012??0???110?111??21010?0110111???

Vulcanodon

???[1,2]??????????????????????1???????01?11?0?00??0?0??01????2?110?1?0?000111??????????????????????????????????????031010[1,2]?00?01111000010011111001 0?11101111001011[0,1]?1????20?10021?0???11?101011011011101 1??111?10102?1001020111110?121?015??

Xingxiulong

?????????????????????1???1?1111???0?10?0????0110011001100000000101?01?00100101?00?101???????0?????????001??000?????????11001111?00100110001?01101000200111001100000000010000110011 0??11?010?00001?????00?000?0????120?00111??0?0????1??????1?101???????????????00100131101000010?1011?002??11??0001000000111100001011010?0?00000?1011100100110 1000???010110001?01110000001?2100110000210002??

Yunnanosaurus
100?1002??00??10011001??1011111???00101110?00??0?1101111001000001?01?0?00010???????????????10000010???0???00010?21000?1???1111000110110100?01101000000110001100000000001000000?0101101000000?00?0???0??001?00??121200??111??000??01??0011?201011002010100[0,1]020?001001310000000011010?0010?110010111?0010110100000110101?101000110011001?011010100??001111001?0?1110?0?011???11?0000110?02??

NHMD_164741
?00110021000101110101121111011011000010011000011001001110000?1000?01?010?????10???????0?01001?100101???0111?1100101010000???

NHMD_164758
?001100210001011?0101121111011011000010011000011001001110001?????????????????????10??0101001110010110101111110010101000??

Macrocollum
1001100210002111111011211110010010000100100000110010010100001000001101??????101???????0?100??1001011010?1?011001010100001 1?01111?002001001111011010000001110111010000000000000100110??010??00000001000010 0?010001111120 00?01100??01101112010100101000211000000100001 00?21??00010200?0?0?001?01100101110100000110000101100 0?010000[0,1]1110110010011010100??00101110000110100000101100000000 1000?1??
;

Ccode

-[/1 0	-[/1 1	-[/1 2	-[/1 3	-[/1 4
-[/1 5	-[/1 6	+[/1 7	-[/1 8	-[/1 9
-[/1 10	-[/1 11	+[/1 12	-[/1 13	-[/1 14
-[/1 15	-[/1 16	-[/1 17	+[/1 18	-[/1 19
-[/1 20	-[/1 21	+[/1 22	-[/1 23	-[/1 24
-[/1 25	-[/1 26	-[/1 27	-[/1 28	-[/1 29
-[/1 30	-[/1 31	-[/1 32	-[/1 33	-[/1 34
-[/1 35	-[/1 36	-[/1 37	-[/1 38	+[/1 39
-[/1 40	-[/1 41	-[/1 42	-[/1 43	-[/1 44
-[/1 45	-[/1 46	-[/1 47	-[/1 48	-[/1 49
-[/1 50	-[/1 51	-[/1 52	-[/1 53	-[/1 54
-[/1 55	+[/1 56	-[/1 57	-[/1 58	-[/1 59
-[/1 60	+[/1 61	-[/1 62	-[/1 63	-[/1 64
-[/1 65	-[/1 66	-[/1 67	+[/1 68	-[/1 69
-[/1 70	-[/1 71	-[/1 72	-[/1 73	-[/1 74
-[/1 75	-[/1 76	-[/1 77	-[/1 78	-[/1 79
-[/1 80	-[/1 81	-[/1 82	-[/1 83	-[/1 84
-[/1 85	-[/1 86	-[/1 87	-[/1 88	-[/1 89
-[/1 90	+[/1 91	-[/1 92	-[/1 93	-[/1 94

-[/1 95 -[/1 96 -[/1 97 -[/1 98 -[/1 99
-[/1 100 +[/1 101 -[/1 102 -[/1 103 -[/1 104
-[/1 105 -[/1 106 -[/1 107 -[/1 108 -[/1 109
-[/1 110 -[/1 111 -[/1 112 -[/1 113 -[/1 114
-[/1 115 +[/1 116 -[/1 117 -[/1 118 -[/1 119
+[/1 120 +[/1 121 -[/1 122 -[/1 123 -[/1 124
-[/1 125 -[/1 126 -[/1 127 +[/1 128 -[/1 129
-[/1 130 +[/1 131 -[/1 132 -[/1 133 -[/1 134
-[/1 135 -[/1 136 -[/1 137 -[/1 138 -[/1 139
-[/1 140 -[/1 141 -[/1 142 -[/1 143 +[/1 144
-[/1 145 -[/1 146 +[/1 147 -[/1 148 +[/1 149
+[/1 150 -[/1 151 -[/1 152 -[/1 153 -[/1 154
-[/1 155 -[/1 156 +[/1 157 -[/1 158 -[/1 159
-[/1 160 -[/1 161 -[/1 162 -[/1 163 -[/1 164
-[/1 165 -[/1 166 +[/1 167 -[/1 168 +[/1 169
+[/1 170 -[/1 171 -[/1 172 -[/1 173 -[/1 174
-[/1 175 -[/1 176 +[/1 177 -[/1 178 -[/1 179
-[/1 180 -[/1 181 -[/1 182 -[/1 183 -[/1 184
-[/1 185 -[/1 186 -[/1 187 -[/1 188 -[/1 189
-[/1 190 -[/1 191 -[/1 192 -[/1 193 -[/1 194
-[/1 195 -[/1 196 -[/1 197 -]/1 198 -[/1 199
-[/1 200 -[/1 201 -[/1 202 -[/1 203 -[/1 204
-[/1 205 -[/1 206 -[/1 207 -[/1 208 +[/1 209
+[/1 210 -[/1 211 +[/1 212 -[/1 213 -[/1 214
-[/1 215 -[/1 216 -[/1 217 -[/1 218 -[/1 219
-[/1 220 -[/1 221 -[/1 222 -[/1 223 -[/1 224
-[/1 225 -[/1 226 -[/1 227 -[/1 228 -[/1 229
-[/1 230 +[/1 231 -[/1 232 -[/1 233 -[/1 234
-[/1 235 +[/1 236 -[/1 237 -[/1 238 -[/1 239
-[/1 240 -[/1 241 -[/1 242 -[/1 243 +[/1 244
-[/1 245 -[/1 246 -[/1 247 -[/1 248 -[/1 249
-[/1 250 -[/1 251 -[/1 252 +[/1 253 -[/1 254
-[/1 255 -[/1 256 -[/1 257 -[/1 258 -[/1 259
-[/1 260 -[/1 261 +[/1 262 -[/1 263 -[/1 264
-[/1 265 -[/1 266 +[/1 267 -[/1 268 -[/1 269
-[/1 270 -[/1 271 -[/1 272 -[/1 273 -[/1 274
-[/1 275 -[/1 276 -]/1 277 -[/1 278 -[/1 279
-[/1 280 +[/1 281 -[/1 282 -[/1 283 -[/1 284
-[/1 285 -[/1 286 -[/1 287 -[/1 288 -[/1 289
-[/1 290 -[/1 291 -[/1 292 -[/1 293 +[/1 294
-[/1 295 -[/1 296 -[/1 297 -[/1 298 -[/1 299
-[/1 300 -[/1 301 -[/1 302 -[/1 303 -[/1 304
-[/1 305 -[/1 306 -[/1 307 -[/1 308 -[/1 309
-[/1 310 -[/1 311 -[/1 312 -[/1 313 -[/1 314
+[/1 315 -[/1 316 -[/1 317 -[/1 318 -[/1 319
-[/1 320 +[/1 321 -[/1 322 -[/1 323 -[/1 324
-[/1 325 -[/1 326 -[/1 327 -[/1 328 +[/1 329
-[/1 330 -[/1 331 -[/1 332 -[/1 333 -[/1 334

-[/1 335 -[/1 336 -[/1 337 -[/1 338 -[/1 339
-[/1 340 -[/1 341 -[/1 342 -[/1 343 -[/1 344
-[/1 345 -[/1 346 -[/1 347 -[/1 348 -[/1 349
-[/1 350 +[/1 351 -[/1 352 -[/1 353 -[/1 354
-[/1 355 -[/1 356 -[/1 357 -[/1 358 -[/1 359
-[/1 360 -[/1 361 -[/1 362 -[/1 363 +[/1 364
-[/1 365 -[/1 366 +[/1 367 -[/1 368 +[/1 369
-[/1 370 -[/1 371 -[/1 372 -[/1 373 +[/1 374
-[/1 375 -[/1 376 -[/1 377 -[/1 378 +[/1 379
-[/1 380 -[/1 381 ;

Ancstates

-0 -1 -2 -3 -4 -5 -6 -7 -8 -9
-10 -11 -12 -13 -14 -15 -16 -17 -18 -19
-20 -21 -22 -23 -24 -25 -26 -27 -28 -29
-30 -31 -32 -33 -34 -35 -36 -37 -38 -39
-40 -41 -42 -43 -44 -45 -46 -47 -48 -49
-50 -51 -52 -53 -54 -55 -56 -57 -58 -59
-60 -61 -62 -63 -64 -65 -66 -67 -68 -69
-70 -71 -72 -73 -74 -75 -76 -77 -78 -79
-80 -81 -82 -83 -84 -85 -86 -87 -88 -89
-90 -91 -92 -93 -94 -95 -96 -97 -98 -99
-100 -101 -102 -103 -104 -105 -106 -107 -108 -109
-110 -111 -112 -113 -114 -115 -116 -117 -118 -119
-120 -121 -122 -123 -124 -125 -126 -127 -128 -129
-130 -131 -132 -133 -134 -135 -136 -137 -138 -139
-140 -141 -142 -143 -144 -145 -146 -147 -148 -149
-150 -151 -152 -153 -154 -155 -156 -157 -158 -159
-160 -161 -162 -163 -164 -165 -166 -167 -168 -169
-170 -171 -172 -173 -174 -175 -176 -177 -178 -179
-180 -181 -182 -183 -184 -185 -186 -187 -188 -189
-190 -191 -192 -193 -194 -195 -196 -197 -198 -199
-200 -201 -202 -203 -204 -205 -206 -207 -208 -209
-210 -211 -212 -213 -214 -215 -216 -217 -218 -219
-220 -221 -222 -223 -224 -225 -226 -227 -228 -229
-230 -231 -232 -233 -234 -235 -236 -237 -238 -239
-240 -241 -242 -243 -244 -245 -246 -247 -248 -249
-250 -251 -252 -253 -254 -255 -256 -257 -258 -259
-260 -261 -262 -263 -264 -265 -266 -267 -268 -269
-270 -271 -272 -273 -274 -275 -276 -277 -278 -279
-280 -281 -282 -283 -284 -285 -286 -287 -288 -289
-290 -291 -292 -293 -294 -295 -296 -297 -298 -299
-300 -301 -302 -303 -304 -305 -306 -307 -308 -309
-310 -311 -312 -313 -314 -315 -316 -317 -318 -319
-320 -321 -322 -323 -324 -325 -326 -327 -328 -329
-330 -331 -332 -333 -334 -335 -336 -337 -338 -339
-340 -341 -342 -343 -344 -345 -346 -347 -348 -349
-350 -351 -352 -353 -354 -355 -356 -357 -358 -359
-360 -361 -362 -363 -364 -365 -366 -367 -368 -369

```
 -370   -371   -372   -373   -374   -375   -376   -377   -378   -379
 -380   -381
;
 xgroup ;
agroup ;
taxcode
+0     +1     +2     +3     +4     +5     +6     +7
+8     +9     +10    +11    +12    +13    +14    +15
+16    +17    +18    +19    +20    +21    +22    +23
+24    +25    +26    +27    +28    +29    +30    +31
+32    +33    +34    +35    +36    +37    +38    +39
+40    +41    +42    +43    +44    +45    +46    +47
+48    +49    +50    +51    +52    +53    +54    +55
+56    +57    +58    +59    +60    +61    +62    +63
+64    +65    +66    +67    +68
;


blocks 0;
hold 50000;
proc/;
```